

AN EXAMINATION OF DENSITY AND VISCOSITY  
DEPENDENT INFILTRATION OF IMMISCIBLE  
NONAQUEOUS PHASE LIQUIDS USING THE  
NUMERICAL MODEL "SWANFLOW"

By

DAVID ALAN BALTHAZOR

Bachelor of Science  
Michigan State University  
East Lansing, Michigan  
1987

Master of Science  
Western Michigan University  
Kalamazoo, Michigan  
1991

Submitted to the Faculty of the  
Graduate College of the  
Oklahoma State University  
in partial fulfillment of  
the requirements for  
the Degree of  
MASTER OF SCIENCE  
July, 1994

AN EXAMINATION OF DENSITY AND VISCOSITY  
DEPENDENT INFILTRATION OF IMMISCIBLE  
NONAQUEOUS PHASE LIQUIDS USING THE  
NUMERICAL MODEL "SWANFLOW"

Thesis Approved:

*Autyapi*

\_\_\_\_\_  
Thesis Advisor

*Gregory J. Wilber*

\_\_\_\_\_  
*Jim Carlson*

*Thomas C. Collins*

\_\_\_\_\_  
Dean of the Graduate College

## ACKNOWLEDGEMENTS

I would like to express special thanks to my advisor and committee chair Dr. Avdhesh K. Tyagi for his supervision, constructive guidance, and encouragement throughout my course of study. I would like to extend my appreciation to my other committee members, Dr. Greg Wilbur and Dr. William Clarkson, for their critical review of this manuscript. I am also grateful to the remaining faculty, staff, and students of the Department of Civil and Environmental Engineering who have made my experience at Oklahoma State University positive and memorable.

To Jeanne and Paige, who gave their love and friendship at a time when I needed them most, I will always be grateful.

Finally, I extend my gratitude to my loving parents for being supportive toward all my academic endeavors.

## TABLE OF CONTENTS

	Page
INTRODUCTION .....	1
Scope of Related Research .....	3
Multiple Phase Fluid Systems .....	10
<i>Saturation Ratio</i> .....	10
<i>Capillary Pressure</i> .....	12
<i>Relative Permeability</i> .....	15
EXPERIMENTAL METHODOLOGY .....	19
Research Methods and Objectives .....	19
The Numerical Model .....	20
<i>Governing Equations for Multiphase Flow</i> .....	21
<i>Constitutive Relationships</i> .....	22
<i>Final Multiphase Flow Equations</i> .....	22
<i>Finite-Difference Formulation</i> .....	23
<i>Assumptions and Limitations</i> .....	24
SWANFLOW Input Parameters .....	26
<i>Hydrogeologic Setting</i> .....	26
<i>Initial Conditions</i> .....	27
<i>Relative Permeability and Capillary Pressure</i> .....	30

<i>Numerical Model Discretization Data</i> . . . . .	30
DISCUSSION OF SIMULATION RESULTS . . . . .	34
Gasoline . . . . .	35
Kerosene . . . . .	40
<i>p</i> -Cymene . . . . .	44
10W-30 Motor Oil . . . . .	48
Water . . . . .	52
Phenol . . . . .	54
<i>o</i> -Nitrotoluene . . . . .	59
Trichloroethene . . . . .	62
Tetrachloromethane . . . . .	65
Vertical and Horizontal NAPL Infiltration Rates . . . . .	68
<i>Vertical NAPL Infiltration Rates</i> . . . . .	68
<i>Horizontal NAPL Infiltration Rates</i> . . . . .	72
Discussion Summary . . . . .	72
CONCLUSIONS . . . . .	78
REFERENCES . . . . .	80
APPENDIXES	
APPENDIX A--SWANFLOW Input Files . . . . .	85
APPENDIX B--SWANFLOW Output Files . . . . .	105

## LIST OF TABLES

Table	Page
1. NAPL Density and Viscosity Data . . . . .	20
2. Hydrogeologic Parameters . . . . .	29
3. Initial Conditions . . . . .	31
4. Capillary Pressure and Relative Permeability Data . . . . .	32
5. Vertical NAPL Infiltration Rates. . . . .	70
6. Horizontal NAPL Infiltration Rates (Unsaturated Zone) . . . . .	73

## LIST OF FIGURES

Figure	Page
1. Migration pattern for an organic liquid more dense than water (left) and less dense than water (right) . . . . .	2
2. Schematic cross section illustrating a porous media containing four phases, i.e., NAPL, water, air, and sorbed contaminant on framework grains . . . . .	11
3. Capillary pressure-wetting fluid saturation for two-phase flow . . . . .	14
4. Typical relative permeability curves for a two-phase system . . . . .	16
5. Ternary diagram showing the relative permeability of NAPL in an air-water-NAPL system as a function of saturation . . . . .	18
6. Finite-difference grid showing locations of the NAPL source block, the lower, draining aquifer, and the block-centered grid nodes . . . . .	28
7. Infiltration of gasoline at one and three years . . . . .	37
8. Infiltration of gasoline at five and 10 years . . . . .	38
9. Infiltration of kerosene at one and three years . . . . .	41
10. Infiltration of kerosene at five and 10 years . . . . .	43
11. Infiltration of <i>p</i> -cymene at one and three years . . . . .	46
12. Infiltration of <i>p</i> -cymene at five and 10 years . . . . .	47
13. Infiltration of 10W-30 motor oil at one and three years . . . . .	49
14. Infiltration of 10W-30 motor oil at five and 10 years . . . . .	51
15. Infiltration of water at one and three years . . . . .	53
16. Infiltration of water at five and 10 years . . . . .	55

17. Infiltration of phenol at one and 3 years . . . . .	57
18. Infiltration of phenol at five and 10 years . . . . .	58
19. Infiltration of <i>o</i> -nitrotoluene at one and three years . . . . .	60
20. Infiltration of <i>o</i> -nitrotoluene at five and 10 years . . . . .	61
21. Infiltration of trichloroethene (TCE) at one and three years . . . . .	63
22. Infiltration of trichloroethene (TCE) at five and 10 years . . . . .	64
23. Infiltration of tetrachloromethane (carbon tetrachloride) at one and three years .	66
24. Infiltration of tetrachloromethane (carbon tetrachloride) at five and 10 years . .	67
25. Breakthrough of vertically-infiltrating NAPL . . . . .	71
26. Horizontal NAPL Infiltration Rates . . . . .	74



## NOMENCLATURE

$c_r$	aquifer compressibility
$g$	gravitational constant
$k$	intrinsic permeability
$k_{ra}$	relative permeability of air (vapor)
$k_{rn}$	relative permeability of NAPL (nonwetting fluid)
$k_{rna}$	relative permeability of NAPL in an air-NAPL system as a function $S_a$
$k_{rnw}^*$	relative permeability of NAPL at the residual saturation of water in a water-NAPL system
$k_{rw}$	relative permeability of water (wetting fluid)
$k_{rnw}$	relative permeability of the NAPL system as a function of $S_w$
$p$	interstitial fluid pressure
$p^\circ$	reference pressure
$p_a$	interstitial air (vapor) pressure
$p_n$	interstitial NAPL (nonwetting fluid) pressure
$p_w$	interstitial water (wetting fluid) pressure
$p_{can}$	capillary pressure between air (vapor) and NAPL (nonwetting fluid)
$p_{caw}$	capillary pressure between air (vapor) and water (wetting fluid)
$p_{cnw}$	capillary pressure between the NAPL (nonwetting fluid) and water (wetting fluid)
$q_a$	air (vapor) mass accumulation (source/sink) term

$q_n$	NAPL (nonwetting fluid) mass accumulation (source/sink) term
$q_w$	water (wetting fluid) mass accumulation (source/sink) term
$t$	time
$A$	cross-sectional area perpendicular to the direction of flow
$D$	depth
DNAPL	dense nonaqueous phase liquid
$K$	hydraulic conductivity
$K_{oc}$	partitioning coefficient based on organic fraction of the aquifer material
$K_{ow}$	octanol-water partition coefficient
$L$	length increment in the flow direction
LNAPL	light nonaqueous phase liquid
$M_n$	mass per unit volume of NAPL
$M_w$	mass per unit volume of water
NAPL	nonaqueous phase liquid
$S_a$	interstitial air (vapor) saturation
$S_n$	interstitial NAPL (nonwetting fluid) saturation
$S_{nwr}$	irreducible or residual NAPL (nonwetting fluid) saturation
$S_w$	interstitial water (wetting fluid) saturation
$S_{wi}$	residual or irreducible water (nonwetting fluid) saturation
$T_n$	transmissibility of NAPL
$T_{ng}$	transmissibility of NAPL under gravitational influence
$T_w$	transmissibility of water
$T_{wg}$	transmissibility of water under gravitational influence

$V_b$	grid block volume
$\phi$	porosity of the medium
$\phi^\circ$	porosity of the medium at the reference pressure, $p^\circ$
$\mu_a$	dynamic viscosity of air (vapor)
$\mu_n$	dynamic viscosity of NAPL (nonwetting fluid)
$\mu_w$	dynamic viscosity of water (wetting fluid)
$\rho_a$	fluid density of the vapor (air) phase
$\rho_n$	fluid density of the nonwetting phase (NAPL)
$\rho_w$	fluid density of water
$\Delta$	difference operator for the finite-difference approximation
$\nabla$	differential operator

## INTRODUCTION

Many hazardous waste sites, including leaking underground storage tanks, involve immiscible nonaqueous phase organic liquids (NAPL) [e.g., *Burmester and Harris*, 1982; *Maugh*, 1979; *U.S. Environmental Protection Agency*, 1980, 1982, 1983; *Villaume*, 1985]. Release of these organic liquid contaminants usually occurs at or near the ground surface, and once released, they are free to migrate downward, under the influence of gravity, through the vadose zone toward the water table. Owing to capillary forces, much of the nonaqueous phase will remain trapped in the unsaturated zone; however, if the spill volume is large enough it eventually reaches the water table. If the nonaqueous phase organic liquid is less dense than water (LNAPL), it will spread laterally upon reaching the top of the water table, and will usually migrate down-gradient from the spill site, as the right side of Figure 1 demonstrates. If the organic liquid is more dense than water (DNAPL), it will continue to migrate through the saturated zone to the base of the aquifer, illustrated by the left side of Figure 1. Once reaching the base, the DNAPL may be transported down-gradient by groundwater flow or may migrate down-dip toward topographic aquifer lows. Additionally, in the vicinity of the water table, soluble components may dissolve in the water phase forming a plume of contaminated water extending outward from the main zone of contamination. A gaseous envelope of chemical vapor may also develop and migrate beyond the main body of contamination

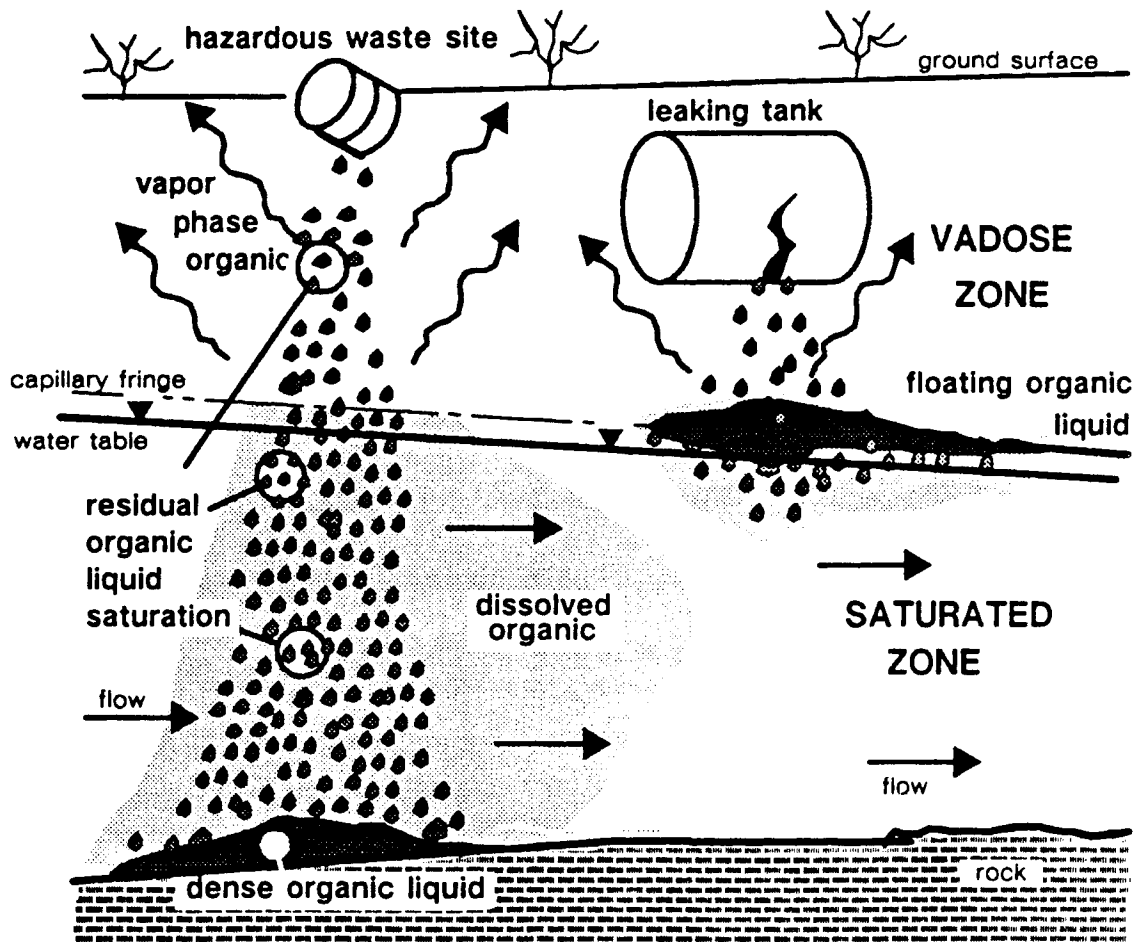


Figure 1. Migration pattern for an organic liquid more dense than water (left) and less dense than water (right) [Wilson et al., 1990].

as the result of volatilization of light components. Such behavior by immiscible contaminants, in addition to dispersion and diffusion phenomena, adsorption onto aquifer solids, and chemical and biological degradation, pose complex challenges to the groundwater-contaminant flow modeler.

The purpose of this study is to evaluate the infiltration pathways of immiscible nonaqueous phase liquids as functions of fluid density and viscosity. Often, groundwater modelers attempt to simulate the movement of a nonaqueous liquid accidentally introduced to subsurface by assuming the NAPL will behave much like the water in the groundwater system. However, the different density and viscosity of the NAPL will result in a dissimilar infiltration pathway. These dissimilarities could impact the design and implementation of a system intended to monitor and recover free product, and should be considered in the evaluation of a contaminated site. Although differences in the infiltration pathway of a NAPL introduced to the subsurface may be generally known for some contaminants, there is little published data which quantify this variation as a function of NAPL fluid properties, i.e., its density and viscosity.

### Scope of Related Research

Much of the current knowledge of the physics of multiphase fluid flow [e.g., *Corey et al.*, 1956; *Land*, 1968; *Leverett and Lewis*, 1941; *Snell*, 1962; *Stone*, 1973] and the relevant numerical solution methods have been developed in the petroleum industry, and are widely published in the petroleum reservoir engineering literature [e.g., *Coats*, 1982; *Peaceman*, 1977; *Young and Stephenson*, 1983]. The simultaneous movement of multiple fluid phases (i.e., crude oil, water, and natural gas) through a single porous

media, as it relates to hydrocarbon emplacement and production is critically important to the reservoir engineer. This concept has long been commonplace within the petroleum industry; however, it was not until 1967 that the movement of a NAPL in a groundwater system was recognized as a multiphase flow problem [*van Dam*, 1967]. *Green et al.* [1970] further expanded the multiphase concept of NAPL transport by questioning the importance of a hydrodynamically passive air phase, an assumption commonly accepted by the hydrologists of the period. Instead, they presented an analysis based upon dynamic air and water phases.

Based on work by *van Dam* [1967], several numerical models were developed to describe mathematically the immiscible flow of a lighter than water NAPL [*Hocmuth and Sunada*, 1985; *Holzer*, 1976]. These early models assumed piston-like flow, i.e., negligible capillarity. Inherent in this assumption is the requirement that the NAPL and water phases have fixed saturations, which is not realistic in field situations where phase saturations can vary considerably [*Pinder and Abriola*, 1986].

During the last decade, several finite-difference and finite-element numerical simulators for NAPL transport in multiphase subsurface systems have been reported in the groundwater literature. Many of the early models were developed to incorporate the concept of capillarity into the immiscible NAPL transport scheme [*Faust*, 1985; *Faust et al.*, 1989; *Kaluarachchi and Parker*, 1989; *Kuppusamy et al.*, 1987; *Osborne and Sykes*, 1986]. However, they do not consider interphase mass transfer of the NAPL components, and either do not include a gas phase or assume an immobile gas phase at uniform atmospheric pressure. Therefore, these simulators do not include the transport of solubilized and vaporized constituents in the water and air phases, respectively. What

follows is a brief discussion of the evolution of these numerical models which have recently been developed.

The model introduced by *Faust* [1985], Simultaneous Water, Air, and NAPL Phase Flow (SWANFLOW), and subsequently updated by *Faust et al.* [1989], analyzed the simultaneous flow of water and NAPL in a three-phase fluid system. The flow model presented uses a finite-difference method in two- and three-dimensional domains, and is based on the mass conservation of each fluid under the assumption of a static air phase at atmospheric pressure. The coupled, nonlinear, partial differential equations are a simplification of the conventional three-phase flow equations used in petroleum reservoir simulation [*Peaceman*, 1977], and can be solved for both saturated and unsaturated conditions. Constitutive relationships employed by the model include relative permeability-saturation, pressure-saturation, and porosity-fluid pressure expressions. In addition, the flow of the nonaqueous phase is in response to viscous and gravity (density dependent) forces.

A finite-element solution for liquid flow in a three-phase porous medium system comprising two space dimensions was presented *Kuppusamy et al.* [1987]. The model involves the simultaneous solution of two coupled, partial differential equations for flow of the water and NAPL phases. It is assumed the air phase is static and remains at constant atmospheric pressure. The model incorporates constitutive relationships for fluid conductivities and saturations as functions of fluid pressures. These relationships were experimentally calibrated by *Parker et al.* [1987], and are included in the finite-element code. No interphase mass transfer is considered.

A simulator by *Kaluarachchi and Parker* [1989] was developed to predict the



simultaneous flow of water and oil in a three-phase system through the unsaturated zone. The two-dimensional, finite-element model, MOFAT-2D, utilizes Galerkin's weighted residual approach and an upstream weighting technique to solve the two coupled, nonlinear, partial differential equations. Brooks and Corey [1966], and van Genuchten [1980] soil properties are also considered. Constitutive relationships are used to describe three-phase relative permeabilities and saturations as functions of fluid pressures. Assumptions include negligible pressure gradients in the air phase (i.e., air pressure is atmospheric), an incompressible porous media, constant fluid properties, and no mass transfer between phases.

The finite-element model, Waterloo Simulator for Two-Phase Immiscible Flow (WSTIF), introduced by *Osborne and Sykes* [1986], is a two-dimensional, two-phase simulator based on Darcy's law and conservation of mass for each liquid, and is intended to predict the migration of an immiscible organic solvent in groundwater. The numerical model is based on a generalized method of weighted residuals in conjunction with the finite-element method to solve the two, coupled, second-order, nonlinear immiscible transport equations. A non-hysteretic capillary pressure-water saturation expression, and a relative permeability-water saturation constitutive relationship are incorporated into the model as well. An incompressible porous media and incompressible fluids are assumed. The transport of the air phase and interphase mass transfer are not considered.

A few of the reported simulators consider interphase mass transfer of one or more NAPL components to the gas and water phases, but assume that the NAPL itself is immobile in the unsaturated zone [*Baehr and Corapcioglu*, 1987; *Corapcioglu and Baehr*, 1987; *Sleep and Sykes*, 1989]. The focus of these simulators is to evaluate the impact of

a NAPL at residual saturation (i.e., immobile conditions), in the unsaturated zone, and its transport as solubilized and vaporized components in the water and air phases, respectively. Such conditions may arise as a spilled contaminant migrates vertically downward through the unsaturated zone, or may be that portion of a spill which remains trapped in a soil after routine remedial efforts to recover the product have ceased.

A one-dimensional, finite-difference model to describe multiphase transport in the unsaturated zone was introduced by *Baehr and Corapcioglu* [1987] and *Corapcioglu and Baehr* [1987]. The simulator considers the fate of an immobile, reactive, multiconstituent, immiscible contaminant, which is allowed to partition between the air, water, sorbed, and immiscible phases. An equilibrium approximation is applied to partition the constituent mass between the four available phases in regions where the contaminant plume exists. Outside the limits of the plume, the equilibrium approximation takes on a simpler form to partition the constituent mass between the air, water, and sorbed phases only. Thermodynamic principles are employed to quantify the interphase partitioning. In addition, molecular transformations of the contaminant, both biotic and abiotic, are incorporated as sink terms into the conservation of mass equation. One nonlinear, partial differential equation is required for each constituent of the immiscible contaminant for the one-dimensional approximation. The one-dimensional formulation allows for conservative estimates of constituent mass released to the atmosphere or aquifer, and of constituent mass remaining in the unsaturated zone.

The simulator developed by *Sleep and Sykes* [1989] is intended to predict the fate of immobilized volatile organic compounds in variably saturated media. The partial differential equations are obtained by combining Darcy's law with the mass continuity

equation, and are solved for a two-dimensional, vertical cross section using Galerkin's method of weighted residuals. The equations are linked by capillary pressures existing at the interfaces between phases. Variably saturated water flow, density-dependent gas flow, and water and gas phase transport are considered by this simulator.

Models presented by *Abriola and Pinder* [1985a, b] and *Forsyth* [1988] allow for interphase mass transfer and flow of the NAPL and water phases, but the gas phase is assumed to be stagnant. *Abriola and Pinder* [1985a, b] developed a series of governing equations for a two-component (nonvolatile and volatile) contaminating phase. Using Darcy's law, the conservation of mass principles, and the volume averaging theory, it was possible to describe the simultaneous transport of a contaminant in three physical forms, including transport as a nonaqueous phase, as a soluble component of a water phase, and as a mobile fraction of a gas phase. Incorporated within the flow equations are the effects of matrix and fluid compressibility, gravity, phase composition, interphase mass exchange, capillarity, diffusion, and dispersion. These resulting equations form a system of three nonlinear partial differential equations for transport of the water phase, and the two organic phases. The five unknowns include nonaqueous-water and water-gas capillary pressures, and the mass fraction of the volatile organic species in the nonaqueous, water, and gas phases. The work of *Forsyth* [1988] involves the basic modeling strategy of *Faust* [1985] and *Faust et al.* [1989]. The simulator includes the interphase mass transfer concepts developed by *Abriola and Pinder* [1985a, b], except the organic phase is composed of a single species.

Recently, researchers including *Falta et al.* [1992a, b], *Sleep and Sykes* [1993a, b], and *Adenekan et al.* [1993] have made significant contributions toward simulation of a

nonaqueous phase in groundwater systems. The model developed by *Falta et al.* [1992a, b], STMVOC, was the first simulator in the groundwater literature to consider interphase mass transfer and the transport of the contaminant in all three fluid components, including gas phase advection, for nonisothermal conditions. Interphase mass transfer of the components between any of the phases is calculated by assuming local chemical equilibrium between the phases. Adsorption of the chemical contaminant to the soil is also included. This code was specifically developed for simulating steam injection for the removal of nonaqueous fluids from shallow subsurface formations.

The three-dimensional simulator developed by *Sleep and Sykes* [1993a, b] considers the fate of a three-phase fluid system in isothermal subsurface conditions. This model includes the flow of the water, gas, and nonaqueous phases, partitioning of an arbitrary number of organic and inorganic species between these phases, and the transport of species in each of these phases.

The most comprehensive simulator to date has recently been introduced by *Adenekan et al.* [1993]. Their model, Multiphase Multicomponent Nonisothermal Organic Transport Simulator (M<sup>2</sup>NOTS), includes the interphase partitioning described by *Falta et al.* [1992a, b] and *Sleep and Sykes* [1993]. In addition, flow of all three NAPL phases in response to viscous, gravity (dependent on NAPL density), and capillary forces in three-dimensional and arbitrary geometries are included. The nonaqueous phase may consist of any number of user specified chemical components, and each component is allowed to partition into all other phases.

## Multiple Phase Fluid Systems

The movement of nonaqueous phase liquids that are immiscible with water through the subsurface may be tracked in any of four phases [Abriola and Pinder, 1985b]. The contaminant may be tracked: (1) as a distinct nonaqueous phase, (2) as a solute, (3) as a vapor, and (4) as a sorbate on the aquifer solids. All four contaminant phases, as illustrated in Figure 2, are free to exist in the unsaturated zone; however, owing to the absence of air, the vapor phase is excluded in the analysis of the saturated zone. The contaminating liquid is free to partition itself between one or all of the available phases in order to achieve phase equilibrium. The partitioning characteristics of each contaminant (or each constituent of a heterogeneous contaminant such as gasoline) can be determined utilizing Henry's law constant in conjunction with vapor pressure, an experimentally determined aqueous solubility (octanol-water partition coefficient,  $K_{ow}$ ), and the partitioning coefficient based on organic fraction of the aquifer material ( $K_{oc}$ ). For more detailed discussions on partitioning and sorption processes, the reader is referred to *Fetter* [1993].

In addition to partitioning phenomena, there are three basic concepts which govern the flow of immiscible fluids in the subsurface. These include saturation ratio, capillary pressure, and relative permeability.

### *Saturation Ratio*

The saturation ratio is the fraction or percent of the total pore space filled with a particular liquid. The liquid may be NAPL, water, or air, and the interstitial saturations are expressed as  $S_n$ ,  $S_w$ , and  $S_a$ , respectively. The total of all the saturation ratios for all

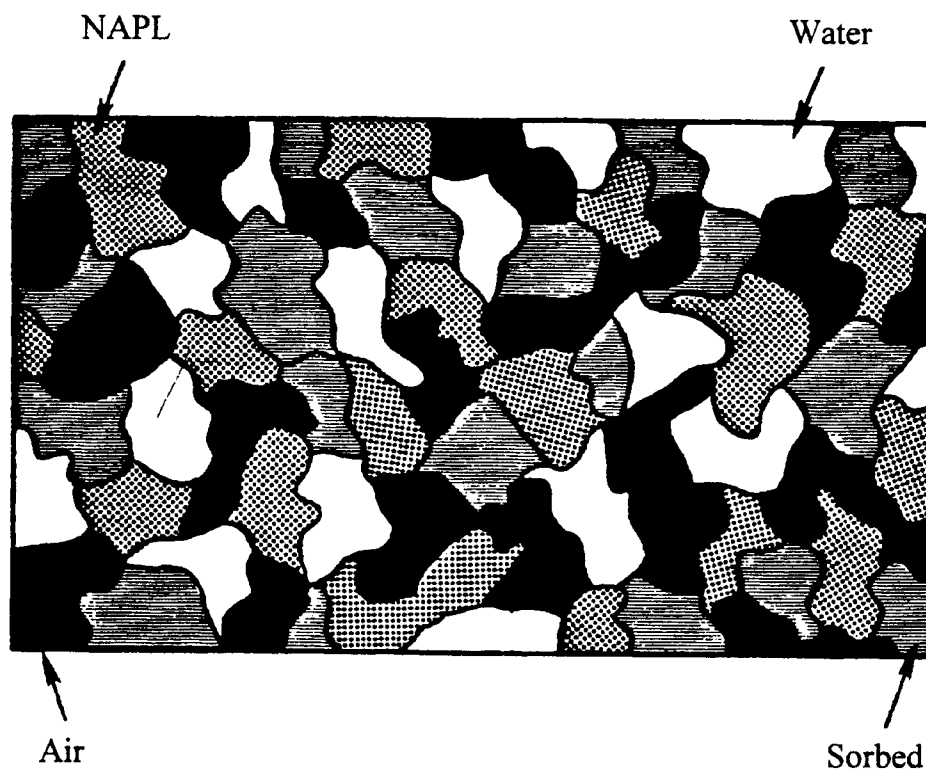


Figure 2. Schematic cross section illustrating a porous media containing four phases, i.e., NAPL, water, air, and sorbed contaminant on framework grains [modified from *Abriola and Pinder, 1985a*].

fluids present must total to one [Fetter, 1993]. That is,

$$S_n + S_w + S_a = 1 \quad (1)$$

### *Capillary Pressure*

If the pore pressures of two immiscible fluids are measured near an interface, different pressures will be noted. That difference is the capillary pressure [Fetter, 1993]. The capillary pressures of interest to contaminant flow modelers are those which occur at the air-NAPL interface in the unsaturated zone, and the NAPL-water interface in the saturated zone [e.g., Faust, 1985; Faust et al., 1989; Guswa, 1985; Osborne and Sykes, 1986]. The expressions used to denote the capillary pressures described above are

$$P_{can} = P_a - P_n \quad (2)$$

$$P_{cnw} = P_n - P_w \quad (3)$$

where  $w$ ,  $n$ , and  $a$  represent the water, nonaqueous, and air phases, respectively,  $p$  is interstitial fluid pressure, and  $p_c$  is the capillary pressure. It is not necessary to define the third capillary pressure, as it is a simple combination of the other two [Peaceman, 1977]

$$P_{caw} = P_a - P_w = P_{can} + P_{cnw} \quad (4)$$

where  $p_{caw}$  is the capillary pressure between air and the wetting-phase fluid, i.e., the water.

The capillary pressure, relative to the saturation of the two immiscible fluids, can be determined experimentally for a given porous medium. The sample is initially water wet, i.e., the saturation of the wetting fluid is 100 percent. The wetting fluid is gradually

displaced from the sample by forcing a nonwetting fluid into the pore space. Because of surface tension and the curvature of the interfaces between the fluids within the small pores, the pressure in the nonwetting fluid is higher than the pressure in the wetting fluid [Peaceman, 1977]. Therefore, as the wetting fluid is "drained" from the sample and the saturation decreases, the capillary pressure will also decrease. Capillary pressure head can then be plotted against the wetting fluid saturation to produce a drainage curve as seen in Figure 3. The saturation at which the wetting fluid can no longer flow under decreasing capillary pressure is referred to as the residual or irreducible wetting saturation ( $S_{wi}$ ). The process is then reversed, displacing the nonwetting fluid with the wetting fluid, increasing the wetting saturation and the capillary pressure. The resulting plot is called an imbibition or wetting curve. When the imbibition curve reaches zero capillary pressure, some of the nonwetting fluid will remain in the porous media. The remaining nonwetting fluid is known as the irreducible or residual nonwetting fluid saturation ( $S_{nwr}$ ).

The different pathways observed between the drainage and imbibition curves is referred to as hysteresis. Hysteresis is a function of saturation history, i.e., which fluid initially occupied the pore space. It can also be shown experimentally that the capillary pressure for drainage cycle is greater than the capillary pressure required for imbibition [Corey, 1986].

Little experimental data concerning three-phase capillary pressures for nonaqueous phase liquids appears in the groundwater literature. The available data are primarily concerned with determining relative permeability data for specific organic contaminants. Some current research includes work by *Dane et al.* [1992], *Ferrand et al.* [1990], *Lenhard* [1992], and *Soll et al.* [1993].



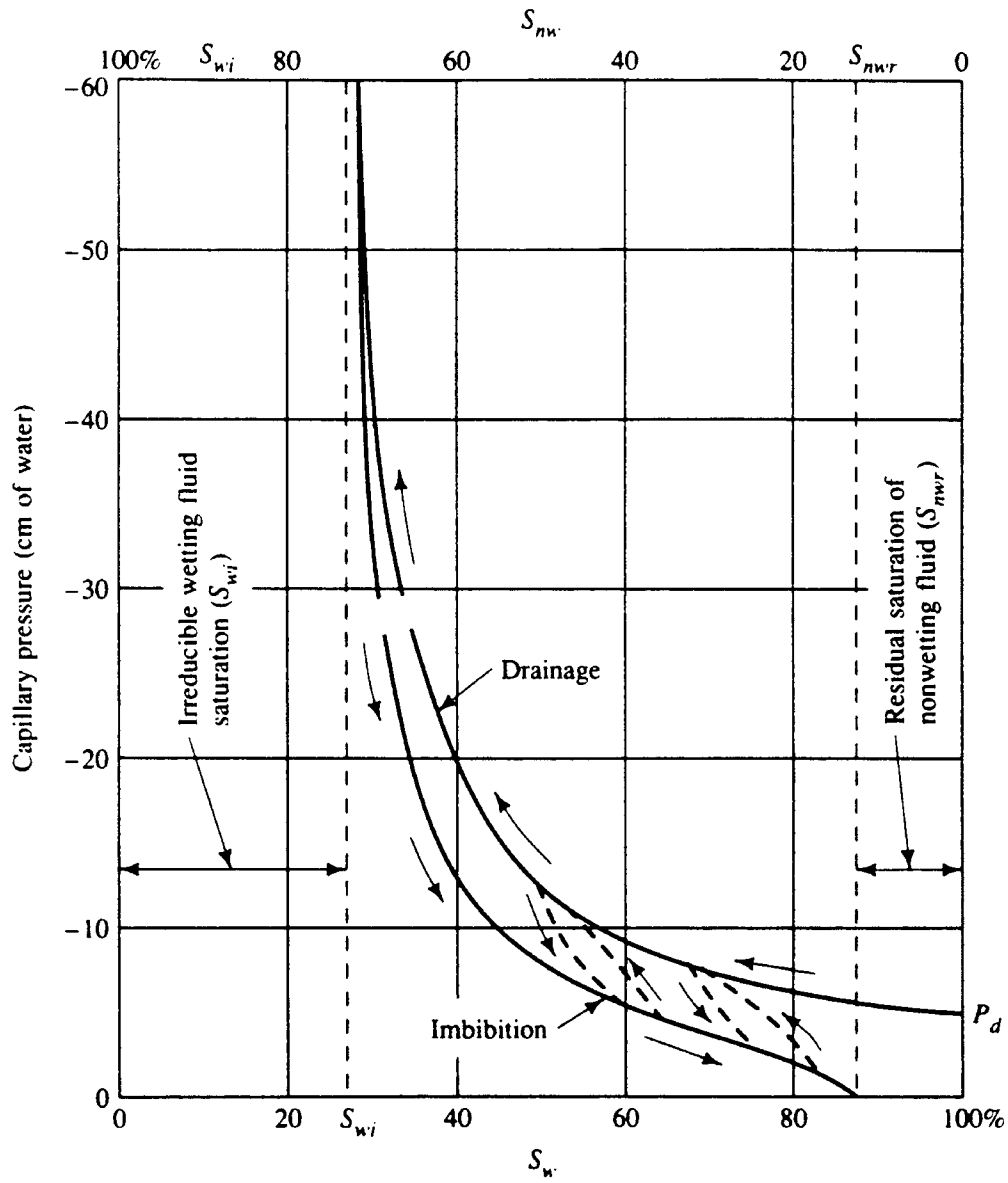


Figure 3. Capillary pressure-wetting fluid saturation for two-phase flow [Fetter, 1993].

### Relative Permeability

As two immiscible fluids flow through a porous media, part of the available pore space will be filled with one fluid and the remainder will be filled with the other. Because the two fluids must compete for pore space through which to flow, the cross-sectional area of the pore available to each fluid now becomes a fraction of the total pore space. The relative permeability is the ratio of the intrinsic permeability for a fluid at a given saturation to the total intrinsic permeability of the rock [Fetter, 1993].

Figure 4 shows two-phase relative permeability curves for a wetting and nonwetting fluid. No flow of the wetting fluid occurs within the irreducible saturation "zone," and the  $S_{wi}$  must be exceeded to initiate flow. The same is true for the residual nonwetting fluid, that is, no flow of the nonwetting phase can occur until the  $S_{nwr}$  is exceeded.

Three-phase relative permeabilities for an air-water-NAPL system are more complex. By obtaining the relative permeabilities for two of the three fluids, the third can be estimated using a procedure devised by Stone [1973]. First, the relative permeability of water,  $k_{rw}$ , as a function of  $S_w$  for a water-NAPL system is determined. Second, the relative permeability of air,  $k_{ra}$ , as a function of  $S_a$  is obtained for an air-NAPL system. Finally, the relative permeability of the nonaqueous liquid,  $k_{rn}$ , in the three-phase system is calculated using equation (5) [Faust, 1985]

$$k_{rn} = k_{rnw}^* \left[ \left( \frac{k_{rnw}}{k_{rnw}^*} + k_{rw} \right) \left( \frac{k_{rna}}{k_{rnw}^*} + k_{ra} \right) - (k_{rw} + k_{ra}) \right] \quad (5)$$

where  $k_{rnw}^*$  is the relative permeability of NAPL at the residual saturation of water in a

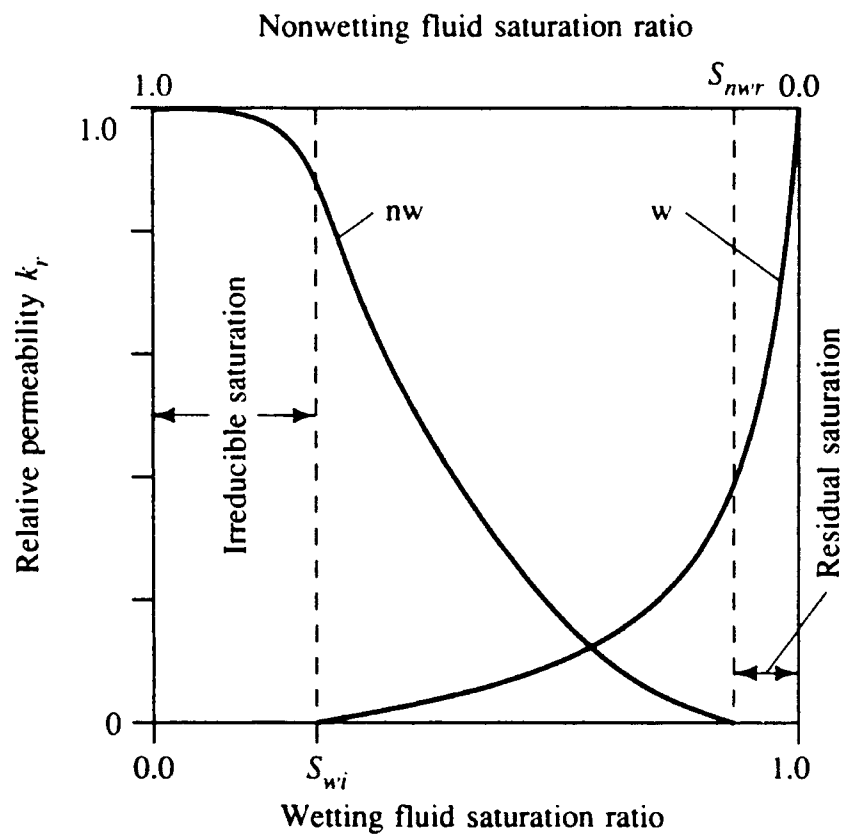


Figure 4. Typical relative permeability curves for a two-phase system [Fetter, 1993].

water-NAPL system,  $k_{rnw}$  is the relative permeability of the NAPL for a water-NAPL system as a function of  $S_w$ , and  $k_{rna}$  is the relative permeability of NAPL in an air-NAPL system as a function  $S_a$ . Figure 5 is a ternary plot of the relative permeability for a NAPL in an air-water-NAPL system, i.e., the unsaturated zone, where water is the wetting fluid.

Experimental data and empirical relationships concerning three-phase relative permeabilities have long been employed in the recovery of crude oil [e.g., *Corey et al.*, 1956; *Land*, 1968; *Snell*, 1962; *Stone*, 1973]; however, comparatively little information is available on these data for organic liquid contaminants [e.g., *Demond and Roberts*, 1993].

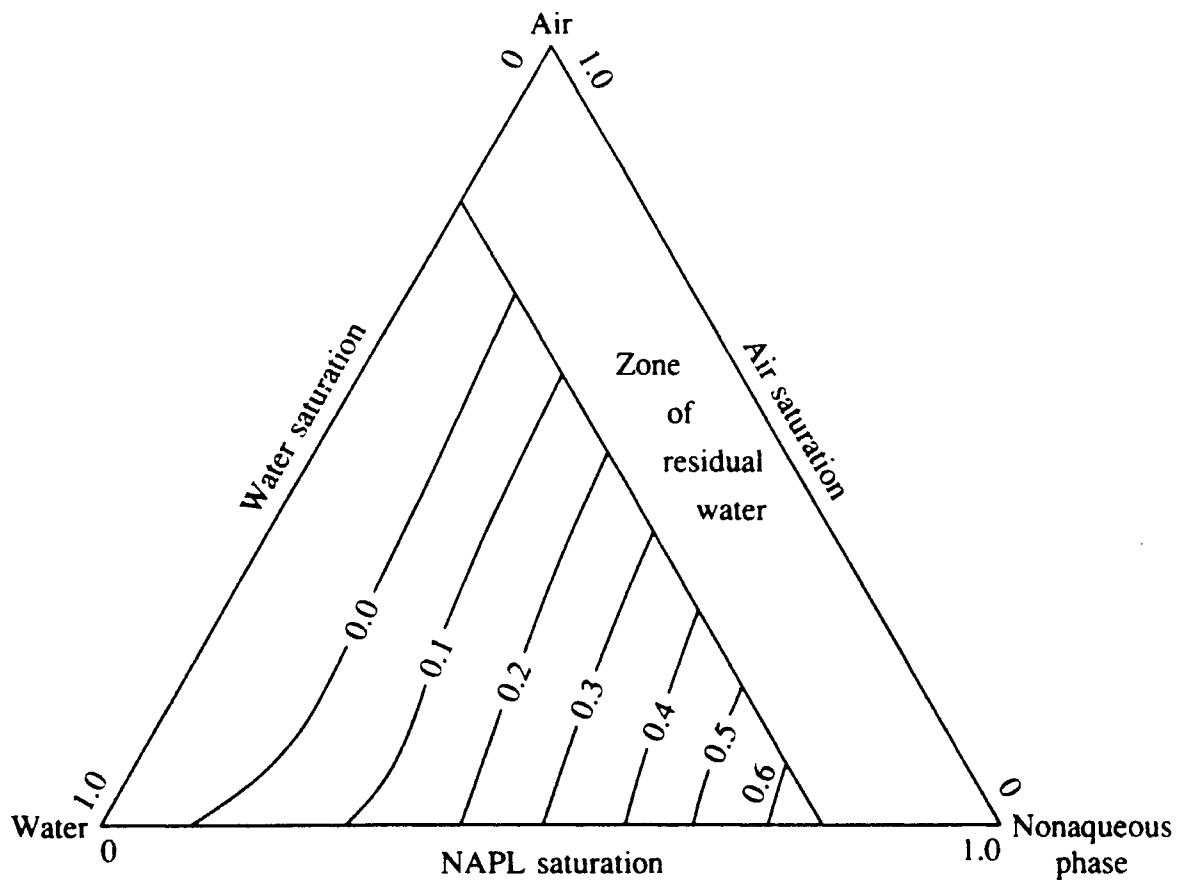


Figure 5. Ternary diagram showing the relative permeability of NAPL in an air-water-NAPL system as a function of saturation [Fetter, 1993].

## EXPERIMENTAL METHODOLOGY

### Research Objectives and Methods Overview

The purpose of this study is to evaluate the infiltration pathways of immiscible nonaqueous phase liquids as functions of fluid density and viscosity. Often, groundwater modelers attempt to simulate the movement of a NAPL accidentally introduced to the subsurface by assuming the NAPL will behave much like the water in the groundwater system. However, the different density and viscosity of the NAPL will result in a dissimilar infiltration pathway. These dissimilarities could impact the design and implementation of a system intended to monitor and recover free product.

This study utilizes numerically simulated cross-sectional flow profiles of nine representative liquids with various densities and viscosities. Table 1 summarizes the liquids and their respective physical constants used in the comparison simulations. For the simulations, all input parameters are kept constant with the exception of NAPL density and viscosity. Simulations were run from the inception of the leak to a time of 10 years. Outputs were produced for one, three, five, and 10 years for each NAPL. Simulated results are plotted and contoured to provide direct visual comparison of the infiltration pathways. Pathway evaluation also includes an examination of vertical and horizontal NAPL migration. The examination of vertical migration is accomplished by comparing breakthrough times at two horizontally-oriented hydrogeologic markers, i.e.,

the groundwater table and the lower draining aquifer. Horizontal migration is evaluated by graphically determining the distance the immiscible plume travels from the source.

TABLE 1. NAPL Density and Viscosity Data\*

NAPL	SWANFLOW Units		Standard Groundwater Units	
	Density (kg/m <sup>3</sup> )	Dynamic Viscosity (kg/m·s)	Specific Gravity (gm/cm <sup>3</sup> )	Dynamic Viscosity (centipoise)
Gasoline	730.0	4.500E-4	0.7300	0.450
Kerosene	810.0	2.050E-3	0.8100	2.050
<i>p</i> -Cymene	857.3	3.402E-3	0.8573	3.402
10W-30 Motor Oil	869.0	1.300E-1	0.8690	130.0
Water	1000.0	1.000E-3	1.0000	1.000
Phenol	1053.3	4.076E-3	1.0533	4.076
<i>o</i> -Nitrotoluene	1162.9	2.370E-3	1.1629	2.370
Trichloroethene	1467.9	5.660E-4	1.4679	0.566
Tetrachloromethane	1584.2	9.690E-4	1.5842	0.969

\*Source: *Mercer et al.* [1990]

### The Numerical Model

The finite-difference model, Simultaneous Water, Air, and Nonaqueous Phase Flow (SWANFLOW), simulates the flow of an immiscible nonaqueous phase fluid under both saturated and unsaturated near-surface conditions [*Faust and Rumbaugh, 1985*]. Mathematical models developed for multiphase simulation are highly nonlinear which result in analytical solutions which are difficult to achieve. Solution techniques for the SWANFLOW model consist of a finite-difference approximation of the differential

equations, the Newton-Raphson method to treat the nonlinearities and to provide faster solution convergence, and the slice successive overrelaxation (SSOR) method for matrix solution [Faust and Rumbaugh, 1985].

### *Governing Equations for Multiphase Flow*

The mathematical description of multiphase flow in porous media is the conservation equation of mass and momentum for each fluid phase present. The equations utilized by the SWANFLOW code are based on a simplification of the conventional three-phase flow equations commonly used in petroleum reservoir simulation intended to simulate three-phase immiscible flow [Faust et al., 1989]. The three equations are

$$\nabla \left[ \frac{k \rho_w k_{rw}}{\mu_w} (\nabla p_w - \rho_w g \nabla D) \right] + q_w = \frac{\partial (\phi \rho_w S_w)}{\partial t} \quad (6)$$

$$\nabla \left[ \frac{k \rho_n k_{rn}}{\mu_n} (\nabla p_n - \rho_n g \nabla D) \right] + q_n = \frac{\partial (\phi \rho_n S_n)}{\partial t} \quad (7)$$

$$\nabla \left[ \frac{k \rho_a k_{ra}}{\mu_a} (\nabla p_a - \rho_a g \nabla D) \right] + q_a = \frac{\partial (\phi \rho_a S_a)}{\partial t} \quad (8)$$

where the subscripts  $w$ ,  $n$ , and  $a$  denote the water, nonaqueous phase, and air constituents, respectively;  $k$  is the intrinsic permeability tensor ( $L^2$ );  $\rho$  is the fluid density ( $M/L^3$ );  $k_r$  is the fluid relative permeability (*dimensionless*);  $\mu$  is the fluid dynamic viscosity ( $M/LT$ );  $p$  is the fluid pressure ( $M/LT^2$ );  $g$  is the gravitational constant ( $L/T^2$ );  $D$  is the depth ( $L$ );  $q$  is the mass source/sink rate ( $M/T$ );  $\phi$  is the porosity of the medium (*dimensionless*);  $S$  is



the volumetric saturation (*dimensionless*);  $\nabla$  is the differential operator; and  $t$  is time ( $T$ ). The above equations include 16 dependent variables in the general case [Peaceman, 1977].

### *Constitutive Relationships*

Five constitutive relationships encompassing an additional 13 independent relationships are necessary to obtain a solution to the flow equations described above. The five most general relationships include:

(1) The volumetric saturations of all three phases total to one--one relationship (see equation 1)

(2) Densities and viscosities are functions of phase pressures--six relationships. For the shallow systems in which most contaminated groundwater is encountered, it is appropriate to assume densities and viscosities are pressure independent [Faust and Rumbaugh, 1985].

(3) The relative permeabilities are functions of saturations--three relationships.

(4) The capillary pressures are functions of saturations--two relationships (see equations 2 and 3).

(5) porosity is a function of pressure for both the unsaturated and saturated zones--one relationship (see equation 19).

### *Final Multiphase Flow Equations*

Equations (6), (7) and (8) are further simplified by assuming the pressure gradients in the air phase are negligible and are at atmospheric conditions. This eliminates the need for equation (8) and allows for the reformulation of (6) and (7) in terms of NAPL

pressure ( $p_n$ ) and water saturation ( $S_w$ ) using the relationships defined in equations (1), (2), and (3). The final governing partial differential flow equations can now be expressed as

$$\nabla \left[ \frac{k \rho_w k_{rw}}{\mu_w} (\nabla p_n - \rho_w g \nabla D) \right] - \nabla \left[ \frac{k \rho_w k_{rw}}{\mu_w} \nabla p_{cnw} \right] + q_w = \frac{\partial (\phi \rho_w S_w)}{\partial t} \quad (9)$$

$$\nabla \left[ \frac{k \rho_n k_{rn}}{\mu_n} (\nabla p_n - \rho_n g \nabla D) \right] + q_n = \frac{\partial (\phi \rho_n (1 - S_w - S_a))}{\partial t} \quad (10)$$

where  $p_{cnw}$  is the capillary pressure between NAPL and water (see equation 3).

### *Finite-Difference Formulation*

The three-dimensional model is based on a finite-difference scheme utilizing a block centered grid that allows for variable spacing and approximation of irregular geometries. The Cartesian grid does not need to be aligned horizontally, permitting the simulation of sloping aquifers. The implicit finite-difference approximations of equations (9) and (10) are given by

$$\Delta \left( T_w^{t+\Delta t} \Delta p^{t+\Delta t} \right) - \Delta \left( T_{wg}^{t+\Delta t} \Delta D \right) - \Delta \left( T_w^{t+\Delta t} \Delta p_{cnw}^{t+\Delta t} \right) + q_w^{t+\Delta t} = \frac{V_b}{\Delta t} \left( M_w^{t+\Delta t} - M_w^t \right) \quad (11)$$

$$\Delta \left( T_n^{t+\Delta t} \Delta p^{t+\Delta t} \right) - \Delta \left( T_{ng}^{t+\Delta t} \Delta D \right) + q_n^{t+\Delta t} = \frac{V_b}{\Delta t} \left( M_n^{t+\Delta t} - M_n^t \right) \quad (12)$$

where  $q_n$  and  $q_w$  are the accumulation terms for NAPL and water ( $M/T$ ), respectively, and  $V_b$  is the grid block volume ( $L^3$ ). The transmissibility terms are defined as

$$T_w = \left( \frac{kA}{L} \right) \frac{\rho_w k_{rw}}{\mu_w} \quad (13)$$

$$T_{wg} = \left( \frac{kA}{L} \right) \frac{\rho_w^2 g k_{rw}}{\mu_w} \quad (14)$$

$$T_n = \left( \frac{kA}{L} \right) \frac{\rho_n k_{rn}}{\mu_n} \quad (15)$$

$$T_{ng} = \left( \frac{kA}{L} \right) \frac{\rho_n^2 g k_{rn}}{\mu_n} \quad (16)$$

where  $T_w$  is the transmissibility of water,  $T_{wg}$  is the transmissibility of water under the influence of gravity required for the unsaturated zone,  $T_n$  is the transmissibility of NAPL,  $T_{ng}$  is the transmissibility of NAPL incorporating the gravitational constant,  $A$  is the cross-sectional area perpendicular to the direction of flow, and  $L$  is the length increment in the flow direction. The mass terms are defined as

$$M_w = \rho_w \phi S_w \quad (17)$$

$$M_n = \rho_n \phi (1 - S_w - S_a) \quad (18)$$

where  $M_w$  and  $M_n$  are the mass per unit volume of water and NAPL, respectively ( $M/L^3$ ).

### *Assumptions and Limitations*

The major assumptions incorporated into the SWANFLOW code include the following.

1. The pressure in the air phase is constant and equal to atmospheric pressure.

2. Water and NAPL viscosity are pressure independent.
3. Water and NAPL density are pressure independent.
4. The relative permeability of water is a function of water saturation.
5. The relative permeability of NAPL is a function of air and water saturation.
6. Capillary pressure is a function of water saturation.
7. Air saturation is a function of NAPL pressure.
8. Porosity is a linear function of pressure.
9. Flow is in a porous medium.
10. Darcy's equation for multiphase flow is valid.
11. Intrinsic permeability is a function of space.
12. There is no interphase mass transfer, e.g., NAPL cannot dissolve in water.

Limitations which must be considered before applying the SWANFLOW code to a specific site are as follows.

1. Transport of the air phase cannot be modeled.
2. Transport of dissolved NAPL is not considered.
3. The model cannot treat highly pressurized systems, such as petroleum reservoirs, where the viscosity and density of the three phases are a function of pressure.

Confined conditions can be simulated.

4. Fractured systems cannot be modeled unless the size of the model's grid blocks is much larger than the scale of the individual fractures.

Many of the recently developed numerical models, e.g., *Falta et al.* [1992a, b], *Sleep and Sykes* [1993a, b], *Adenekan et al.*, [1993], consider many of these limitations which are imposed on the SWANFLOW code. These numerical codes are written to

include such components as dissolved phase transport, vapor phase transport, and interphase mass transfer, in addition to flow modeling of the immiscible nonaqueous phase. However, as the complexity of the model increases, the data sets required to operate them becomes increasingly more comprehensive. In some instances, the necessary input data may not be readily available, and may require experimental derivation. Although SWANFLOW may appear simplistic in comparison, it is actually a complex, sophisticated model which affords the user valuable, useful information from input data which are readily available. This is provided the user understands and considers the assumptions and limitations listed above.

### SWANFLOW Input Parameters

The SWANFLOW code can accommodate any consistent set of units within the input files. However, this often results in abandoning the more "standard" groundwater units commonly used in industry. For the reader's convenience, conversions between the standard units and the units used in the input data files are provided.

#### *Hydrogeologic Setting*

The hydrogeologic setting for the simulations involves an undetected surface leak of a nonaqueous phase liquid onto a stratigraphic unit considered to be an aquitard [Huyakorn *et al.*, 1983]. Thickness of this aquitard remains constant across the study area and extends to a depth of 4.75 meters below the ground surface. The water table occurs at a depth of 1.5 meters, resulting in both saturated and unsaturated conditions within the aquitard. The influence of the capillary fringe on fluid migration is not included in the

SWANFLOW code, and a sharp boundary between the unsaturated and saturated zones is assumed to exist. Immediately below is the aquifer which provides a local source of drinking water. Since the aquifer drains the overlying aquitard, any NAPL leakage into the aquifer will likely impact the quality of the drinking water. Only the upper most 0.25 meters of the aquifer is included in the simulation (Figure 6). Groundwater flow velocity is negligible and not considered in the simulation.

The porosity of the media is related to interstitial fluid pressure and aquifer compressibility by means of the following expression

$$\phi = \phi^{\circ} [1 + c_r (p - p^{\circ})] \quad (19)$$

where  $\phi^{\circ}$  is the porosity at the reference pressure,  $p^{\circ}$ , and  $c_r$  is the aquifer compressibility. The reference porosity is 0.3 at the reference pressure 0.0 N/m<sup>2</sup> which occurs at the groundwater table. Aquifer compressibility is 1.0E-15 m<sup>2</sup>/N. Intrinsic permeability ( $k$ ) is equivalent for the  $x$ -,  $z$ -, and  $y$ -directions at 10<sup>-12</sup> m<sup>2</sup>, and remains constant throughout the aquifer and the aquitard.

Table 2 and Figure 6 summarize the hydrogeologic parameters used in the simulations.

### *Initial Conditions*

The natural recharge rate, NAPL source rate, initial water saturations, and initial interstitial NAPL pressures are assumed as initial conditions before contaminant leakage occurred.

The natural recharge rate, resulting from rainfall within the study area, is 3.94 in/yr (3.17E-6 kg/s/m<sup>2</sup>) [Huyakorn et al., 1983].

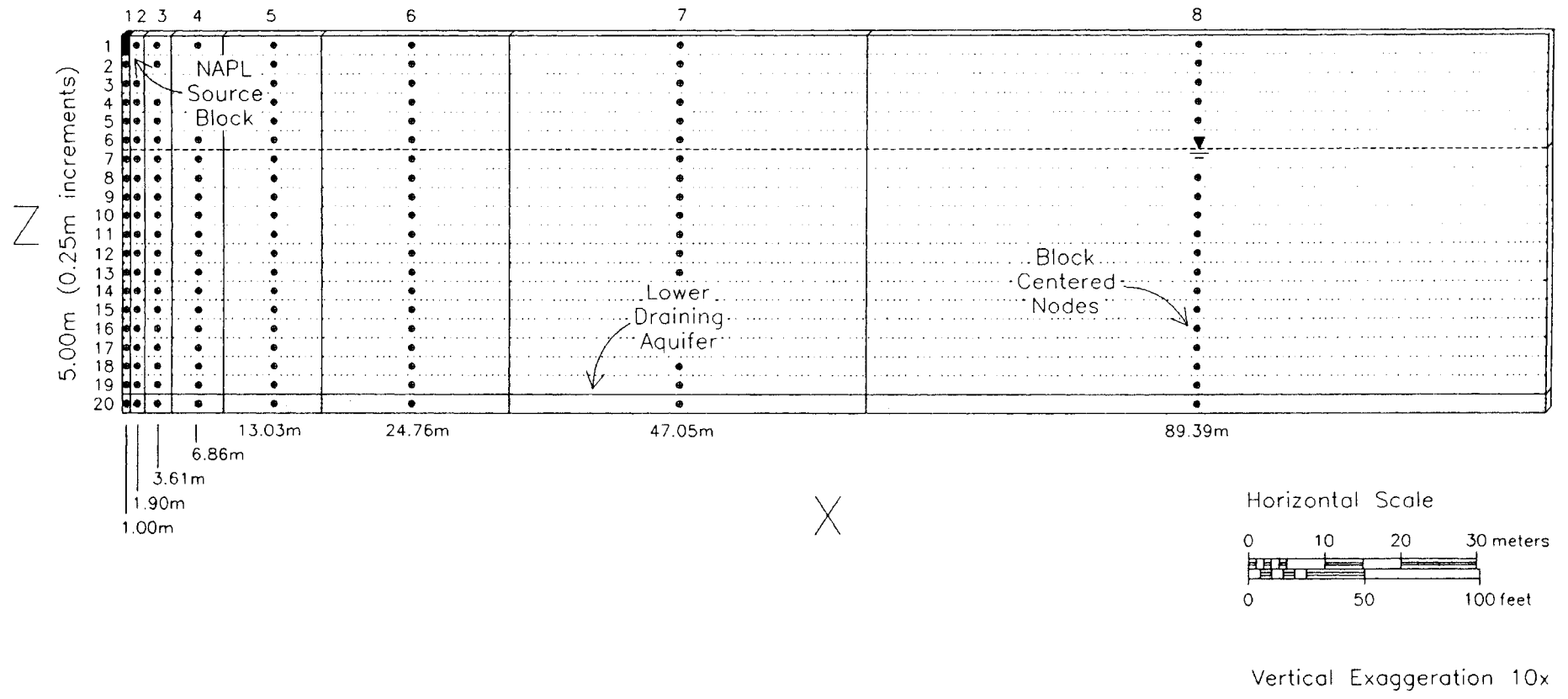


Figure 6. Finite-difference grid showing locations of the NAPL source block, the lower, draining aquifer, and the block-centered grid nodes.

TABLE 2. Hydrogeologic Parameters

Property	SWANFLOW Model Units
Total Aquitard Thickness	4.75 m
Represented Aquifer Thickness	0.25 m
Depth to Groundwater	1.50 m
Reference Porosity ( $\phi^o$ )	0.30
Reference Pressure ( $p^o$ )	0.00 N/m <sup>2</sup>
Intrinsic Permeability ( $k$ )	1.00E-12 m <sup>2</sup>
Hydraulic Conductivity ( $K$ )	0.84 m/d
Media Compressibility ( $c_p$ )	1.00E-15 m <sup>2</sup> /N

The nonaqueous phase liquid is introduced to the system as a continuous source at grid block ( $x=1, z=1$ ) (Figure 6) at a rate of 300 gal/yr ( $3.60\text{E-}8 \text{ m}^3/\text{s}$ ). The SWANFLOW code requires entry of the NAPL source term into the input file as spill mass per unit time (kg/s), which is a function of spill volume and NAPL density.

The initial volumetric water saturations are based on a yearly averaged soil moisture profile of the contamination site which was originally described by *Huyakorn et al.* [1983]. The saturation profile is assumed to be a steady-state condition, which is dependent on the natural recharge in the area of the spill site. The volume of water entering the system through natural recharge is equivalent the volume lost through the base of the finite-difference grid. Within the unsaturated zone, water saturations uniformly increased with depth at a rate of 7.5% per meter and range in value from approximately 84% at the surface to a maximum of 100% at the water table. Below the water table, within the saturated zone, initial volumetric water saturations are constant at



100% (Table 3).

Initial interstitial NAPL pressures are equivalent to the hydrostatic pressure head, which is a function of the distance above or below the water table, the gravitational constant, and the density of water. Within the unsaturated zone, pressure heads are negative, i.e., suction head, and become more negative with increasing distance from the water table. Suction head is the results from the down-flow of the natural recharge water through the unsaturated zone. Likewise, pressure heads are positive in the saturated zone and increase with increasing depth into the saturated zone depth. Pressure at the water table is zero and is uniform in each horizontal layer. The initial conditions are assumed to have been in effect at the time the simulation began, that is, before the spill occurred.

#### *Relative Permeability and Capillary Pressure*

The relative permeability and capillary pressure data utilized in the simulations were derived by *Guswa* [1985], and are representative of the relative permeabilities observed in a two-phase water-nonaqueous phase system, and a two-phase nonaqueous phase-air system for a fine sand matrix. Three-phase relative permeabilities are determined by SWANFLOW using the data in Table 4 and equation (5).

#### *Numerical Model Discretization Data*

The two-dimensional finite-difference grid extends 187.60 meters from the source in the positive  $x$ -direction and 5.00 meters vertically-downward in the  $z$ -direction, discretizing the cross section into 160 blocks. The  $x$ -coordinate is divided into eight unequal "columns" which increase in size by a factor of 1.9 in the positive  $x$ -direction. Although not represented in the finite-difference grid, SWANFLOW assumes the grid is

TABLE 3. Initial Conditions

Property	SWANFLOW Units	Standard Groundwater Units
Natural Recharge	3.17E-6 kg/s/m <sup>2</sup>	3.94 in/yr
NAPL Source Rate*	3.60E-8 m <sup>3</sup> /s	300 gal/yr

Depth (m)	Water Saturation (decimal %)	NAPL Pressure (N/m <sup>2</sup> )
0.125	0.850	-14,700
0.375	0.875	-12,250
0.625	0.900	-9,800
0.875	0.925	-7,350
1.125	0.950	-4,900
1.375	0.975	-2,450
1.625	1.000	0
1.875	1.000	2,450
2.125	1.000	4,900
2.375	1.000	7,350
2.625	1.000	9,800
2.875	1.000	12,250
3.125	1.000	14,700
3.375	1.000	17,150
3.625	1.000	19,600
3.875	1.000	22,000
4.125	1.000	24,500
4.375	1.000	26,950
4.625	1.000	29,400
4.875	1.000	31,850

\*The units of NAPL source rate required by SWANFLOW are actually kg/s.

TABLE 4. Capillary Pressure and Relative Permeability Data\*

Capillary Pressure (N/m <sup>2</sup> )	Water Saturation (decimal %)	Two-Phase Relative Permeabilities	
		Water	NAPL
103425.0	-0.10	0.00	1.00
103425.0	0.00	0.00	1.00
103425.0	0.10	0.00	0.82
103425.0	0.20	0.00	0.68
27580.0	0.30	0.04	0.55
10343.0	0.40	0.10	0.43
7585.0	0.50	0.18	0.31
7447.0	0.60	0.30	0.20
7309.0	0.70	0.44	0.12
7171.0	0.80	0.60	0.05
7033.0	0.90	0.80	0.00
6895.0	1.00	1.00	0.00
6895.0	1.10	1.00	0.00

Capillary Pressure (N/m <sup>2</sup> )	Air Saturation (decimal %)	Two-Phase Relative Permeabilities	
		NAPL	Air
-98000.0	1.00	-0.32	1.00
0.0	0.00	0.68	0.00

\*Source: *Guswa* [1985]

symmetrical; therefore, negative  $x$  values can be implied and presumed equivalent to the simulated values generated for the positive  $x$  segment. The  $z$ -coordinate is equally divided into 20 "layers" each 0.25 meters in length (Figure 6). The simulation is considered quasi three-dimensional given a  $y$ -direction that is defined by one "slice" having a width of one meter. Although the third dimension, i.e., the  $y$ -direction, is not fully represented by the finite-difference grid, SWANFLOW calculates fluid movement as though the third dimension were included. Fluids are free to enter and exit the grid. NAPL and water mass balances are calculated at each time step to check for proper fluid distributions.

Time steps within SWANFLOW are regulated by the maximum allowable saturation change which can occur during each time step. Maximum saturation change values range from 7.5-10% (0.075-0.010), and depend on the NAPL being simulated (Appendix A).

## DISCUSSION OF SIMULATION RESULTS

As previously stated, the goal of this study is to examine the influence of gravitational forces, i.e., the density difference between water and the nonaqueous phase, as well as the impact of viscous forces, on the infiltration of an immiscible nonaqueous phase liquid into an aquitard/aquifer system.

The nine liquids used in the following simulations (Table 1) were selected not only for their common occurrence at contaminated sites, but also for the wide range of density and viscosity values they possess. The liquids can be divided into three categories: (1) less-dense-than-water nonaqueous phase liquids (LNAPL), (2) more-dense-than-water nonaqueous phase liquids (DNAPL), and (3) water. The water was treated in the same manner as an infiltrating NAPL, i.e. an immiscible fluid, and was included for comparison purposes and as a benchmark.

As indicated, the SWANFLOW code does not consider dissolution or volatilization and provides a conservative estimate of the extent of NAPL migration. For a highly volatile NAPL such as gasoline, any contaminant which migrates to a position at or near the ground surface will likely vaporize and enter the atmosphere. The volatilization of gasoline will effectively reduce saturation levels. However, the numerical model does not consider for losses resulting from NAPL volatilization. Also, contaminants which are relatively soluble, such as phenol, would experience a loss of mass as the NAPL dissolves

into the surrounding groundwater. Again, these are not considered by this model.

Based on the data presented herein, it is suggested that the infiltration of NAPL, especially LNAPL, through the unsaturated zone is strongly influenced by the interstitial pressure, i.e., suction head, of the nonaqueous liquid. If the density of the NAPL is sufficiently low, flow of NAPL from high to low pressure will predominate, and the vertically-driven gravitational flow will be significantly hindered. Moderately dense NAPL will exhibit infiltration pathways containing both pressure and gravity components. In contrast, the flow of DNAPL is gravity dominated, and shows no apparent influence of NAPL pressure gradients.

For the purpose of this study, only NAPL saturations are presented; values are provided in decimal percent unless otherwise indicated. SWANFLOW output also generates water saturation and air saturation data for each time step; however, these data are not treated quantitatively, and only receive qualitative attention. Discussion of the simulation results follows.

### Gasoline

Gasoline represents the least dense of the less-dense-than-water nonaqueous phase liquids which were evaluated in this study. At the start of the simulation, only water and air were present in the system. See Table 3 for initial conditions for the simulations. At time  $t=0$ , gasoline began to infiltrate from a slow, continuous, surficial leak at a rate of 300 gallons per year, indicated in Figure 6 by the shaded grid block (1,1) in the upper left corner of the finite-difference grid. The reader is reminded the quasi three-dimensional nature of the simulations requires that  $y$  always equal 1; therefore, the finite-difference

grid block locations are defined by the  $x$  and  $z$  values only. The gasoline source and natural recharge term remain constant throughout the 10 year duration of the simulation. Simulated output is generated at one, three, five, and 10 years (Appendix B).

Figure 7 displays the numerical model solutions for one and three years. At time  $t=1$  year, gasoline saturation contours range from 0-40%. The greatest saturation of LNAPL present in the domain is 42.5%, and occurs at grid block (1,1) (Appendix B). Water and air have been displaced by the infiltrating gasoline, indicated by a decrease in their respective saturations. Although water is being added to the system as natural recharge, the same amount of water is also exiting through the base of the finite-difference grid, creating the steady-state conditions previously described. Thus, the three phases, gasoline, water, and air, coexist in the available void space. It can be shown experimentally that any pore within the area of spill influence may contain a single phase or any possible combination of the three phases, i.e., NAPL, water, and air [Wilson *et al.*, 1990]. At one year, the contaminant plume has reached the depth of one meter below the ground surface, and extends 30 meters laterally from the source. At time  $t=3$  years, the gasoline plume has expanded, but remains wholly within the unsaturated zone. Therefore, the available porosity may contain any or all three phases, i.e., gasoline, water, air, within the area of spill influence. The LNAPL extends approximately 60 meters laterally from its origin with a maximum depth of 1.3 meters below the ground surface. Saturation contour levels range from 0-40% (Figure 7) with the maximum LNAPL saturation of 46.4%, located at block (1,1) (Appendix B).

Figure 8 provides the numerical solutions for five and 10 years. At time  $t=5$  years, the gasoline plume continues to expand both horizontally and vertically; however,

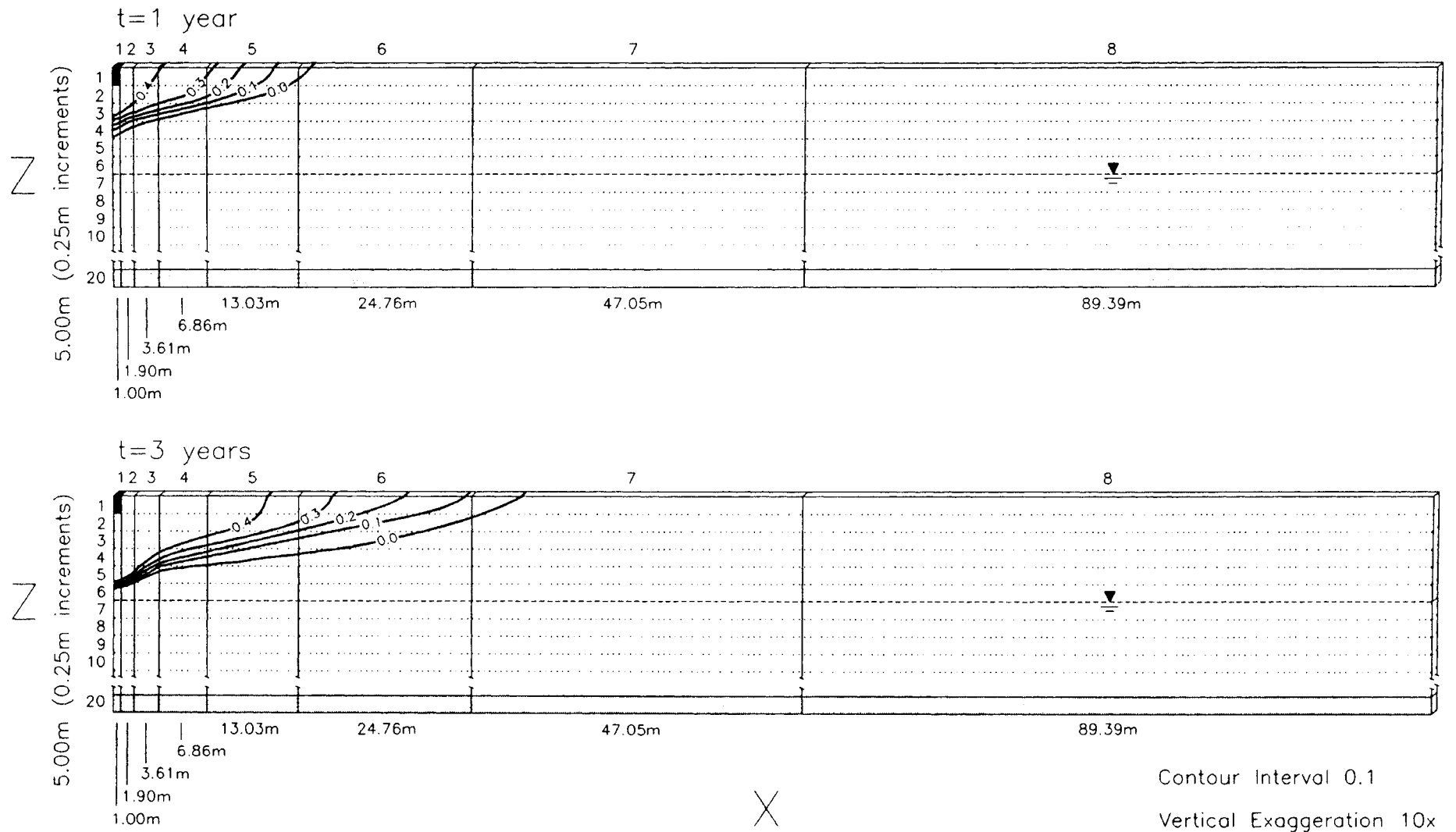


Figure 7. Infiltration of gasoline at one and three years.



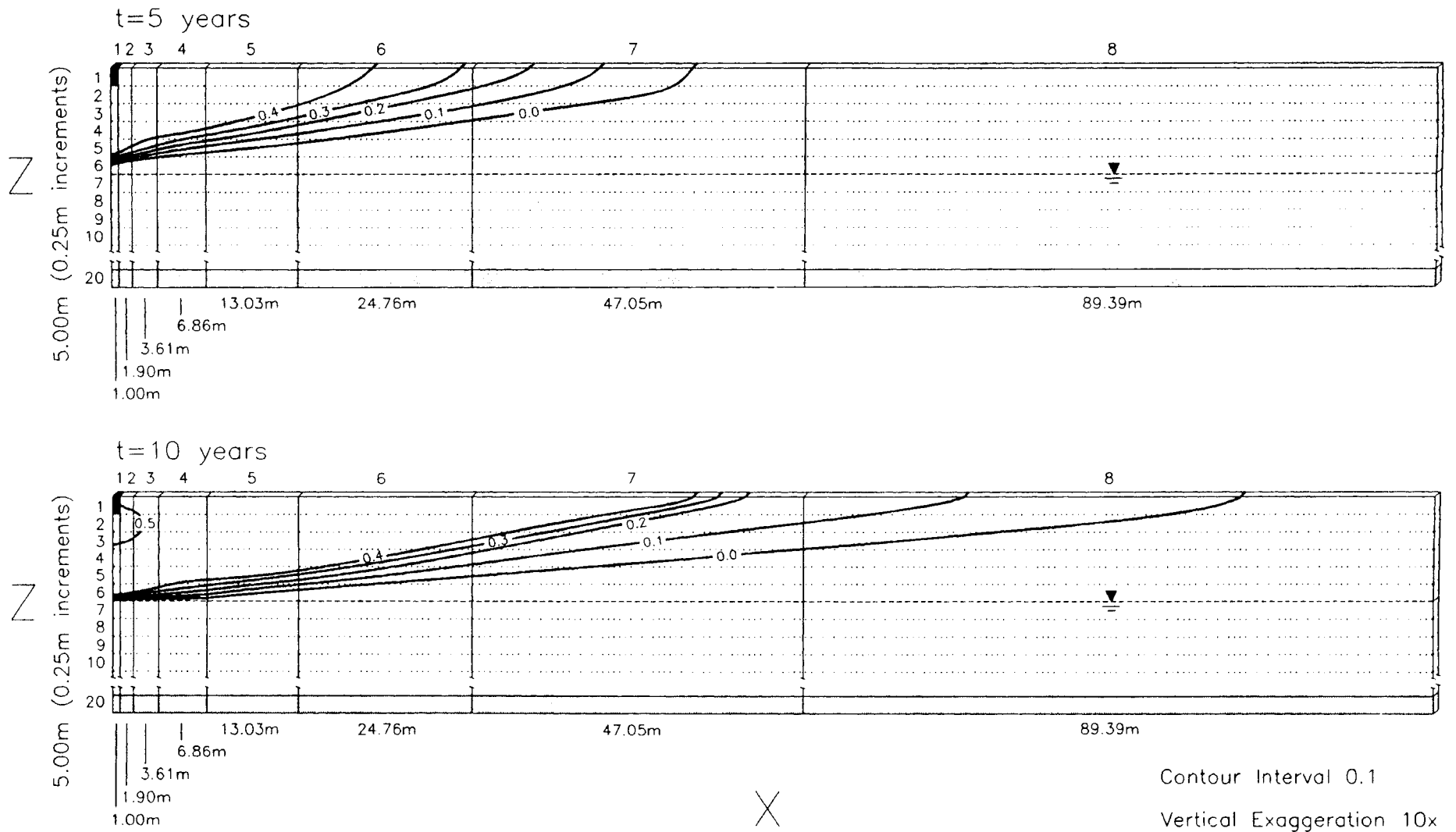


Figure 8. Infiltration of gasoline at five and 10 years.

has yet to break through the water table. The contaminant plume has reached 90 meters laterally from the source, and attained a depth of 1.4 meters below the ground surface. Gasoline saturation contours range from 0-40% with the greatest saturation in the domain at grid block (1,1) having the value 48.1% (Appendix B). As in the previous time steps, water and air within the zone of spill influence has been displaced by the infiltrating gasoline, indicated by the decrease in their respective saturations.

At time  $t=10$  years, the gasoline plume shows still further enlargement in the  $x$ - and  $z$ -directions, extending approximately 175 meters laterally from the source, and has expanded vertically-down to intersect the water table at 1.5 meters; however, no NAPL has entered the saturated zone. Saturation contours range from 0-50% (Figure 8) with the maximum LNAPL saturation of 50.6%, located at block (1,2) (Appendix B).

The infiltration pathway of gasoline produced by the SWANFLOW simulation indicates lateral plume migration to be predominant. Horizontal migration of the gasoline plume has extended 175 meters from the source, while only penetrating to a depth of approximately 1.5 meters after 10 years of simulation. The horizontal movement of the LNAPL is likely the result of capillary pressure effects. The influence of capillary pressure on migration is greater for the less-dense-than-water nonaqueous phase liquids as gravity effects, which result in vertically-downward movement, proportionally decrease as NAPL density decreases. A decrease in the gravitational control on NAPL movement allows other forces, such as capillary pressure, a greater degree of influence on NAPL movement through the subsurface. All of the LNAPL, which has been introduced into the subsurface, remains wholly within the unsaturated zone, although breakthrough into the saturated zone does occur almost immediately after completion of the 10 year

simulation (see subsequent discussion on Vertical and Horizontal NAPL Infiltration Rates). The area of spill influence consists of a variable mixture of gasoline, water, and air. The maximum LNAPL saturation is 50.6%, suggesting the contaminant "lens," commonly referred to in groundwater literature, contains all three phases, and is not represented by 100% NAPL. This application shows that the lens concept may not apply for all possible types of contaminants and hydrogeologic settings. Although field observations often indicate a homogeneous NAPL lens, these observations are typically provided through monitoring wells. However, within the well the capillary forces which influence NAPL movement do not exist. Capillary pressure is a property of the macroscopic geometry of the void spaces in the porous media [Fetter, 1993]. The removal of the pore spaces, i.e., introduction of a well bore, eliminates capillary pressure forces within the affected area. This suggests the well bore is not an accurate representation of the surrounding media, and can be used to explain the differences in lens composition between field observations and the simulated results produced by SWANFLOW.

### Kerosene

Kerosene, like gasoline, is one of the lighter less-dense-than-water nonaqueous phase liquids considered in this study. Initial conditions are identical to those used in the simulation of gasoline and consist of only water and air within the unsaturated zone, and water only within the saturated zone (Table 3). Simulated output is generated at one, three, five, and 10 year intervals.

Figure 9 provides the numerical solutions at one and three years. At time  $t=1$

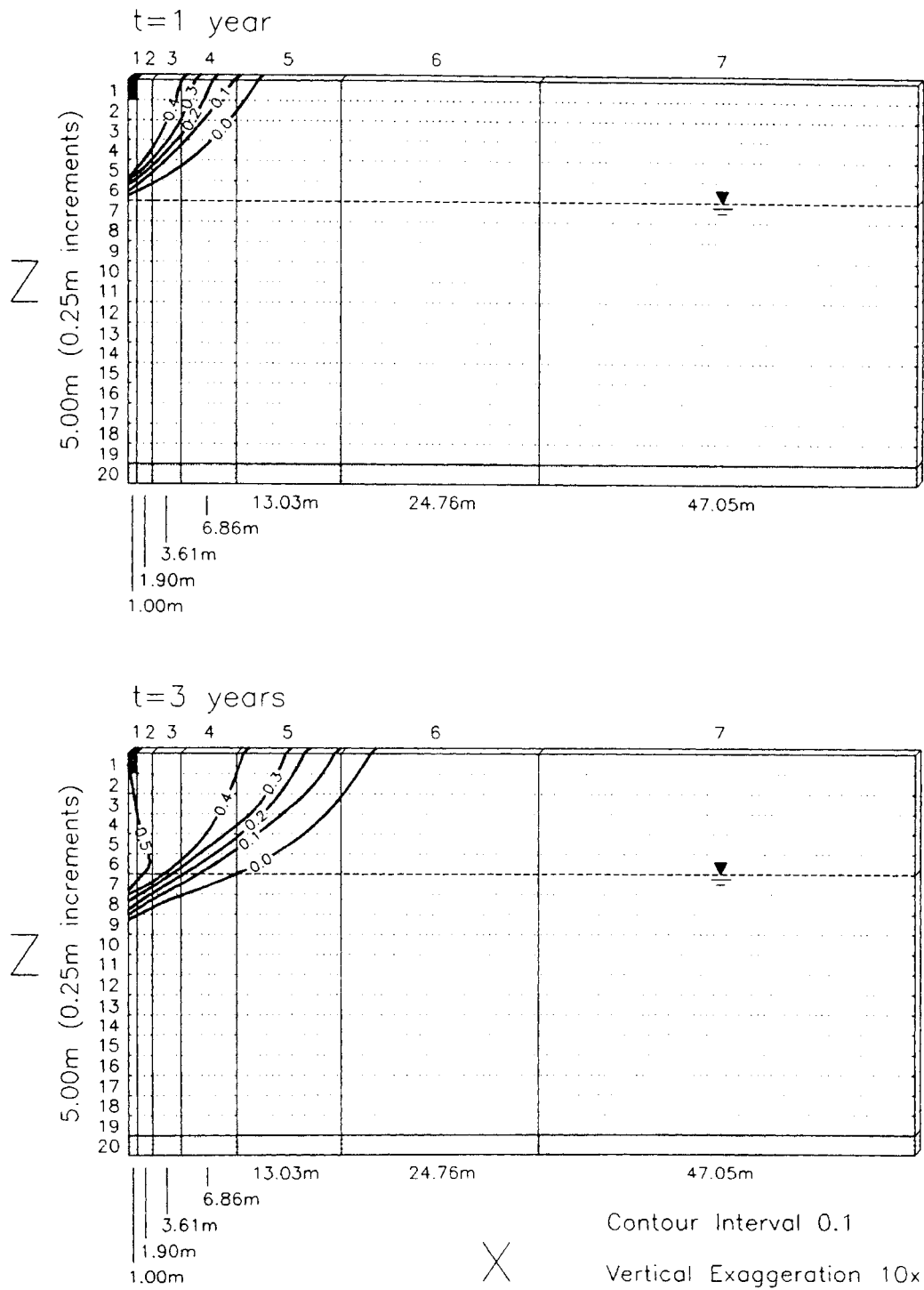


Figure 9. Infiltration of kerosene at one and three years.

year, the contoured kerosene saturation values range from 0-40%. The greatest saturation of LNAPL present in the domain is 49.8%, and occurs at grid block (1,5) (Appendix B). Water and air have been displaced by the infiltrating kerosene, evidenced by a decrease in their respective saturations, and indicate kerosene, water, and air, coexist in the available void space within the area of spill influence. Any pore within the area of spill influence may contain a single phase or any possible combination of the three [Wilson *et al.*, 1990]. At one year, the contaminant plume has reached a maximum depth of 1.4 meters. Lateral plume migration extends approximately 17 meters from the source.

At time  $t=3$  years, the kerosene plume has expanded downward completely through the unsaturated zone and is now partly contained within the saturated zone. Movement into the saturated zone is likely results from the physical depression of the groundwater table due to the overlying mass of the kerosene plume. As before, porosity within the unsaturated zone may contain any or all three phases while the interstices of the saturated zone within the area of spill influence contain water and LNAPL only. The LNAPL extends approximately 32 meters laterally from its origin with a maximum depth of 2.1 meters below the ground surface. Saturation contour levels range from 0-50% (Figure 9) with the maximum LNAPL saturation of 50.6%, located at block (1,6) (Appendix B).

Figure 10 provides the numerical solutions at five and 10 years. At time  $t=5$  years, the kerosene plume continues to expand both horizontally and vertically, enlarging the area of the contaminant influence progressively deeper into the saturated zone. The contaminant plume now extends 45 meters laterally from the source, and has reached a depth of 2.3 meters below the ground surface. Kerosene saturation contours range from

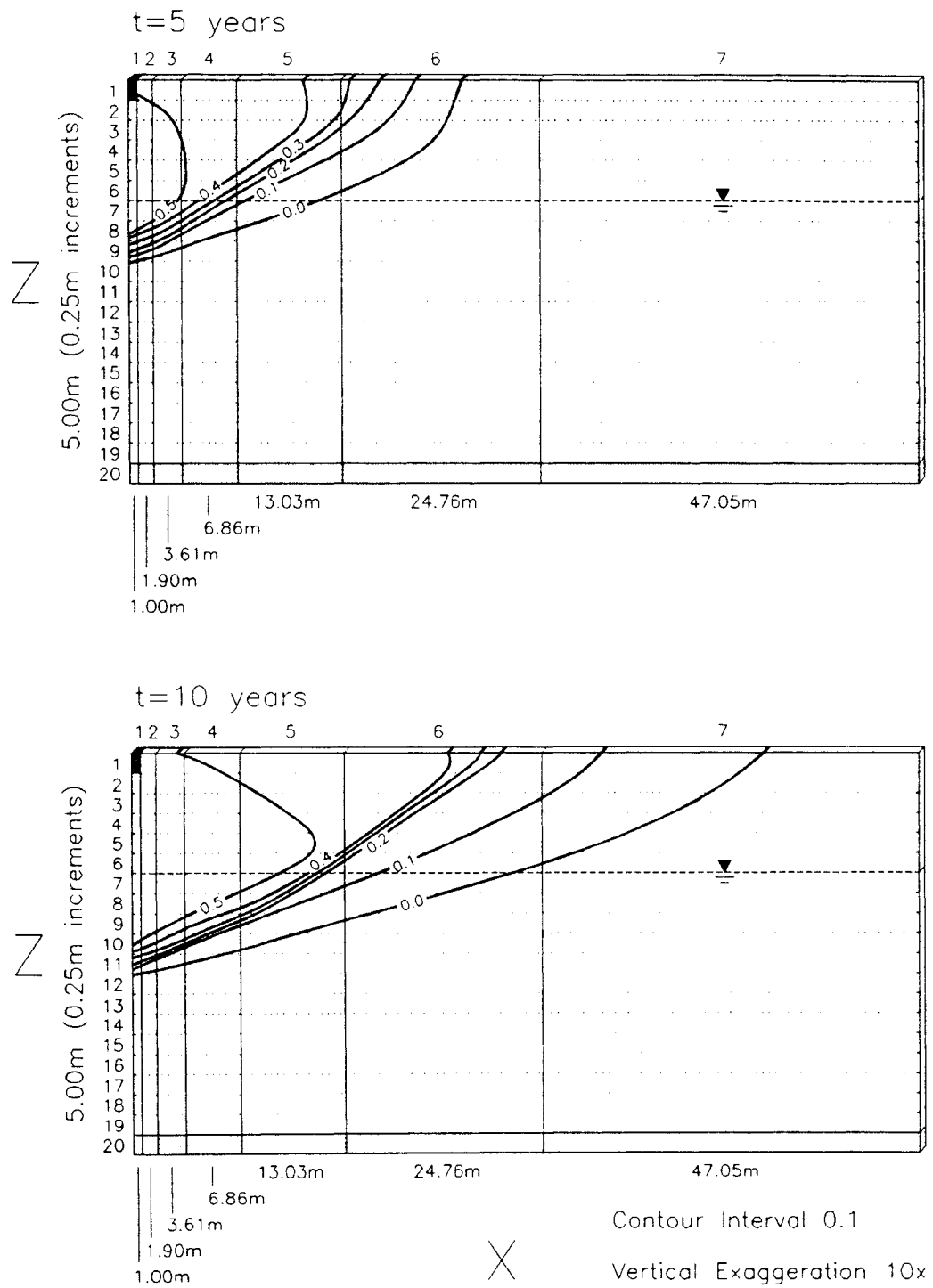


Figure 10. Infiltration of kerosene at five and 10 years.

0-50% (Figure 10) with the greatest saturation in the domain at grid block (1,6), having the value 53.2% (Appendix B).

At time  $t=10$  years, the kerosene plume shows still further enlargement in the  $x$ - and  $z$ -directions, extending approximately 86 meters laterally from the source, and has expanded vertically-downward to 2.8 meters below the ground surface. Saturation contours range from 0-50% (Figure 10) with the maximum LNAPL saturation of 57.0%, located at block (1,6) (Appendix B).

The area of contaminant influence produced by the infiltration of kerosene and generated by SWANFLOW indicates lateral plume migration to be predominant. Horizontal migration of the contaminant plume has a maximum extent of 86 meters from the source, while penetrating only 2.8 meters into the aquitard after 10 years of simulation. The majority of the area of spill influence remains within the unsaturated zone with comparatively less occurring within the saturated zone. Composition of the plume is likely a variable mixture of kerosene, water, and air. The maximum simulated LNAPL saturation is 57.0%, indicating the contaminant "lens" contains all three phases present within the unsaturated zone, and two phases in the saturated zone, air being the absent phase. The contaminant lens does show pooling at and above the water table as would be expected for a less-dense-than-water nonaqueous phase liquid.

#### *p*-Cymene

The LNAPL *p*-cymene [1-methyl-4-(1-methylethyl)-benzene] is slightly more dense than gasoline and kerosene, but still considerably less dense than water. Again, initial conditions are as previously described and consist of water and air. The air phase

found in the unsaturated zone only (Table 3).

Figure 11 displays numerical solutions for one and three years after the initial introduction of *p*-cymene into the aquitard. At time  $t=1$  year, the contoured *p*-cymene saturation values range from 0-40%. The greatest saturation of LNAPL present in the domain is 48.5%, and occurs at grid block (1,6) (Appendix B). A decrease in water and air saturations indicates displacement by the infiltrating *p*-cymene; *p*-cymene, water, and air, coexist in the available void space within the area of spill influence. At one year, the contaminant plume has reached a maximum depth of 1.9 meters below the ground surface. Lateral plume migration extends approximately 12 meters from the source.

At time  $t=3$  years, the *p*-cymene plume extends approximately 27 meters laterally from its origin and has attained a maximum depth of 2.6 meters below the ground surface. Saturation contour levels range from 0-50% (Figure 11) with the maximum LNAPL saturation of 52.7%, located at block (1,6) (Appendix B).

Figure 12 provides the numerical solutions for the output times of five and 10 years. At time  $t=5$  years, the *p*-cymene plume continues to expand both horizontally and vertically, enlarging the area of the contaminant influence still deeper into the saturated zone. The contaminant plume extends 43 meters laterally from the source, and has attained a depth of 2.9 meters below the ground surface. The *p*-cymene saturation contours range from 0-50% (Figure 12) with the greatest saturation in the domain at grid block (1,6), having the value 55.2% (Appendix B).

At time  $t=10$  years, the *p*-cymene plume shows still further enlargement in the  $x$ - and  $z$ -directions, extending approximately 62 meters laterally from the source, and has expanded vertically-downward to 3.5 meters below the ground surface. The maximum



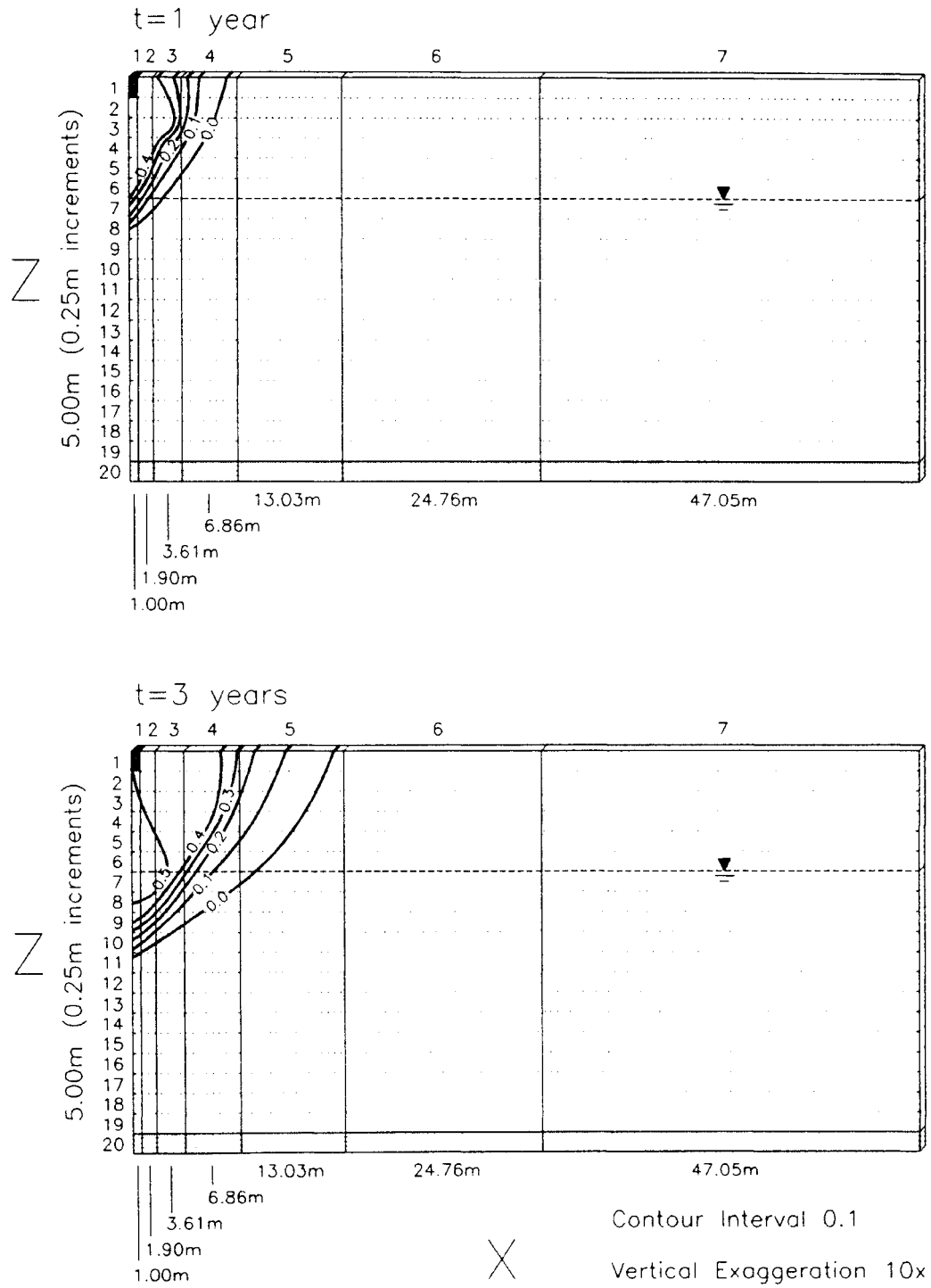


Figure 11. Infiltration of *p*-cymene at one and three years.

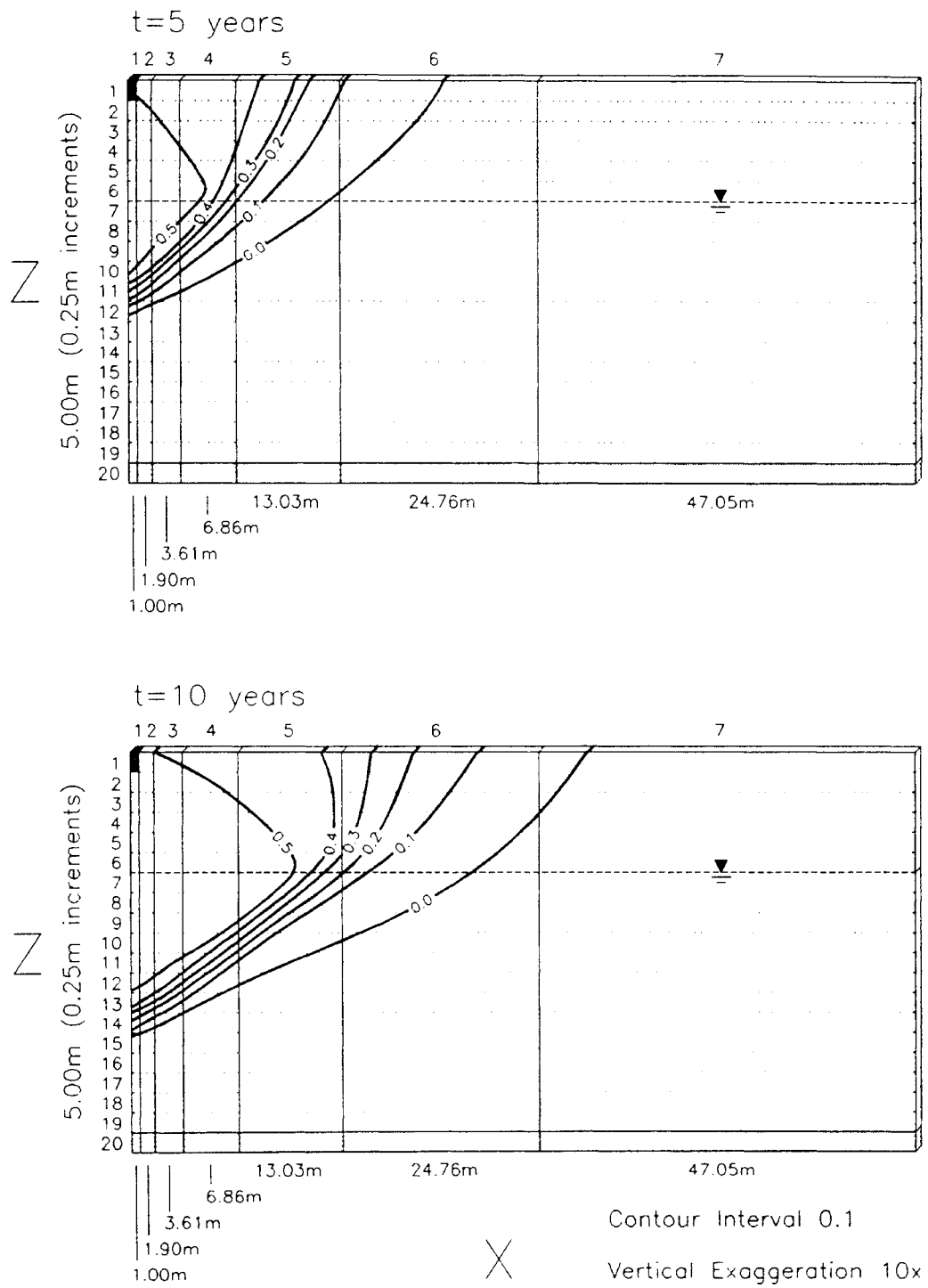


Figure 12. Infiltration of *p*-cymene at five and 10 years.

plume thickness is 3.5 meters directly below the source block. Saturation contours range from 0-50% (Figure 12) with the maximum LNAPL saturation of 58.7%, located at block (1,2) (Appendix B).

The area of contaminant influence produced by the infiltration of *p*-cymene and generated by SWANFLOW indicates lateral plume migration to be predominant. Horizontal migration of the contaminant plume has attained a maximum distance of 62 meters from the source, while penetrating only 3.5 meters into the subsurface at 10 years. The *p*-cymene infiltration event is similar to kerosene, likely due to their nearly equivalent density and viscosity values (see Table 1).

#### 10W-30 Motor Oil

The inclusion of 10W-30 motor oil in this study is to examine the infiltration pathway of a NAPL with a high dynamic viscosity. In the case of motor oil, viscosity is approximately two orders of magnitude greater than *p*-cymene with a nearly equivalent density (Table 1). As with the previous simulations, no NAPL was present in the system at the start of the simulation. Water and air saturations are defined by the initial conditions given in Table 3.

Figure 13 provides the numerical model solutions at one and three years. At time  $t=1$  year, saturation contour levels are given for 0, 20, 40, and 60%. The greatest oil saturation present in the domain is 66.2%, and occurs at grid block (1,1) (Appendix B). Water and air have been displaced by the infiltrating oil in the unsaturated and saturated zones, indicated by a decrease in their respective saturations. At one year, the oil plume has migrated completely through the unsaturated zone and penetrates 1.6 meters into the

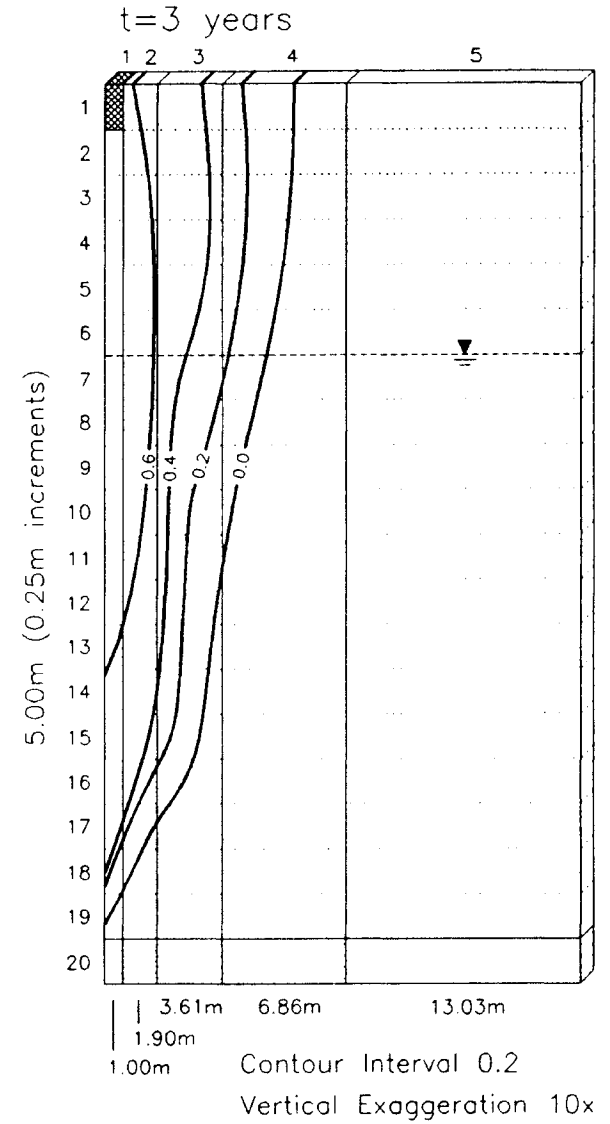
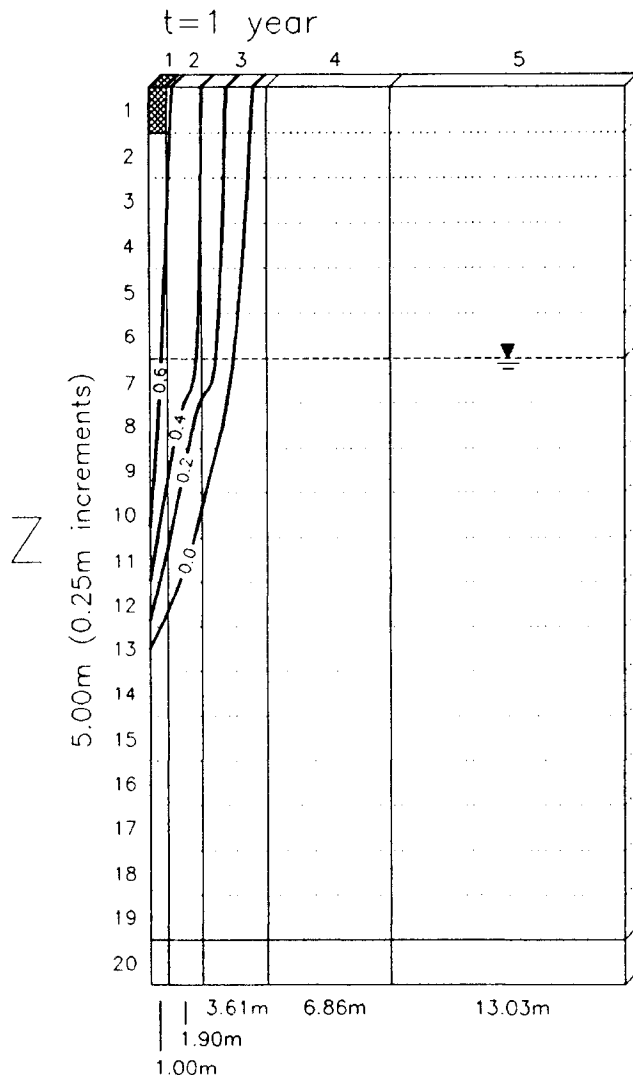


Figure 13. Infiltration of 10W-30 motor oil at one and three years.

saturated zone. The area of spill influence extends 5.6 meters laterally from the source.

At time  $t=3$  years, the oil plume has expanded both vertically and horizontally.

The plume extends approximately 9.9 meters laterally from its origin with a maximum depth of 4.6 meters below the ground surface. Saturation contour levels range from 0-60% (Figure 13) with maximum oil saturation at grid block (1,1) increasing from 66.2% to 68.9% (Appendix B).

Figure 14 supplies the numerical solutions for five and 10 years. At time  $t=5$  years, the oil plume has expanded horizontally and vertically, and the area of influence produced by oil infiltration has enlarged to include the lower draining aquifer. The introduction of motor oil to the lower aquifer actually occurs at 3.4 years. The contaminant plume is detectable 11.0 meters laterally from the source. The maximum depth exceeds the area of the finite-difference grid and is greater than 5.0 meters in depth. The highest oil saturation reported by the SWANFLOW code occurs at grid block (1,1) and has a value of 70.0%. The highest saturation reported at the aquitard-aquifer interface is 50.6% at block (1,19) (Figure 14, Appendix B).

At time  $t=10$  years, the oil plume shows still further enlargement in the  $x$ -direction and has attained a lateral distance of 20.6 meters from the source. Maximum oil saturation is 70.1% reported at block (1,1). Maximum NAPL saturation reported at the aquitard-aquifer interface is 51.1% at block (1,19), a slight increase over the value reported for the same grid location at five years, suggesting further expansion of the area of spill influence into the lower draining aquifer.

The area of contaminant influence produced by the infiltration of 10W-30 motor oil generated by the SWANFLOW code has decreased horizontally and increased

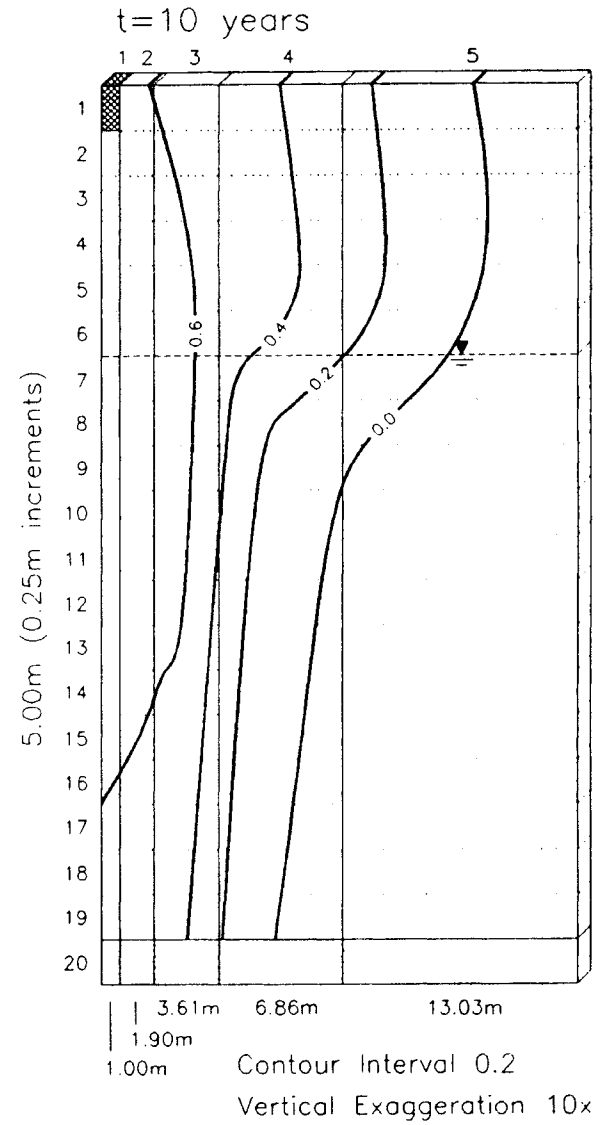
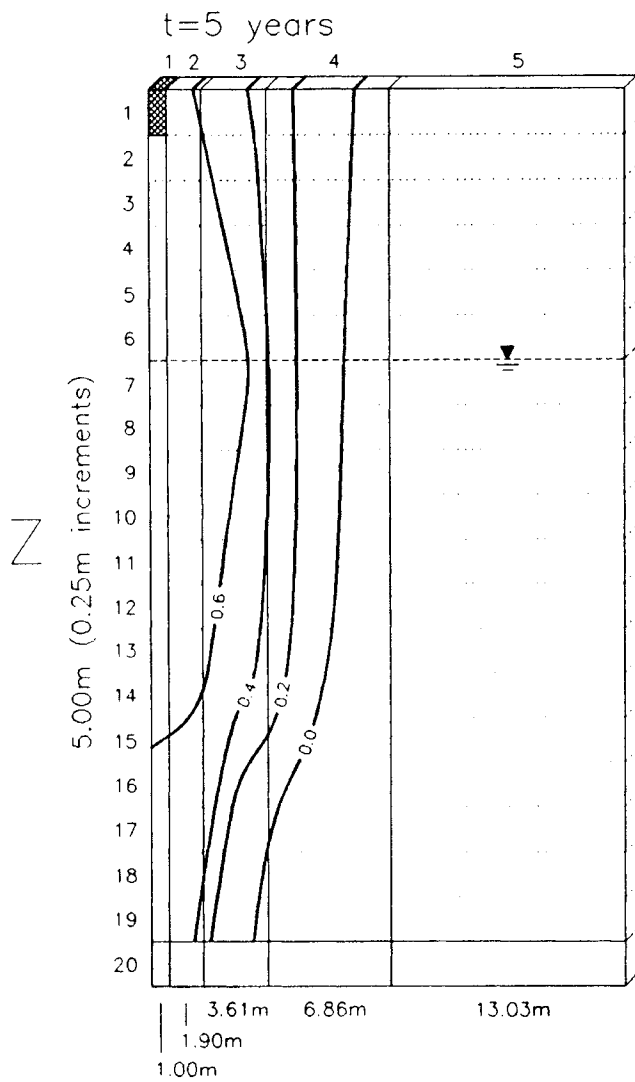


Figure 14. Infiltration of 10W-30 motor oil at five and 10 years.

vertically when compared with the pathway previously described for *p*-cymene. Also, the maximum saturation determined for the motor oil simulation is considerably higher than the saturation of the *p*-cymene, 70.1% versus 58.7%, respectively. As the densities of the two less-dense-than-water nonaqueous phase liquids are approximately equivalent, the differences observed in their infiltration pathways, i.e., area of spill influence and maximum saturation, are likely due to the higher viscosity of the motor oil versus *p*-cymene.

### Water

An infiltration event consisting of water entering the finite-difference grid at a point source was performed to serve as a benchmark by which to compare NAPL infiltration. It is assumed the "spilled" water is immiscible in the groundwater and behaves independently of the water introduced through natural recharge. All the initial conditions previously described are retained for the simulation.

Figure 15 displays numerical solutions for one and three years after the initial introduction of water at the surface. At time  $t=1$  year, the contoured water saturation values range from 0-30%. The greatest water saturation present in the domain is 33.6%, and occurs at grid block (1,1) (Appendix B). A decrease in the initial water and air saturations indicates displacement by the infiltrating water, which has entered the finite-difference grid since the beginning of the simulation. At one year, the plume has reached a maximum depth of 5 meters below the ground surface. Maximum saturation of the infiltrating water at the aquitard-aquifer interface is 10.2% at block (1,19). Horizontal plume migration extends a maximum of 6.5 meters from the source.

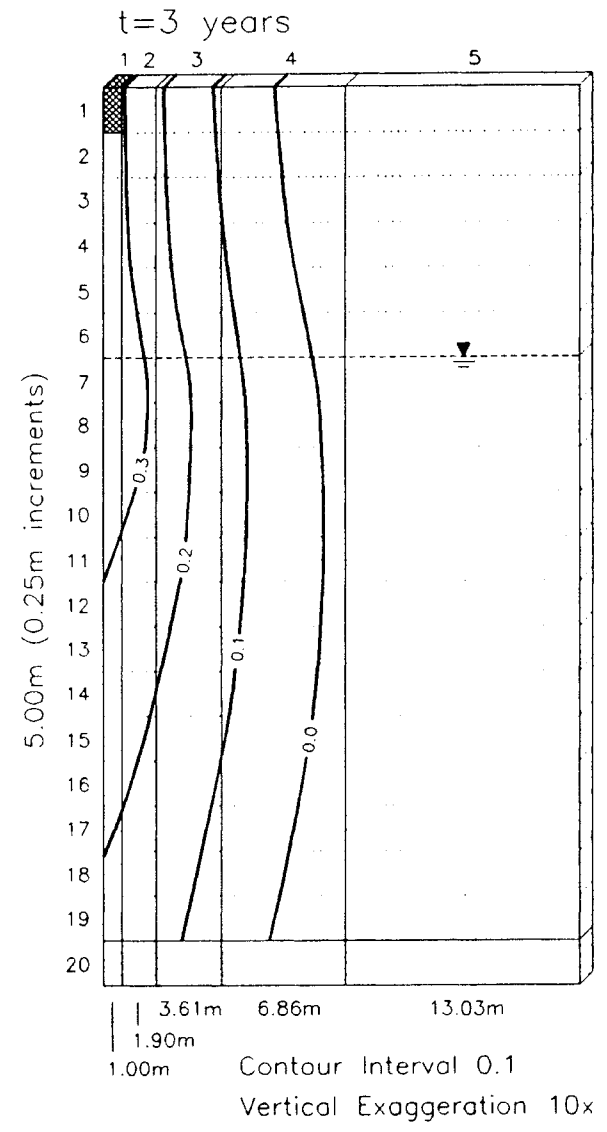
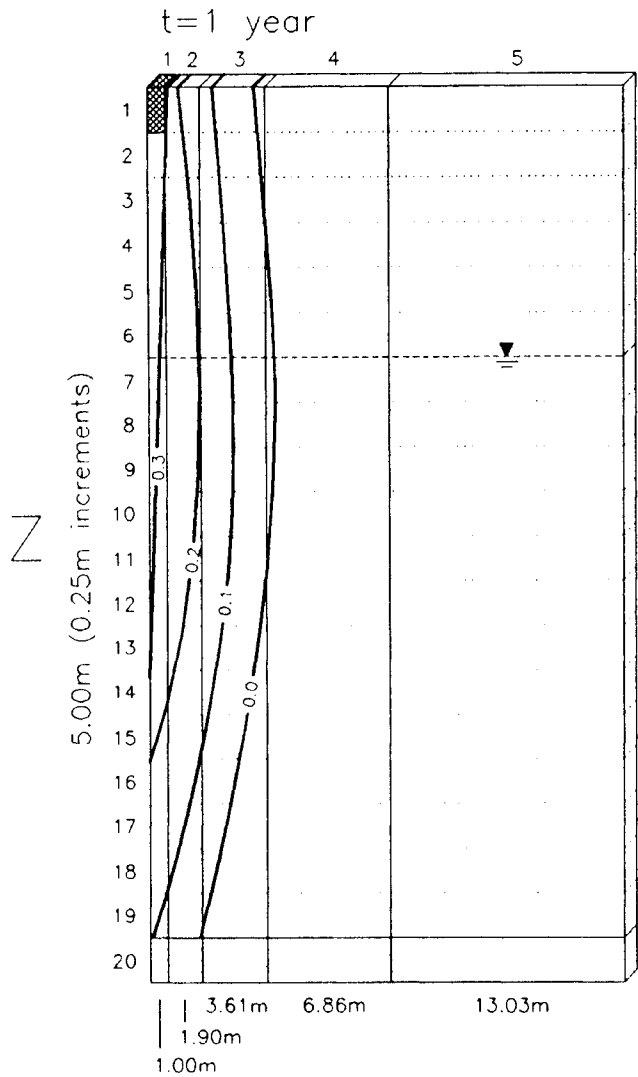


Figure 15. Infiltration of water at one and three years.



At time  $t=3$  years, the introduced water extends approximately 11.6 meters laterally from its origin, and continues to enter the lower draining aquifer (Figure 16). Saturation contour levels range from 0-30%, with the maximum saturation of 35.5%, reported for the infiltrating water at grid block (1,7). The maximum saturation determined at the aquitard-aquifer interface is 10.2% (Appendix B).

Figure 16 provides the numerical solutions for the output times of five and 10 years. At time  $t=5$  years, the water plume continues to expand both horizontally and vertically, enlarging the area of spill influence throughout the unsaturated and saturated zones. The plume now reaches a lateral distance 16.7 meters from the source. Maximum horizontal distance corresponds to a depth of approximately 2.1 meters below the ground surface. The water saturation contours on Figure 16 range from 0-30%. The highest saturation of the introduced water within the domain occurs at grid block (1,7), having a value of 35.8%. The maximum saturation reported at the aquitard-aquifer interface is 12.4% occurring at the grid block (1,19) (Appendix B).

At time  $t=10$  years, the water plume shows further enlargement in the  $x$ -direction, extending approximately 20.0 meters laterally from the source. Maximum lateral movement corresponds to a depth of 2.4 meters below the surface. Saturation contours range from 0-30% (Figure 12) with the maximum "NAPL" saturation of 35.9%, at block (1,7). The maximum saturation reported at the aquitard-aquifer interface remains at 12.4% at the grid block (1,19) (Appendix B).

### Phenol

Phenol is the first of the more-dense-than-water nonaqueous liquids (DNAPL)

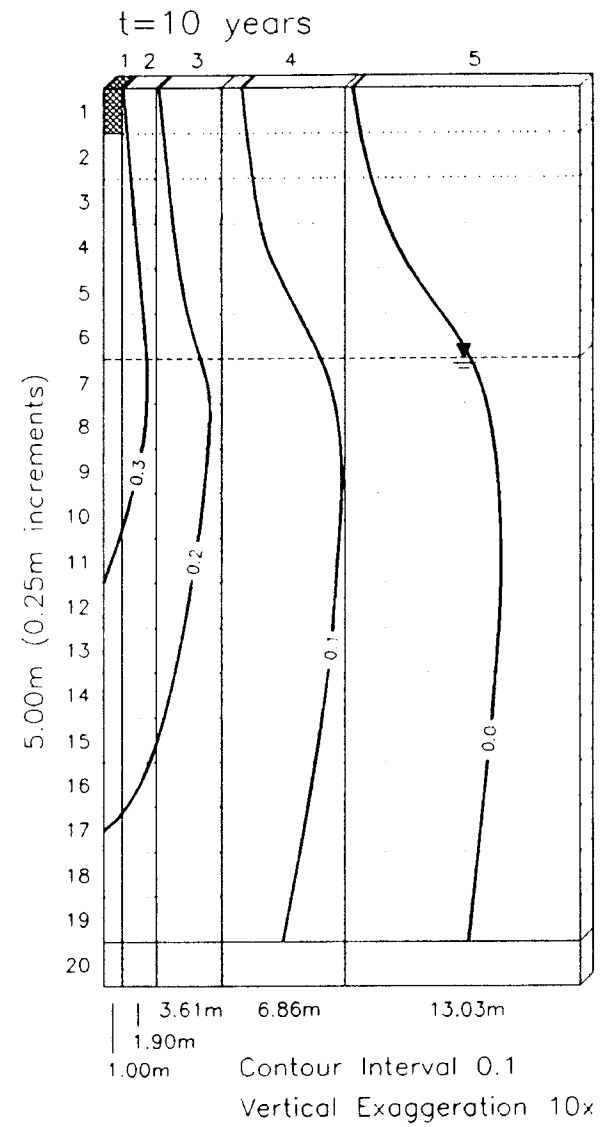
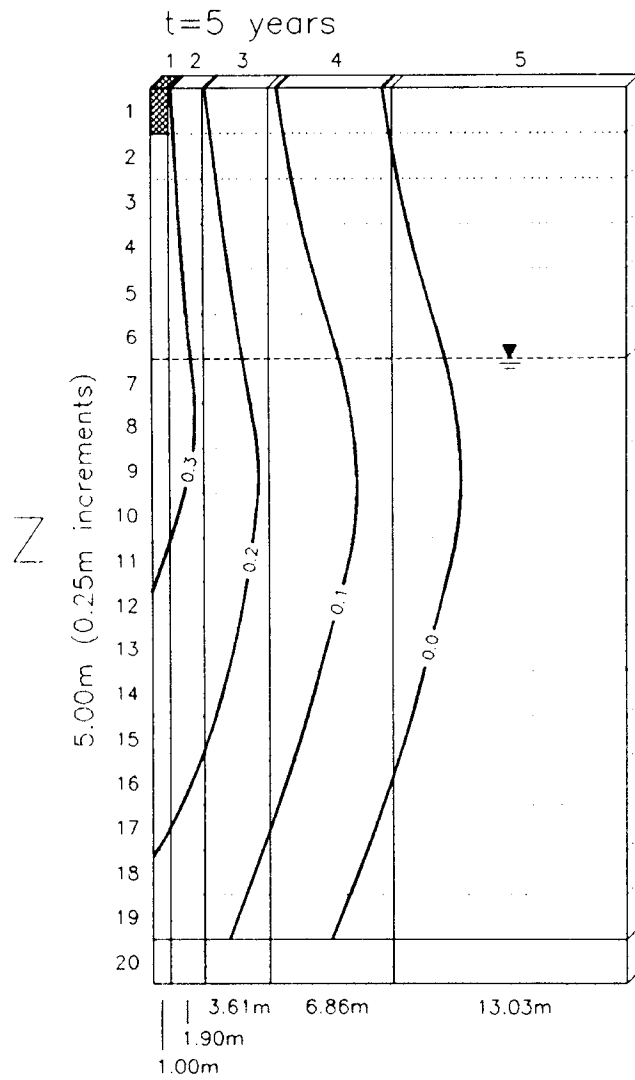


Figure 16. Infiltration of water at five and 10 years.

evaluated in this study. At time  $t=1$  year, the contoured phenol saturation values range from 0-30% (Figure 17). The greatest saturation of DNAPL present in the domain is 36.3%, and occurs at grid block (1,2) (Appendix B). After one year of simulation, the contaminant plume has migrated downward through the unsaturated zone, through the saturated portion of the aquitard, and has extended into the lower draining aquifer. Movement of the DNAPL into the saturated zone is due to the greater density of phenol as compared to water; the density difference allows for gravity-driven vertical migration of the phenol. Maximum horizontal plume migration is 4.4 meters from the source.

For times  $t=3, 5,$  and 10 years (Figures 17 and 18), conditions present within the finite-difference grid representing the infiltration of phenol show virtually no change. The maximum DNAPL saturation remains constant at 36.3% for grid block (1,2) indicating a relatively uniform saturation profile has been established below the source. The exception is the area of spill influence which continues to increase, although not significantly. At the basal portion of the aquitard, i.e., layer 19, a noticeable widening of the phenol plume has occurred. The maximum distance of measurable spill influence has increased from 4.4 meters at one year to 7.7 meters at 10 years.

The infiltration pathway of phenol produced by the SWANFLOW simulation indicates vertical plume migration to be predominant. At one year, the phenol has long since reached the underlying aquifer that drains the aquitard. This actually happens at 240 days (see subsequent discussion on Vertical and Horizontal NAPL Infiltration Rates). The horizontal migration at one year is only 4.4 meters from the source and reaches 7.7 meters at 10 years. Given the vertically dominated infiltration of the phenol, it is likely a majority of the contaminant introduced into the subsurface will eventually pass through

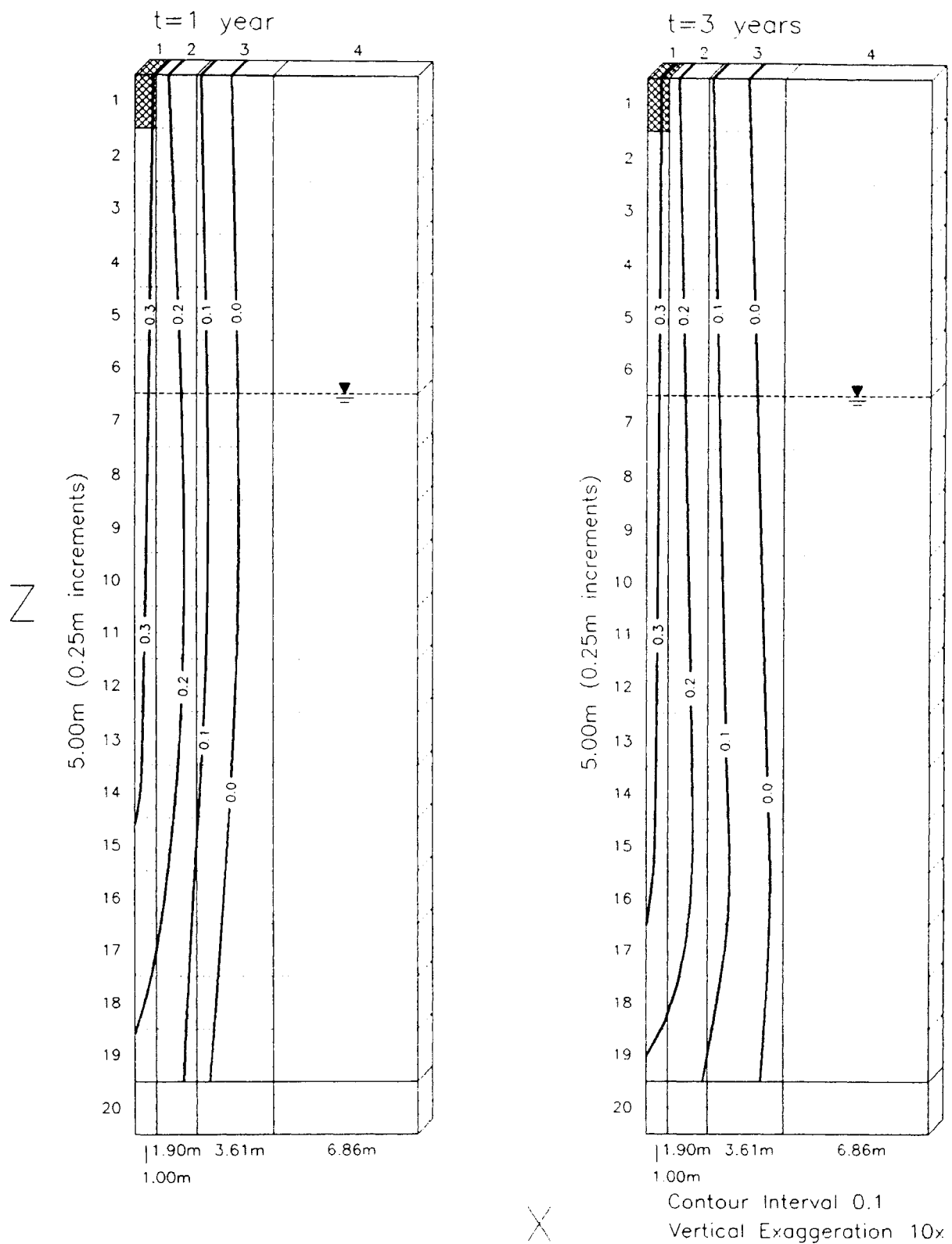


Figure 17. Infiltration of phenol at one and 3 years.

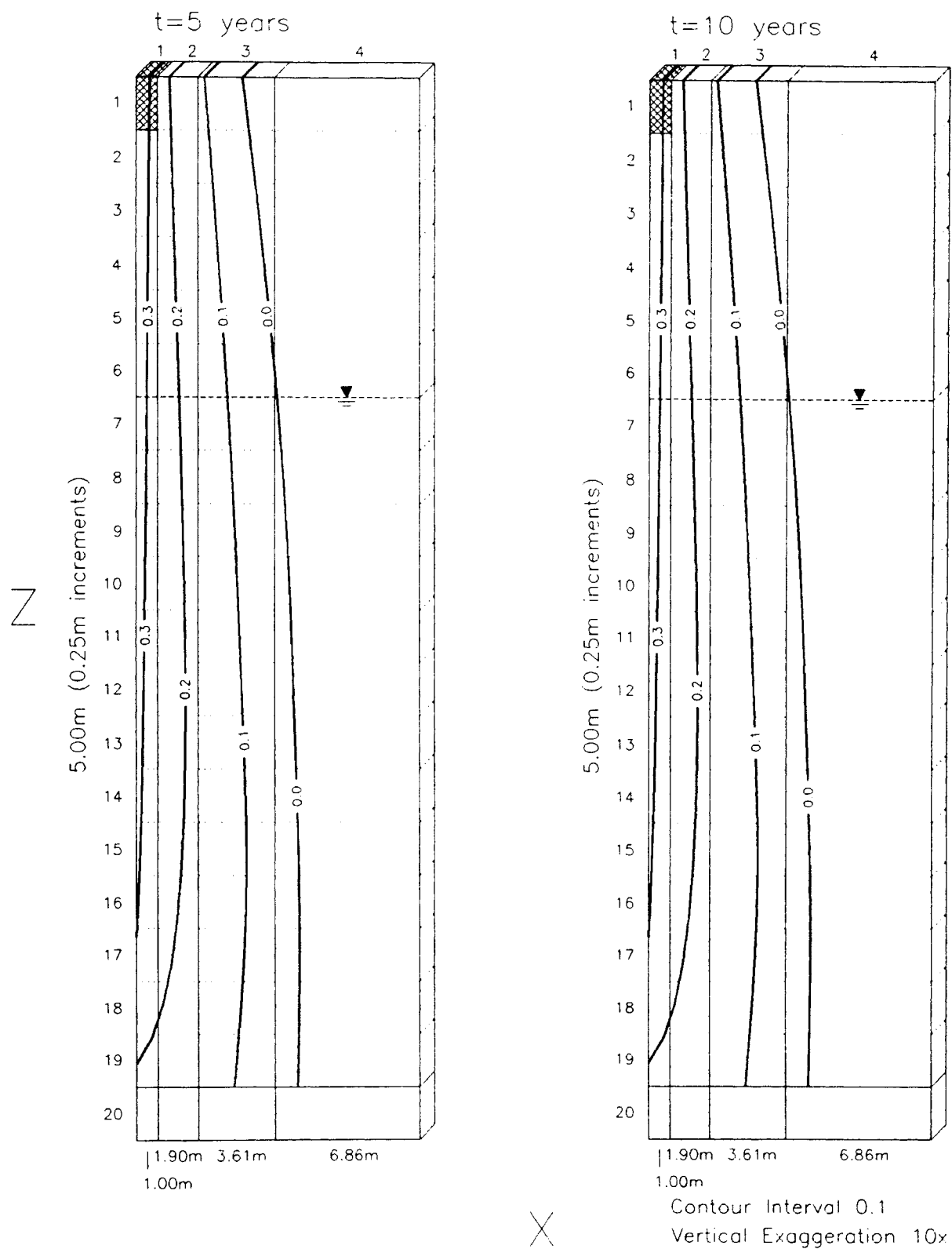


Figure 18. Infiltration of phenol at five and 10 years.

the aquitard and into the lower aquifer. The maximum reported DNAPL saturation is 36.3% indicating the area of spill influence consists of a variable mixture of phenol and water in the saturated zone, and phenol, water, and air in the unsaturated zone.

#### *o*-Nitrotoluene

*o*-Nitrotoluene is the second representative of the more-dense-than-water nonaqueous liquids included in this study. Initial conditions are the same as those described above (Table 3).

At time  $t=1$  year, the contoured *o*-nitrotoluene saturation values range from 0-30% (Figure 19). The greatest saturation of DNAPL present in the domain is 22.6%, and occurs at grid block (1,1) (Appendix B). At one year, the dense fluid has long since reached the underlying aquifer that drains the aquitard. This happens 77 days after the beginning of the simulation. Maximum lateral migration of the DNAPL plume is 4.8 meters from the original source.

For times  $t=3, 5,$  and 10 years (Figures 19 and 20), no significant changes are observed in the geometries of the *o*-nitrotoluene plume. The maximum DNAPL saturation remains unchanged and constant at 22.6% in grid block (1,1) indicating a relatively uniform saturation profile has been established below the source. There is some increase in the width of the area of contaminant influence noted at the basal portion of the aquitard between the times of one and three years (Figure 19). However, the overall maximum distance of measurable spill influence remains unchanged at 4.8 meters at three years, and throughout the remainder of the 10 year simulation.

The infiltration pathway of *o*-nitrotoluene produced by the SWANFLOW

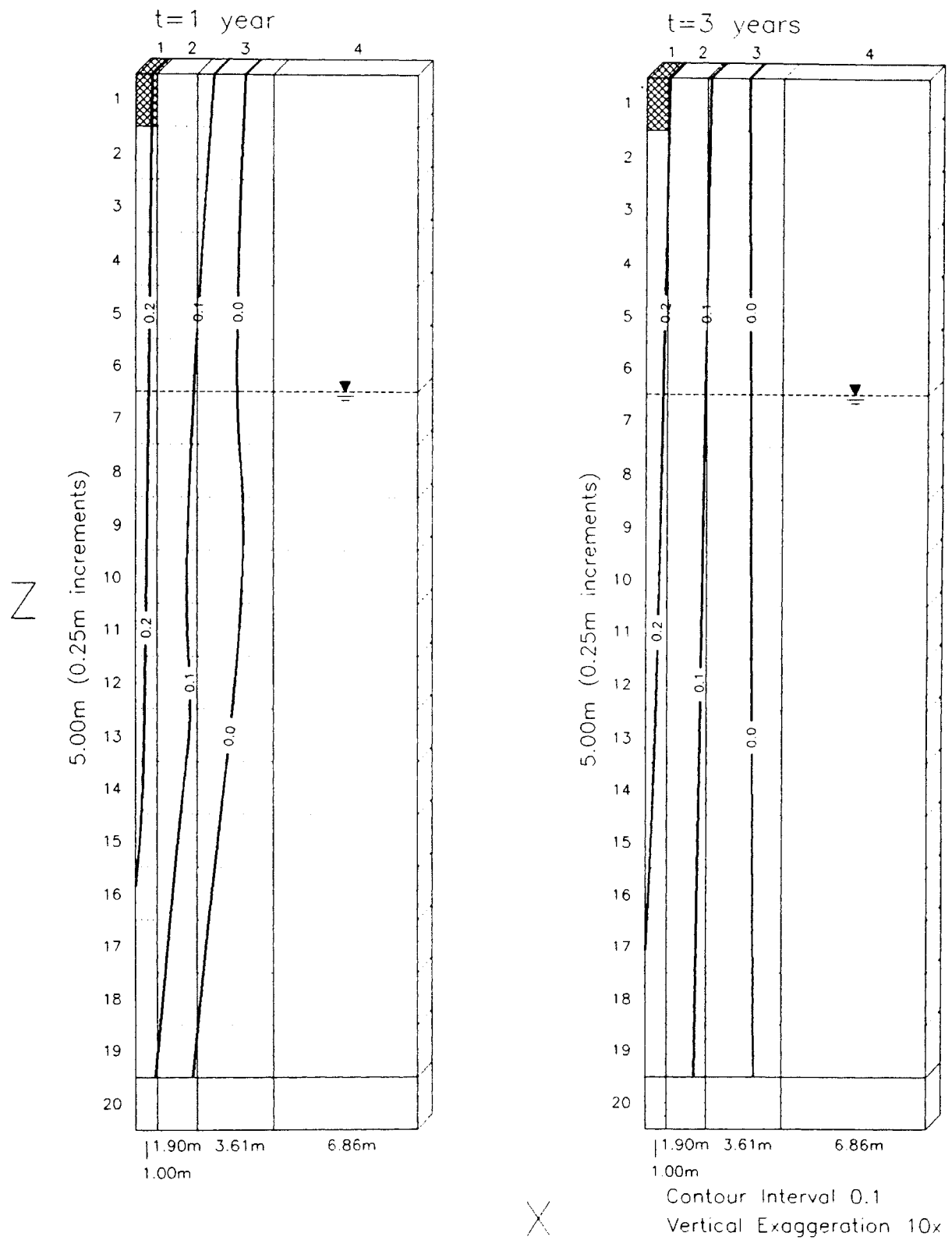


Figure 19. Infiltration of *o*-nitrotoluene at one and three years.

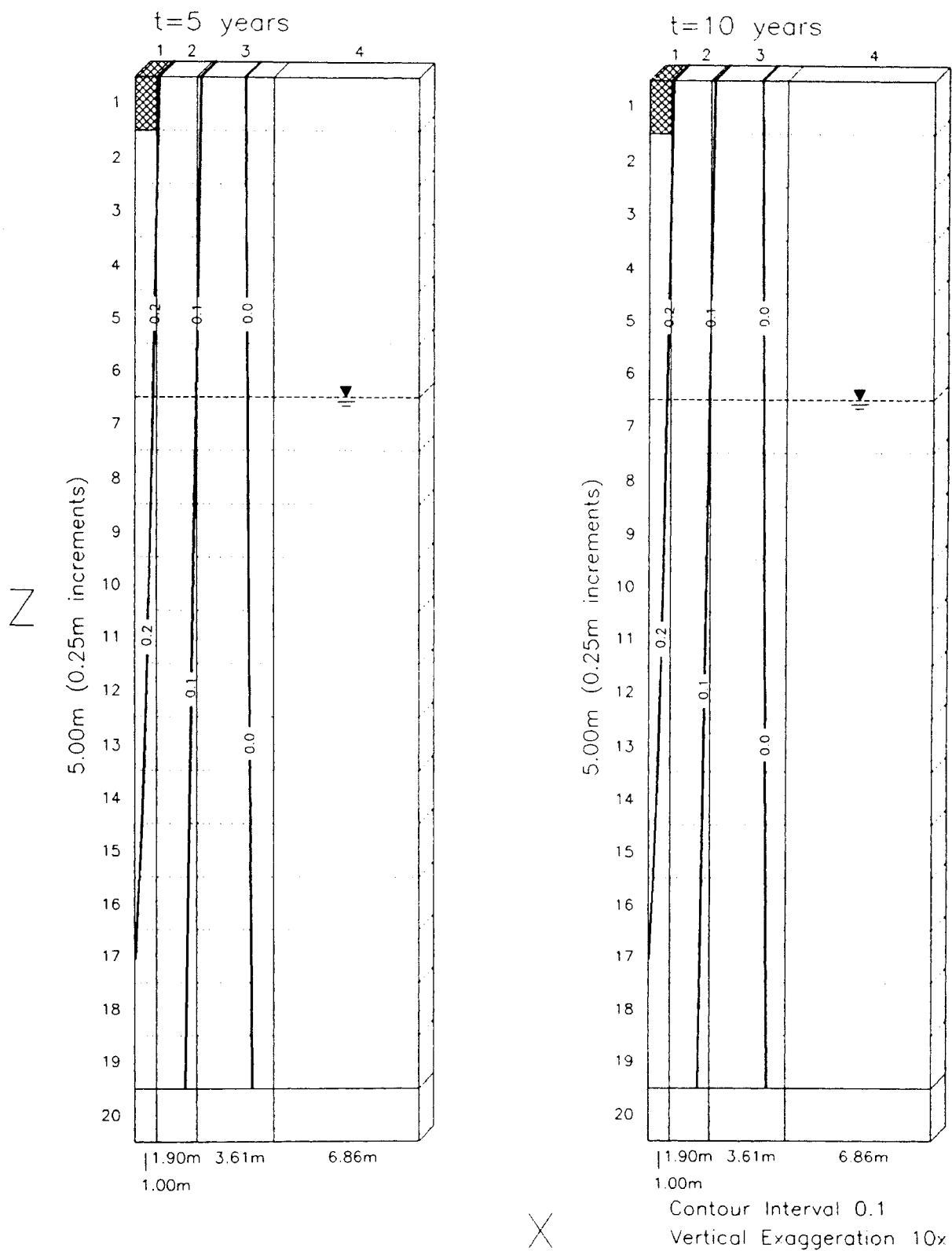


Figure 20. Infiltration of *o*-nitrotoluene at five and 10 years.



simulation indicates vertical plume migration to be predominant. As with the simulated infiltration of phenol, the vertically-dominated infiltration of the *o*-nitrotoluene, it is likely a majority of the contaminant introduced into the subsurface will eventually pass through the aquitard and into the lower draining aquifer.

### Trichloroethene

Trichloroethene (TCE) is one of the more dense DNAPLs, with a density nearly 50% greater than water. Initial conditions are presented in the discussions above and in Table 3. NAPL entry occurs at grid block (1,1) as indicated in Figure 6. The TCE source remains constant throughout the 10 year duration of the simulation. Simulated output is generated at one, three, five, and 10 year intervals (Figures 21 and 22, Appendix B).

The numerical solution at one year provides the contoured TCE saturation a range of values from 0-30% (Figure 21). The greatest saturation of DNAPL present in the domain is 16.9%, and occurs at grid block (1,1) (Appendix B). Water and air have been displaced by the infiltrating TCE, evidenced by a decrease in their respective saturations. After one year of simulation, the contaminant plume has migrated downward through the unsaturated zone, through the saturated portion of the aquitard, and has extended into the lower draining aquifer. Maximum horizontal plume migration is 2.8 meters from the original source.

For times  $t=3, 5,$  and 10 years (Figures 21 and 22), conditions present within the finite-difference grid show little change. The maximum DNAPL saturation remains constant at 16.9% for grid block (1,1). The exception is the area of spill influence which

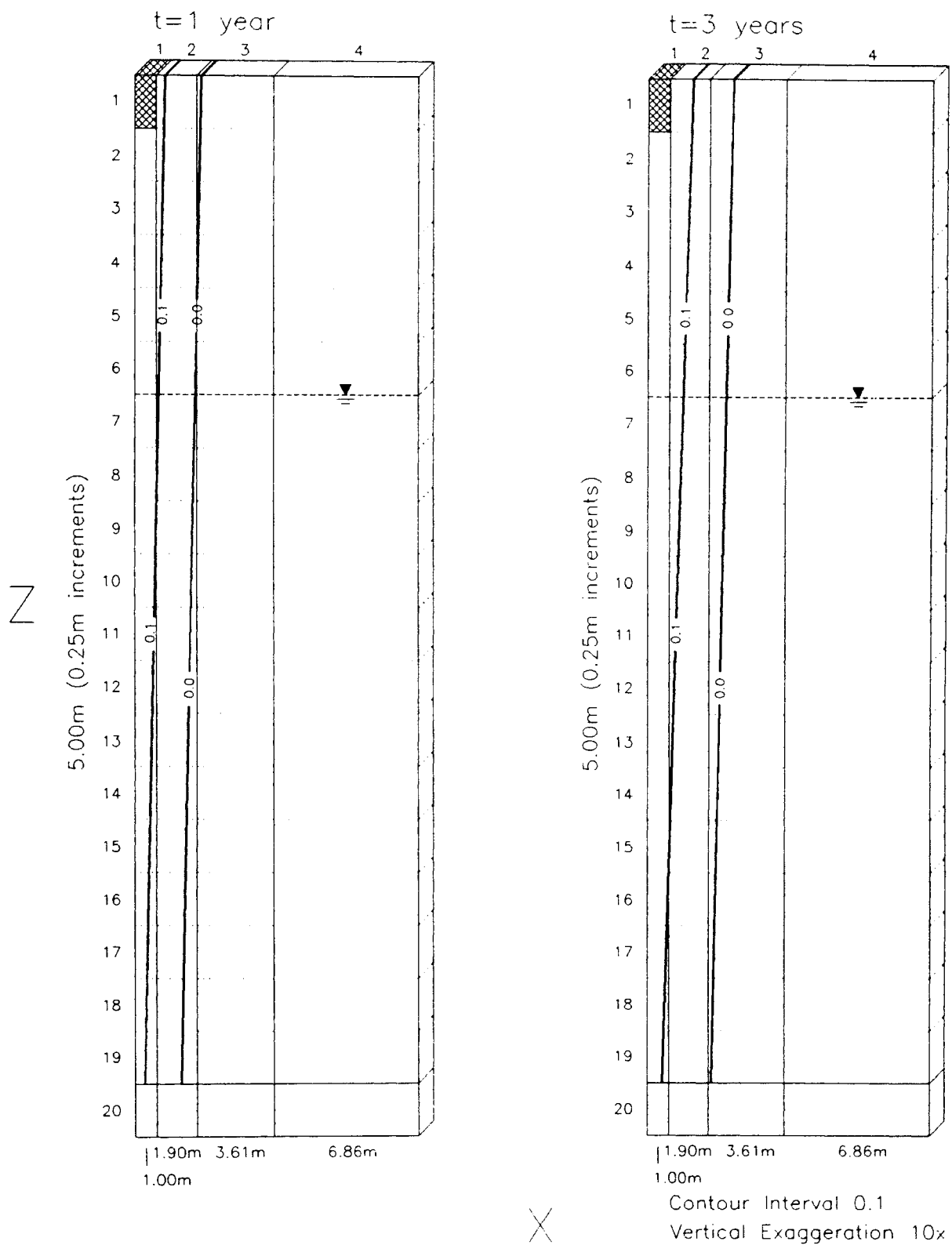


Figure 21. Infiltration of trichloroethene (TCE) at one and three years.

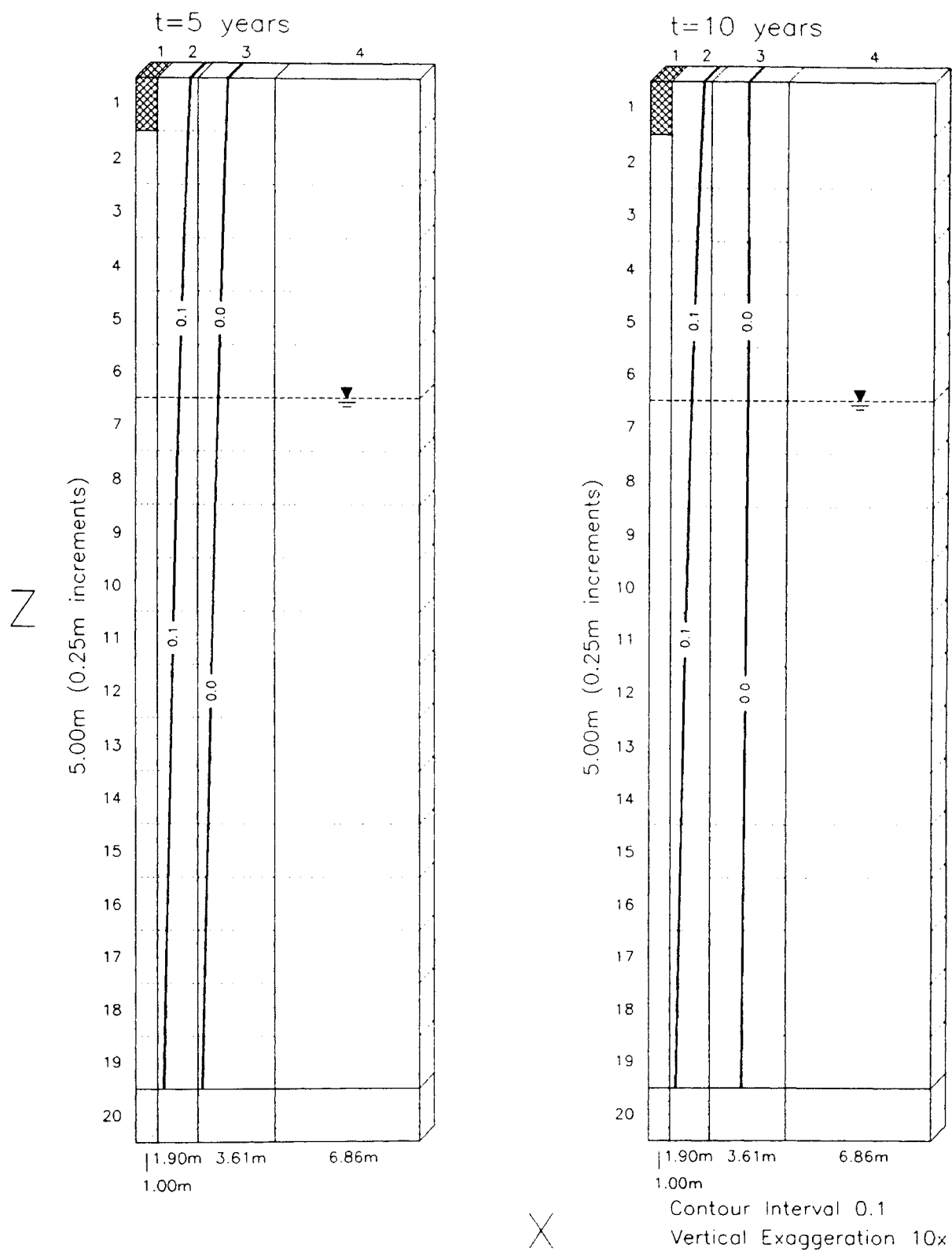


Figure 22. Infiltration of trichloroethene (TCE) at five and 10 years.

continues to show a uniform increase, although not a significant increase. The maximum distance of measurable spill influence has increased from 2.8 meters at one year to 4.2 meters at 10 years.

The infiltration pathway of TCE produced by the SWANFLOW simulation indicates vertical plume migration to be predominant. At 61 days, the TCE has reached the underlying aquifer that drains the aquitard. Given the vertically-dominated trend of infiltration for more-dense-than-water nonaqueous phase liquids, the majority of the contaminant will likely pass through the aquitard and into the lower aquifer. The maximum reported DNAPL saturation is 16.9%, while the maximum horizontal plume migration is 4.2 meters.

#### Tetrachloromethane

Tetrachloromethane (carbon tetrachloride) is the most dense NAPL included in this study, having a density 58% greater than that of water. Initial conditions are presented in the discussions above and summarized in Table 3. NAPL entry occurs at grid block (1,1) as indicated in Figure 6, which remains continuous throughout the 10 year duration of the simulation. Simulated output is generated at one, three, five, and 10 year intervals (Figures 23 and 24, Appendix B).

Figure 23 displays the numerical solution at one years. The contoured tetrachloromethane saturation values range from 0-30%. The greatest saturation of DNAPL present in the domain is 17.1%, and occurs at grid block (1,1) (Appendix B). Maximum lateral migration of the DNAPL plume is 2.2 meters from the original source.

For times  $t=3, 5,$  and 10 years (Figures 23 and 24), conditions present within the

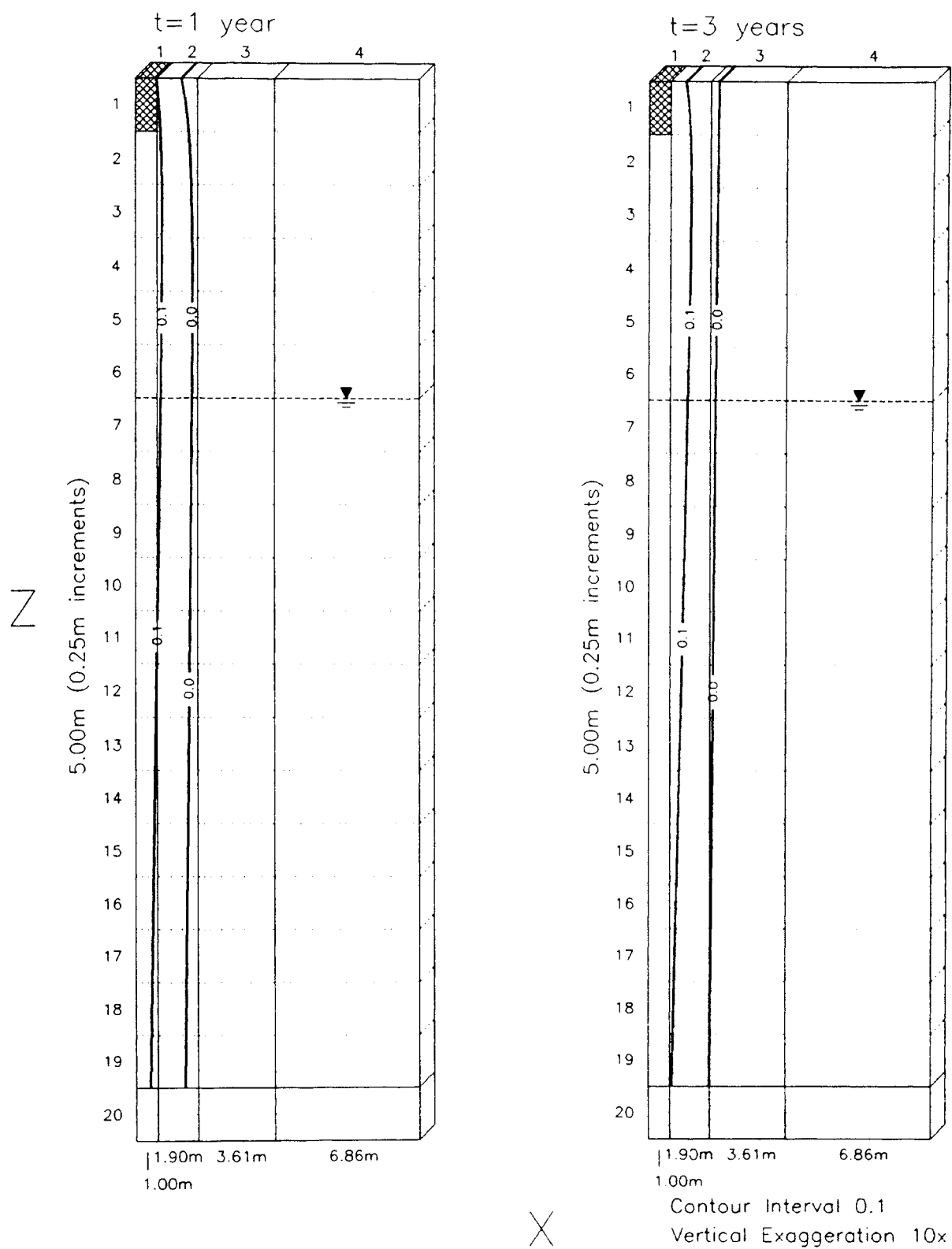


Figure 23. Infiltration of tetrachloromethane (carbon tetrachloride) at one and three years.

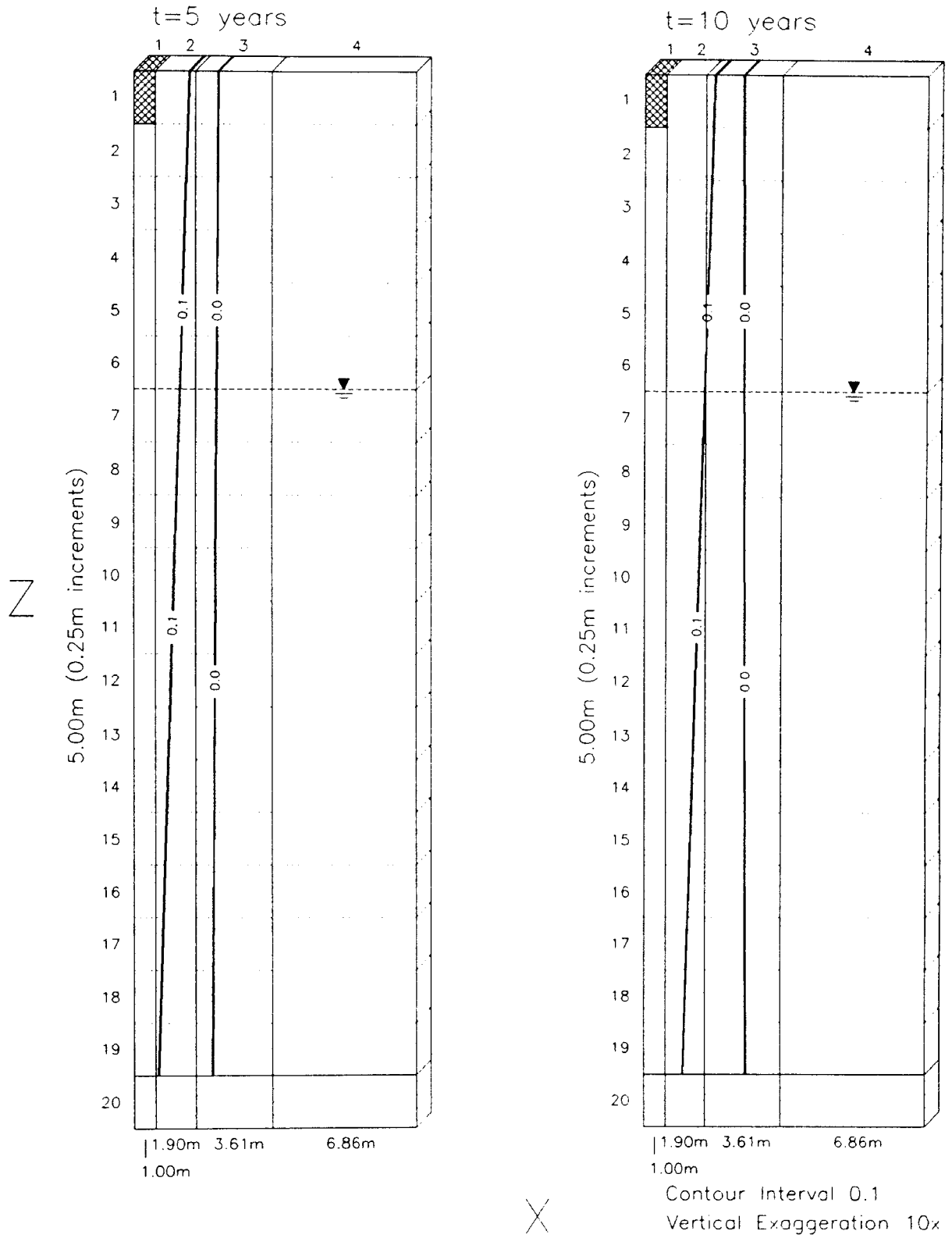


Figure 24. Infiltration of tetrachloromethane (carbon tetrachloride) at five and 10 years.

finite-difference grid show little change. The maximum DNAPL saturation remains constant at 17.1% for grid block (1,1) indicating a relatively uniform saturation profile has been established. The exception is the area of spill influence which continues to show a slight increase. The maximum distance of measurable spill influence has increased from 2.2 meters at one year to 4.3 meters at 10 years.

The area of contaminant influence produced by the infiltration of tetrachloromethane, as generated by the SWANFLOW code, exhibits an increase in the when compared with the pathway previously described for trichloroethene. An increase in the horizontal migration of contaminant in the subsurface is contrary to the trend observed for the phenol, *o*-nitrotoluene, and trichloroethene. These more-dense-than-water nonaqueous phase liquids demonstrate a decrease in horizontal migration as density increases. Also, the maximum saturation of DNAPL predictably decreases as the density increases. However, the maximum saturation of tetrachloromethane increases when compared to TCE, contrary to the observed trend. The tetrachloromethane appears to behave as if it were less dense than trichloroethene, whereas, it is actually more dense. The differences observed in the infiltration pathways of trichloroethene and tetrachloromethane, i.e., area of spill influence and maximum saturation, are likely due to the higher viscosity of the tetrachloromethane versus TCE.

### Vertical and Horizontal NAPL Infiltration Rates

#### *Vertical NAPL Infiltration Rates*

To quantify the vertical infiltration pathways of the nonaqueous phase liquids described above, breakthrough times at the groundwater table and the lower draining

aquifer were compared for the nine liquids. Breakthrough at the groundwater table and lower draining aquifer is said to occur when the simulated NAPL reaches layers 7 and 20, respectively. Vertical infiltration rates are calculated in meters per day. Table 5 provides a summary of vertical breakthrough times determined from the SWANFLOW output (Appendix B). Summary data are plotted in Figure 25 to provide a graphical display of these breakthrough times to facilitate comparison. From Figure 25, it is readily apparent that the vertical infiltration rate is a function of NAPL density. Although viscosity has also been shown to influence infiltration (see discussions on motor oil and tetrachloromethane), it appears to have less influence as compared to density differences. Within the unsaturated and saturated zones, infiltration rates show a steady increase corresponding to the increase in NAPL density (Table 5). A second notable trend seen on Figure 25 and in Table 5 is the difference behavior between LNAPL and DNAPL as the nonaqueous liquid moves between the unsaturated and saturated zones. As would be expected, LNAPL infiltration rates are higher within the unsaturated zone than in the saturated zone, e.g., gasoline has an infiltration rate of  $0.405\text{E-}3$  meters per day within the unsaturated zone compared to  $0.069\text{E-}3$  meters per day in the saturated zone, approximately an order of magnitude difference. This slowing of LNAPL infiltration is most likely due to buoyancy effects experienced at and below the water table. Contrary to this is the behavior of DNAPL, which exhibits an increased infiltration rate as the contaminant moves from the unsaturated zone to the saturated zone. For example, tetrachloromethane infiltrates the unsaturated zone at a rate of  $59.241\text{E-}3$  meters per day, and increases to  $90.529\text{E-}3$  meters per day within the saturated zone, a 53% increase. This is likely due to the absence of the air phase within the saturated zone. Elimination



TABLE 5. Vertical NAPL Infiltration Rates

NAPL	Breakthrough at the Groundwater Table (days)	Unsaturated Zone Infiltration Rate (m/d)	NAPL/Water Infiltration Ratio Unsaturated Zone (unitless)	Breakthrough at the Lower Draining Aquifer (days)	Saturated Zone Infiltration Rate (m/d)	NAPL/Water Infiltration Ratio Saturated Zone (unitless)
Gasoline	3703.7*	0.405E-3	0.015	50,578.7*	0.069E-3	0.006
Kerosene	568.3	2.640E-3	0.098	27,314.8*	0.122E-3	0.012
<i>p</i> -Cymene	261.6	5.733E-3	0.213	11,469.9*	0.290E-3	0.028
10W-30 Motor Oil	135.4	11.078E-3	0.411	1,238.4	2.947E-3	0.280
Water	55.7	26.930E-3	1.000	364.5	10.525E-3	1.000
Phenol	53.9	27.829E-3	1.033	240.7	17.398E-3	1.653
<i>o</i> -Nitrotoluene	38.7	38.760E-3	1.439	115.6	42.263E-3	4.015
Trichloroethene	24.9	60.241E-3	2.237	60.8	90.529E-3	8.601
Tetrachloromethane	25.1	59.761E-3	2.219	60.8	91.036E-3	8.650

\*Simulation runs are not within the scope of this study and are intended for comparison purposes only. Additional simulations were run to when breakthrough occurred. Output files are not provided.

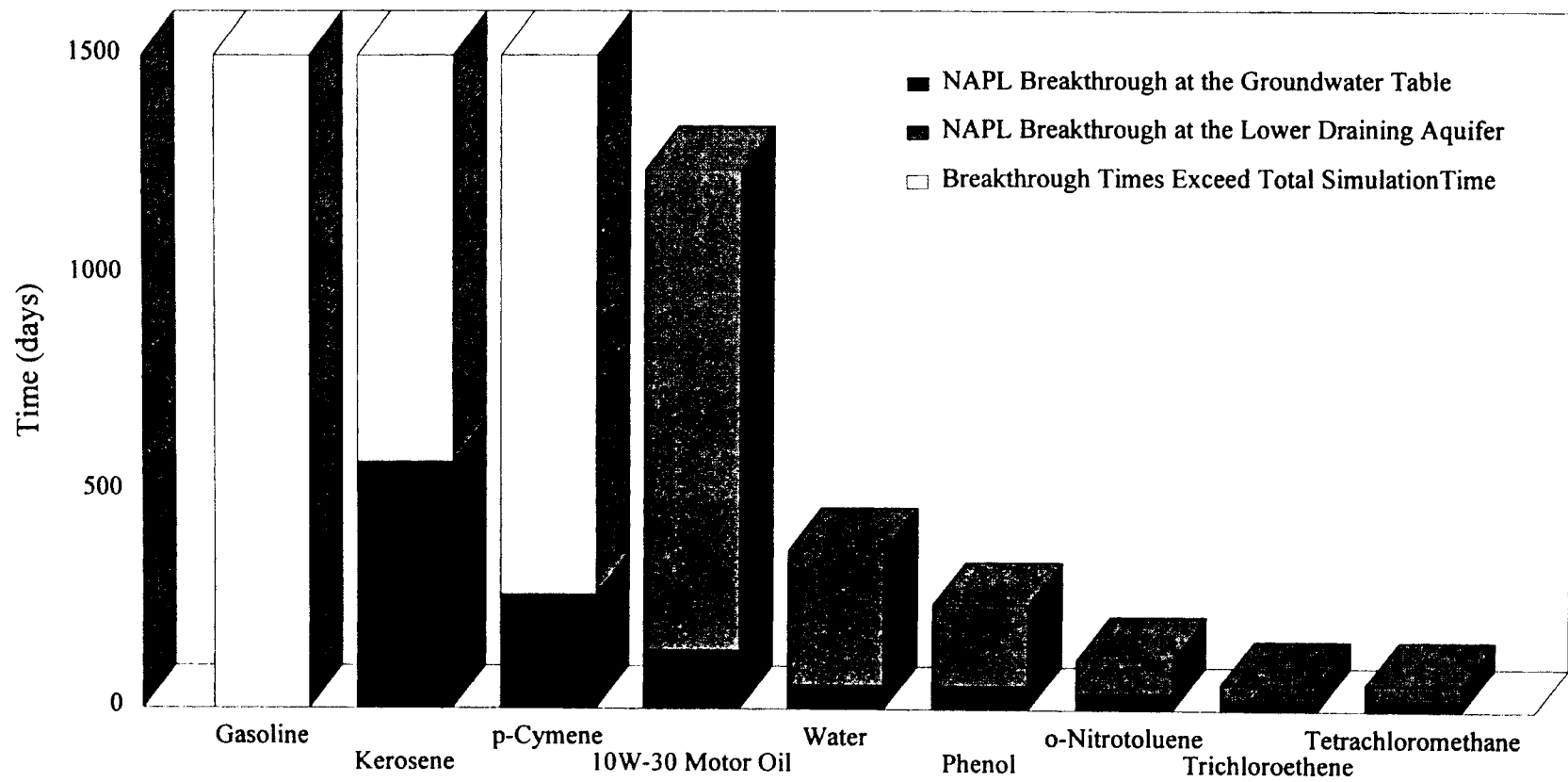


Figure 25. Breakthrough of vertically-infiltrating NAPL.

of the air phase results in a higher relative permeability for the NAPL, i.e., less competition for the available pore space in the absence of the third phase. Higher simulated vertical infiltration rates for DNAPL within the saturated zone versus the unsaturated zone are the result.

#### *Horizontal NAPL Infiltration Rates*

To evaluate horizontal infiltration, the maximum distance the NAPL migrated from the source was determined graphically from the contour plots of the nine liquids at one, three, five, and 10 years. These values are tabulated and plotted in Table 6 and Figure 26, respectively.

Figure 26 indicates a general decrease in the maximum extent of horizontal infiltration with increasing density. The influence of viscosity, as described for the LNAPL and DNAPL pairs, does result in some fluctuation between the graphed and "expected" values; however, the general trend persists throughout the spectrum of contaminant densities used for the simulations.

#### Discussion Summary

The concept of a floating "lens" [e.g., *Holzer, 1976*], often used to characterize the spill of a less-dense-than-water nonaqueous phase liquid, appears imprecise. The lens is more likely to be a thick zone of varying proportions of NAPL and water (and air if the unsaturated zone is under consideration). This suggests observations from monitoring wells, which essentially ignore capillary pressure effects, may not be representative of the conditions present in the adjacent aquifer. Capillary pressure is a property of the

TABLE 6. Horizontal NAPL Infiltration Rates (Unsaturated Zone)

NAPL	Total Horizontal Infiltration After 1 year (m)	Total Horizontal Infiltration After 3 years (m)	Total Horizontal Infiltration After 5 years (m)	Total Horizontal Infiltration After 10 years (m)	Horizontal Infiltration Rate for 10 years (m/d)	NAPL/Water Infiltration Ratio for 10 years (unitless)
Gasoline	30	60	90	175	47.945E-3	8.751
Kerosene	17	32	45	86	23.562E-3	4.300
<i>p</i> -Cymene	12	27	43	62	16.986E-3	3.100
10W-30 Motor Oil	5.6	9.9	11.0	20.6	5.644E-3	1.030
Water	6.5	11.6	16.7	20.0	5.479E-3	1.000
Phenol	4.4	7.7	7.7	7.7	2.110E-3	0.385
<i>o</i> -Nitrotoluene	4.8	4.8	4.8	4.8	1.315E-3	0.240
Trichloroethene	2.8	4.2	4.2	4.2	1.151E-3	0.210
Trichloromethane	2.2	4.3	4.3	4.3	1.178E-3	0.215

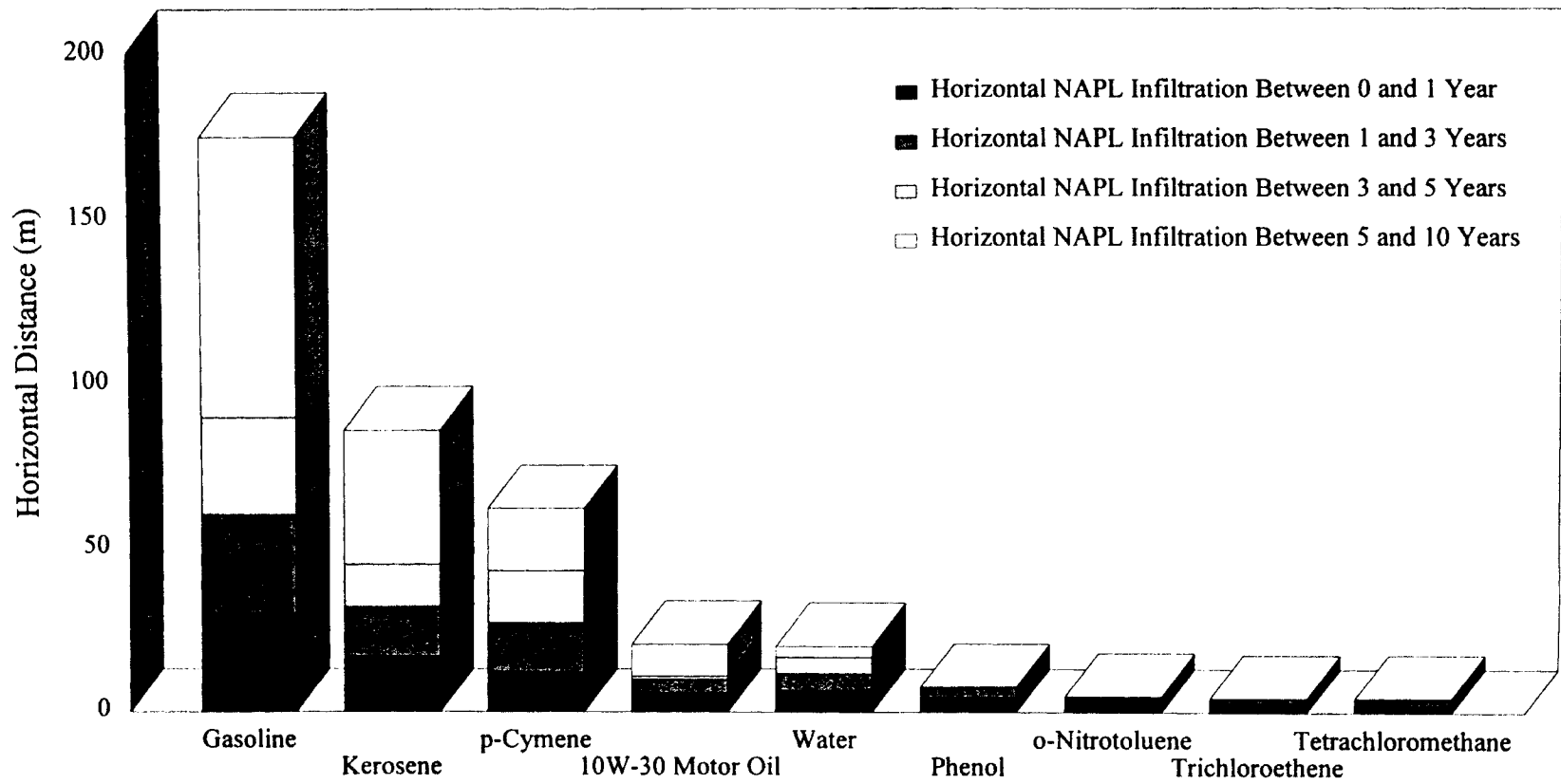


Figure 26. Horizontal NAPL infiltration rates.

macroscopic geometry of the void spaces in the porous media [Fetter, 1993]. The removal of the pore spaces, i.e., introduction of a well bore, eliminates capillary pressure forces within the affected area.

The lateral migration of the LNAPL can occur even within the unsaturated zone. Lateral spreading of the contaminant lens cannot be attributed solely to physical spreading at the water table due to buoyant forces acting on the less dense NAPL. Capillary forces likely play a significant role in lateral LNAPL movement.

The geometry of the area of spill influence, that is, the horizontal versus vertical dimensions, is a function of NAPL density and viscosity. However, density and viscosity act independently of one another. Low density NAPL, such as gasoline, produce an area of spill influence which is dominated by lateral migration with little vertical infiltration, which is likely a function of capillary forces. As LNAPL density increases and approaches that of water, the vertical component of migration becomes more prevalent than lateral migration. The infiltration of a high density NAPL, such as tetrachloromethane, results in an area of spill influence dominated by the vertical migration component due to gravity or buoyant forces.

The role of viscosity on infiltration varies for LNAPL and DNAPL. For a less-dense-than-water nonaqueous phase liquid, an increase in viscosity causes the LNAPL to behave as if its density has increased. For example, the area of contaminant influence produced by the infiltration of 10W-30 motor oil, generated by the SWANFLOW code, has decreased horizontally and increased vertically when compared with the pathway of *p*-cymene. Since the densities of the two less-dense-than-water nonaqueous phase liquids are approximately equivalent, the differences observed in their infiltration pathways, i.e.,

area of spill influence, is likely due to the higher viscosity of the motor oil versus the *p*-cymene. The effect of viscosity on DNAPL infiltration is the inverse of the description of the viscosity effects on LNAPL infiltration, i.e., an increase in viscosity behaves similarly to a decrease in density. This is evidenced by the comparison between trichloroethene and tetrachloromethane infiltration.

Immiscible fluid saturation appears to be a function of the fluid density and viscosity, again acting independently of one another. Generally, less-dense-than-water immiscible fluids attained higher saturation levels during the simulations than did the more dense liquids. Within the LNAPL grouping, immiscible fluid saturations increased as density increased. Conversely, the more-dense-than-water immiscible nonaqueous phase fluid saturations progressively decreased as density increased. Maximum saturation is also influenced by dynamic viscosity. As the dynamic viscosity of a nonaqueous liquid increases, a corresponding increase in the maximum saturation can be noted. The influence of viscosity differences on immiscible fluid saturations are somewhat more subtle than density differences, but can still be discerned. A comparison of infiltration characteristics of two less-dense-than-water nonaqueous phase liquids, e.g., *p*-cymene and 10W-30 motor oil, which have approximately the same density but an approximate two order of magnitude difference in dynamic viscosity, suggests a notable difference in their infiltration pathways can be attributed to the difference in viscosity. The maximum immiscible fluid saturation for motor oil is 11.4% greater than *p*-cymene. This difference is likely due to the greater dynamic viscosity of the motor oil. This is further supported by comparing the maximum saturations of trichloroethene (16.9%) and tetrachloromethane (17.1%). The dynamic viscosity of the tetrachloromethane is

approximately two times that of the trichloroethene (Table 1). Recall that as the density of a DNAPL increases, the maximum saturation decreases; therefore, we would expect the maximum tetrachloromethane saturation to be less than TCE. However, the maximum saturation of tetrachloromethane is greater, and it the result of its higher dynamic viscosity.

Breakthrough times for the downward-infiltrating nonaqueous immiscible liquids indicate infiltration rates increase as density increases. This is likely due to buoyant forces encountered by the less dense liquids. The implication of these results is that dense immiscible liquids present the greatest danger in terms of migration potential in that they travel faster and deeper. Lower density liquids, which travel slower and tend to remain at shallow depths, are more amenable to corrective measures. However, the increased area of spill influence can create additional remediation problems.

Generally, increasing NAPL density results in a decrease in the maximum extent of horizontal infiltration. The influence of viscosity, as described for the LNAPL and DNAPL pairs, does result in some fluctuation between the simulated and "expected" values based on density alone.



## CONCLUSIONS

1. The concept of a floating lens consisting of only NAPL, often used to characterize the spill and infiltration of a less dense than water nonaqueous phase liquid (LNAPL), appears imprecise. The lens is more likely to be a thick zone of varying proportions of nonaqueous phase liquid and water (and air if the unsaturated zone is under consideration).

2. The geometry of the area of spill influence, i.e., the rate of horizontal versus vertical NAPL infiltration, are influenced by NAPL density and viscosity. These influences, however, act independently from each other. As the density of the NAPL increases, the rate at which the contaminant migrates horizontally decreases, while the vertical infiltration rate increases. The influence of dynamic viscosity on NAPL infiltration is somewhat more complex, and is dependent on whether the NAPL being considered is a less dense than water (LNAPL) or more dense than water (DNAPL). For less dense liquids, an increase in viscosity results in decreased horizontal infiltration and increased vertical infiltration. If viscosity is decreased, the opposite holds true. For more dense liquids, the influence of viscosity is the inverse of that described for LNAPL.

3. The maximum immiscible fluid saturation is a function of fluid density and viscosity. First, as the density of an LNAPL increases and approaches the density of water, the maximum NAPL saturation also increases. Second, as the density of a DNAPL

increases from the density of water, the maximum NAPL saturation decreases. Finally, for two nonaqueous phase liquids having approximately the same density and differing viscosities, the higher maximum saturation will be associated with the greater viscosity. This is true for both LNAPL and DNAPL.

## REFERENCES

- Abriola, L.M., and G.F. Pinder, A multiphase approach to the modeling of porous media contamination by organic compounds, 1, Equation development, *Water Resources Research*, 21(1), 11-18, 1985a.
- Abriola, L.M., and G.F. Pinder, A multiphase approach to the modeling of porous media contamination by organic compounds, 2, Numerical simulation, *Water Resources Research*, 21(1), 19-26, 1985b.
- Adenekan, A.E., T.W. Patzek, and K. Pruess, Modeling of multiphase transport of multicomponent organic contaminants and heat in the subsurface: Numerical model formulation, *Water Resources Research*, 29(11), 3727-3740, 1993.
- Baehr, A.L., and M.Y. Corapcioglu, A compositional multiphase model for groundwater contamination by petroleum products, 2, Numerical Solution, *Water Resources Research*, 23(1), 201-214, 1987.
- Brooks, P.M., and A.T. Corey, Hydraulic properties of porous media, *Hydrology Paper* 3, University of Colorado, Fort Collins, Colorado, 1966.
- Burmester, D.E., and R.H. Harris, Groundwater contamination: An emerging threat, *Technology Review*, 84(7), 50-52, 1982.
- Coats, K.H., Reservoir simulation: State of the art, *Journal of Petroleum Technology*, 34(8), 1633-1642, 1982.
- Conrad, S.H., J.L. Wilson, W.R. Mason, and W.J. Peplinski, Visualization of residual organic liquid trapped in aquifers, *Water Resources Research*, 28(2), 467-478, 1992.
- Corapcioglu, M.Y., and A.L. Baehr, A compositional multiphase model for groundwater contamination by petroleum products, 1, Theoretical considerations, *Water Resources Research*, 23(1), 191-200, 1987.
- Corapcioglu, M.Y., and M.A. Hossain, Ground-water contamination by high-density immiscible slugs in gravity-driven gravel aquifers, *Ground Water*, 28(3), 403-412, 1990.

- Corey, A.T., *Mechanics of immiscible fluids in porous media*, Water Resources Publications, Littleton, Colorado, 1986.
- Corey, A.T., C.H. Rathjens, J.H. Henderson, and M.R.J. Wyllie, Three-phase relative permeability, *American Institute of Mining, Metallurgical, and Petroleum Engineers Transactions, Petroleum Branch*, 207, 349-351, 1956.
- Dane, J.H., M. Oostrom, and B.C. Missildine, An improved method for the determination of capillary pressure-saturation curves involving TCE, water and air, *Journal of Contaminant Hydrology*, 11, 69-81, 1992.
- Demond, A.H., and P.V. Roberts, Estimation of two-phase relative permeability relationships for organic liquid contaminants, *Water Resources Research*, 29(4), 1081-1090, 1993.
- Falta, R.W., K. Pruess, I. Javandel, and P.A. Witherspoon, Numerical modeling of steam injection for the removal of nonaqueous phase liquids from the subsurface, 1, Numerical formulation, *Water Resources Research*, 28(2), 433-449, 1992a.
- Falta, R.W., K. Pruess, I. Javandel, and P.A. Witherspoon, Numerical modeling of steam injection for the removal of nonaqueous phase liquids from the subsurface, 2, Code validation and application, *Water Resources Research*, 28(2), 451-465, 1992b.
- Faust, C.R., Transport of immiscible fluids within and below the unsaturated zone, A numerical model, *Water Resources Research*, 21(4), 587-596, 1985.
- Faust, C.R., J.H. Guswa, and J.W. Mercer, Simulation of three-dimensional flow of immiscible fluids within and below the unsaturated zone, *Water Resources Research*, 25(12), 2449-2464, 1989.
- Faust, C.R., and J.O. Rumbaugh, SWANFLOW: Simultaneous water, air, and nonaqueous phase flow, Version 1.0, *International Ground Water Modeling Center*, Institute for Ground-Water Research and Education, Colorado School of Mines, Golden, Colorado 1985.
- Fayers, F.J., and T.A. Hewett, A review of current trends in petroleum reservoir description and assessment of the impacts on oil recovery, *Advances in Water Resources*, 15, 341-365, 1992.
- Ferrand, L.A., P.C.D. Milly, G.F. Pinder, and R.P. Turrin, A comparison of capillary pressure-saturation relations for drainage in two- and three-fluid porous media, *Advances in Water Resources*, 13(2), 54-63, 1990.
- Fetter, C.W., *Contaminant Hydrology*, Macmillan Publishing Company, New York, 1993.

- Forsyth, P.A., Simulation of nonaqueous phase groundwater contamination, *Advances in Water Resources*, 11, 74-83, 1988.
- Green, D.W., H. Dabiri, C.F. Weinaug, and R. Prill, Numerical modeling of unsaturated groundwater flow and comparison of the model to a field experiment, *Water Resources Research*, 6(3), 862-874, 1970.
- Guswa, J.H., Application of multi-phase flow theory at a chemical waste landfill, Niagara Falls, New York, in *Proceedings of the Second International Conference on Groundwater Quality Research*, pp. 108-111, National Center for Ground Water Research, Oklahoma State University, Stillwater, Oklahoma, 1985.
- Hochmuth, D.P., and D.K. Sunada, Groundwater model of two phase immiscible flow in course material, *Ground Water*, 23(5), 617-626, 1985.
- Holzer, T.L., Application of groundwater flow theory to a subsurface oil spill, *Ground Water*, 14(3), 138-145, 1976.
- Huyakorn, P.S., S.D. Thomas, J.W. Mercer, and B.H. Lester, SATURN: A finite element model for simulating saturated-unsaturated flow and radionuclide transport, report prepared for Electric Power Research Institute, *Geotrans, Inc.*, Sterling, Virginia, 1983.
- Kaluarachchi, J.J., and J.C. Parker, An efficient finite element method for modeling multiphase flow, *Water Resources Research*, 25(1), 43-54, 1989.
- Kuppusamy, T., J. Sheng, J.C. Parker, and R.J. Lenhard, Finite-element analysis of multiphase immiscible flow through soils, *Water Resources Research*, 23(4), 625-631, 1987.
- Land, C.S., Calculation of imbibition relative permeability for two- and three-phase flow from rock properties, *Society of Petroleum Engineers Journal*, 8, 149-156, 1968.
- Lenhard, R.J., Measurement and modeling of three-phase saturation-pressure hysteresis, *Journal of Contaminant Hydrology*, 9, 243-269, 1992.
- Lenhard, R.J., and J.C. Parker, J.C., A model for hysteretic constitutive relations governing multiphase flow, 2, Permeability-saturation relations, *Water Resources Research*, 23(12), 2197-2206, 1987.
- Lenhard, R.J., J.C. Parker, and J.J. Kaluarachchi, Comparing simulated and experimental hysteretic two-phase transient fluid flow phenomena, *Water Resources Research*, 27(8), 2113-2124, 1991.

- Leverett, M.C., and W.B. Lewis, Steady flow of gas-oil-water mixtures through unconsolidated sands, *American Institute of Mining and Metallurgical Engineers Transactions*, 142, 107-116, 1941.
- Maugh, T.H., Toxic waste disposal a growing problem, *Science*, 204, 819-823, 1979.
- Mercer, J.W., D.C. Skipp, and D. Giffin, Basics of pump-and-treat ground-water remediation technology, *Research Report EPA/600/8-90/003*, U.S. Environmental Protection Agency, Ada, Oklahoma, 1990.
- Osborne, M., and J. Sykes, Numerical modeling of immiscible organic transport at the Hyde Park landfill, *Water Resources Research*, 22(1), 25-33, 1986.
- Parker, J.C., and R.J. Lenhard, A model for hysteretic constitutive relations governing multiphase flow, 1, Saturation-pressure relations, *Water Resources Research*, 23(12), 2187-2196, 1987.
- Parker, J.C., R.J. Lenhard, and T. Kuppusamy, A parametric model for constitutive properties governing multiphase flow in porous media, *Water Resources Research*, 23(4), 618-624, 1987.
- Peaceman, D.W., *Fundamentals of Numerical Reservoir Simulation*, Elsevier Scientific Publishing Company, New York, 1977.
- Pinder, G.F., and L.M. Abriola, On the simulation of nonaqueous phase organic compounds in the subsurface, *Water Resources Research*, 22(9), 109S-119S, 1986.
- Ryan, P.A., and Y. Cohen, One-dimensional subsurface transport of a nonaqueous phase liquid containing sparingly water soluble organics: A front-tracking model, *Water Resources Research*, 27(7), 1487-1500, 1991.
- Sleep, B.E., and J.F. Sykes, Modeling the transport of volatile organics in variably saturated media, *Water Resources Research*, 25(1), 81-92, 1989.
- Sleep, B.E., and J.F. Sykes, Compositional simulation of groundwater contamination by organic compounds, 1, Model development and verification, *Water Resources Research*, 29(6), 1697-1708, 1993a.
- Sleep, B.E., and J.F. Sykes, Compositional simulation of groundwater contamination by organic compounds, 2, Model applications, *Water Resources Research*, 29(6), 1709-1718, 1993b.
- Snell, R.W., Three-phase relative permeability in an unconsolidated sand, *Journal of the Institute of Petroleum*, 48, 80-88, 1962.

- Soll, W.E., M.A. Celia, J.L. Wilson, Micromodel studies of three-fluid porous media systems: Pore scale processes relating to capillary pressure-saturation relationships, *Water Resources Research*, 29(9), 2963-2974, 1993.
- Stone, H.L., Estimation of three-phase relative permeability and residual oil data, *The Journal of Canadian Petroleum Technology*, 12, 53-61, 1973.
- U.S. Environmental Protection Agency, Proposed groundwater protection strategy, *Office of Drinking Water*, U.S. Environmental Protection Agency, Washington, D.C., 1980.
- U.S. Environmental Protection Agency, Proposed groundwater protection strategy, *Environmental Protection Agency Journal*, 9(5), 24-25, 1982.
- U.S. Environmental Protection Agency, Hazardous waste site descriptions: National priority list-final rule, *Office of Solid Waste and Emergency Response Report WH-5624*, U.S. Environmental Protection Agency, Washington, D.C., 1983.
- van Dam, J., The migration of hydrocarbons in a water bearing stratum, in *The Joint Problems of the Oil and Water Industries*, edited by P. Hepple, pp. 55-96, Elsevier Scientific Publishing Company, New York, 1967.
- van Genuchten, M., A closed-form equation for predicting the hydraulic conductivity of unsaturated soils, *Soil Science Society of America Journal*, 44, 892-898, 1980.
- Villaume, J.F., Investigations at sites contaminated with dense non-aqueous phase liquids, *Groundwater Monitoring Review*, 5(2), 60-74, 1985.
- Wilson, J.L., S.H. Conrad, W.R. Mason, W. Peplinski, and E. Hagan, Laboratory investigation of residual liquid organics from spills, leaks, and the disposal of hazardous wastes in groundwater, *Research Report EPA/600/6-90/004*, U.S. Environmental Protection Agency, Ada, Oklahoma, 1990.
- Young, L.C., and R.E. Stephenson, A generalized compositional approach for reservoir simulation, *Society of Petroleum Engineers Journal*, 23(5), 727-742, 1983.

APPENDIX A  
SWANFLOW Input Files



```

1. title*
2-D Unsaturated-Saturated Infiltration of Gasoline
2. date
7 May 1994
3. run identifier
RUN1
4. x, z, y, number of Newton-Raphson iterations, bandwidth, total time steps, steps between printing output, print
potentials, number of SSOR iterations, coordinate system
8 20 1 4 0 100 1 0 0 1 0
5-1. balance error, initial time, water density, NAPL density, water viscosity, NAPL viscosity
0.02000 0. 1000.00 730.00 1.000E-3 4.500E-4
5-2. gravity term x-direction, gravity term z-direction, SSOR relaxation factor, SSOR convergence tolerance
-9.80 0.00000 1.00 0.100E-04
6-1. number of capillary pressure-relative permeability tables
1
6-2a. number of entries in table
13
6-2b. capillary pressure, water saturation, relative permeability water, relative permeability NAPL
103425.0 -0.10 0.00000 1.00000
103425.0 0.00 0.00000 1.00000
103425.0 0.10 0.00000 0.82000
103425.0 0.20 0.00000 0.68000
27580.0 0.30 0.04000 0.55000
10343.0 0.40 0.10000 0.43000
7585.0 0.50 0.18000 0.31000
7447.0 0.60 0.30000 0.20000
7309.0 0.70 0.44000 0.12000
7171.0 0.80 0.60000 0.05000
7033.0 0.90 0.80000 0.00000
6895.0 1.00 1.00000 0.00000
6895.0 1.10 1.00000 0.00000
6-2c. number of entries in table, relative permeability of NAPL at residual water saturation
2 0.680
6-2d. capillary pressure between NAPL and air, air saturation, relative permeability NAPL, relative permeability air
-98000.0 1.00 -0.3200 1.000
0.0 0.00 0.6800 0.000
7-1. number of permeability classes
1
7-2. permeability x-, z-, y-directions
0.100E-11 0.100E-11 0.100E-11
8-1. number of porosity classes
1
8-2. reference porosity, aquifer compressibility, reference pressure
0.300 1.0E-15 0.0
9a. grid spacing x-direction
1.000 1.900 3.610 6.859 13.032 24.761 47.046 89.387
9b. grid spacing z-direction
0.250 0.250 0.250 0.250 0.250 0.250 0.250 0.250
0.250 0.250 0.250 0.250 0.250 0.250 0.250 0.250
0.250 0.250 0.250 0.250
9c. grid spacing y-direction
1.000
10-1. number of property combination sets
1
10-2. capillary pressure-relative permeability class number, permeability class number, porosity class number
1 1 1
11. number of active blocks per slice
152
12. grid block number
1 2 3 4 5 6 7 8
9 10 11 12 13 14 15 16
17 18 19 20 21 22 23 24
25 26 27 28 29 30 31 32
33 34 35 36 37 38 39 40
41 42 43 44 45 46 47 48
49 50 51 52 53 54 55 56
57 58 59 60 61 62 63 64
65 66 67 68 69 70 71 72
73 74 75 76 77 78 79 80
81 82 83 84 85 86 87 88
89 90 91 92 93 94 95 96
97 98 99 100 101 102 103 104
105 106 107 108 109 110 111 112
113 114 115 116 117 118 119 120
121 122 123 124 125 126 127 128
129 130 131 132 133 134 135 136
137 138 139 140 141 142 143 144
145 146 147 148 149 150 151 152
-1 -1 -1 -1 -1 -1 -1 -1
14-1. initial conditions-uniform or nonuniform
1
14-3. initial NAPL pressure in each of the numbered grid blocks
-14700.00 -14700.00 -14700.00 -14700.00 -14700.00 -14700.00 -14700.00 -14700.00
-12250.00 -12250.00 -12250.00 -12250.00 -12250.00 -12250.00 -12250.00 -12250.00
-9800.00 -9800.00 -9800.00 -9800.00 -9800.00 -9800.00 -9800.00 -9800.00
-7350.00 -7350.00 -7350.00 -7350.00 -7350.00 -7350.00 -7350.00 -7350.00
-4900.00 -4900.00 -4900.00 -4900.00 -4900.00 -4900.00 -4900.00 -4900.00
-2450.00 -2450.00 -2450.00 -2450.00 -2450.00 -2450.00 -2450.00 -2450.00
0.00 0.00 0.00 0.00 0.00 0.00 0.00 0.00
2450.00 2450.00 2450.00 2450.00 2450.00 2450.00 2450.00 2450.00
4900.00 4900.00 4900.00 4900.00 4900.00 4900.00 4900.00 4900.00
7350.00 7350.00 7350.00 7350.00 7350.00 7350.00 7350.00 7350.00
9800.00 9800.00 9800.00 9800.00 9800.00 9800.00 9800.00 9800.00
12250.00 12250.00 12250.00 12250.00 12250.00 12250.00 12250.00 12250.00
14700.00 14700.00 14700.00 14700.00 14700.00 14700.00 14700.00 14700.00
17150.00 17150.00 17150.00 17150.00 17150.00 17150.00 17150.00 17150.00
19600.00 19600.00 19600.00 19600.00 19600.00 19600.00 19600.00 19600.00
22050.00 22050.00 22050.00 22050.00 22050.00 22050.00 22050.00 22050.00
24500.00 24500.00 24500.00 24500.00 24500.00 24500.00 24500.00 24500.00

```

\*The numbered, italicized lines, corresponding to input card numbers, are for the reader's information only and are not included in the input file.

26950.00	26950.00	26950.00	26950.00	26950.00	26950.00	26950.00	26950.00
29400.00	29400.00	29400.00	29400.00	29400.00	29400.00	29400.00	29400.00
31850.00	31850.00	31850.00	31850.00	31850.00	31850.00	31850.00	31850.00

14-4. initial water saturation in each of the numbered grid blocks\*

0.8500	0.8500	0.8500	0.8500	0.8500	0.8500	0.8500	0.8500
0.8750	0.8750	0.8750	0.8750	0.8750	0.8750	0.8750	0.8750
0.9000	0.9000	0.9000	0.9000	0.9000	0.9000	0.9000	0.9000
0.9250	0.9250	0.9250	0.9250	0.9250	0.9250	0.9250	0.9250
0.9500	0.9500	0.9500	0.9500	0.9500	0.9500	0.9500	0.9500
0.9750	0.9750	0.9750	0.9750	0.9750	0.9750	0.9750	0.9750
1.0000	1.0000	1.0000	1.0000	1.0000	1.0000	1.0000	1.0000
1.0000	1.0000	1.0000	1.0000	1.0000	1.0000	1.0000	1.0000
1.0000	1.0000	1.0000	1.0000	1.0000	1.0000	1.0000	1.0000
1.0000	1.0000	1.0000	1.0000	1.0000	1.0000	1.0000	1.0000
1.0000	1.0000	1.0000	1.0000	1.0000	1.0000	1.0000	1.0000
1.0000	1.0000	1.0000	1.0000	1.0000	1.0000	1.0000	1.0000
1.0000	1.0000	1.0000	1.0000	1.0000	1.0000	1.0000	1.0000
1.0000	1.0000	1.0000	1.0000	1.0000	1.0000	1.0000	1.0000
1.0000	1.0000	1.0000	1.0000	1.0000	1.0000	1.0000	1.0000
1.0000	1.0000	1.0000	1.0000	1.0000	1.0000	1.0000	1.0000
1.0000	1.0000	1.0000	1.0000	1.0000	1.0000	1.0000	1.0000
1.0000	1.0000	1.0000	1.0000	1.0000	1.0000	1.0000	1.0000
1.0000	1.0000	1.0000	1.0000	1.0000	1.0000	1.0000	1.0000
1.0000	1.0000	1.0000	1.0000	1.0000	1.0000	1.0000	1.0000
1.0000	1.0000	1.0000	1.0000	1.0000	1.0000	1.0000	1.0000
1.0000	1.0000	1.0000	1.0000	1.0000	1.0000	1.0000	1.0000

15. initial time step, min time step, max saturation change per time step, time step multiplier, time to read new recurrent data, number source/sink blocks, source/sink change

1000000	10000	0.10000	1.500	3.1536E07	8	1
---------	-------	---------	-------	-----------	---	---

16-1. column number (i), slice number (j), total mass source rate, mass fraction of water in source term

1	1	2.9459E-5	0.1206
---	---	-----------	--------

16-2. layers over which source/sink is applied

1	0	0	0	0	0	0	0	0	0	0	0
2	1	6.0249E-6	1.0000	0	0	0	0	0	0	0	0
3	1	1.1447E-5	1.0000	0	0	0	0	0	0	0	0
4	1	2.1750E-5	1.0000	0	0	0	0	0	0	0	0
5	1	4.1325E-5	1.0000	0	0	0	0	0	0	0	0
6	1	7.8517E-5	1.0000	0	0	0	0	0	0	0	0
7	1	1.4918E-4	1.0000	0	0	0	0	0	0	0	0
8	1	2.8344E-4	1.0000	0	0	0	0	0	0	0	0

15. initial time step, min time step, max saturation change per time step, time step multiplier, time to read new recurrent data, number source/sink blocks, source/sink change

1000000	10000	0.10000	1.500	9.4608E07	8	1
---------	-------	---------	-------	-----------	---	---

16-1. column number (i), slice number (j), total mass source rate, mass fraction of water in source term

1	1	2.9459E-5	0.1206
---	---	-----------	--------

16-2. layers over which source/sink is applied

1	0	0	0	0	0	0	0	0	0	0	0
2	1	6.0249E-6	1.0000	0	0	0	0	0	0	0	0
3	1	1.1447E-5	1.0000	0	0	0	0	0	0	0	0
4	1	2.1750E-5	1.0000	0	0	0	0	0	0	0	0
5	1	4.1325E-5	1.0000	0	0	0	0	0	0	0	0
6	1	7.8517E-5	1.0000	0	0	0	0	0	0	0	0
7	1	1.4918E-4	1.0000	0	0	0	0	0	0	0	0
8	1	2.8344E-4	1.0000	0	0	0	0	0	0	0	0

15. initial time step, min time step, max saturation change per time step, time step multiplier, time to read new recurrent data, number source/sink blocks, source/sink change

1000000	10000	0.10000	1.500	1.5768E08	8	1
---------	-------	---------	-------	-----------	---	---

16-1. column number (i), slice number (j), total mass source rate, mass fraction of water in source term

1	1	2.9459E-5	0.1206
---	---	-----------	--------

16-2. layers over which source/sink is applied

1	0	0	0	0	0	0	0	0	0	0	0
2	1	6.0249E-6	1.0000	0	0	0	0	0	0	0	0
3	1	1.1447E-5	1.0000	0	0	0	0	0	0	0	0
4	1	2.1750E-5	1.0000	0	0	0	0	0	0	0	0

\*The numbered, italicized lines, corresponding to input card numbers, are for the reader's information only and are not included in the input file.

```

5      1 4.1325E-5      1.0000
1      0 0 0 0 0 0 0 0 0 0 0 0 0 0
0      0 0 0 0 0 0 0 0 0 0 0 0 0 0
6      1 7.8517E-5      1.0000
1      0 0 0 0 0 0 0 0 0 0 0 0 0 0
0      0 0 0 0 0 0 0 0 0 0 0 0 0 0
7      1 1.4918E-4      1.0000
1      0 0 0 0 0 0 0 0 0 0 0 0 0 0
0      0 0 0 0 0 0 0 0 0 0 0 0 0 0
8      1 2.8344E-4      1.0000
1      0 0 0 0 0 0 0 0 0 0 0 0 0 0
0      0 0 0 0 0 0 0 0 0 0 0 0 0 0
15.  initial time step, min time step, max saturation change per time step, time step multiplier, time to read new
      recurrent data, number source/sink blocks, source/sink change*
1000000      10000      0.10000      1.500 3.1536E08      8      1
16-1. column number (i), slice number (j), total mass source rate, mass fraction of water in source term
1      1 2.9459E-5      0.1206
16-2. layers over which source/sink is applied
1      0 0 0 0 0 0 0 0 0 0 0 0 0 0
0      0 0 0 0 0 0 0 0 0 0 0 0 0 0
2      1 6.0249E-6      1.0000
1      0 0 0 0 0 0 0 0 0 0 0 0 0 0
0      0 0 0 0 0 0 0 0 0 0 0 0 0 0
3      1 1.1447E-5      1.0000
1      0 0 0 0 0 0 0 0 0 0 0 0 0 0
0      0 0 0 0 0 0 0 0 0 0 0 0 0 0
4      1 2.1750E-5      1.0000
1      0 0 0 0 0 0 0 0 0 0 0 0 0 0
0      0 0 0 0 0 0 0 0 0 0 0 0 0 0
5      1 4.1325E-5      1.0000
1      0 0 0 0 0 0 0 0 0 0 0 0 0 0
0      0 0 0 0 0 0 0 0 0 0 0 0 0 0
6      1 7.8517E-5      1.0000
1      0 0 0 0 0 0 0 0 0 0 0 0 0 0
0      0 0 0 0 0 0 0 0 0 0 0 0 0 0
7      1 1.4918E-4      1.0000
1      0 0 0 0 0 0 0 0 0 0 0 0 0 0
0      0 0 0 0 0 0 0 0 0 0 0 0 0 0
8      1 2.8344E-4      1.0000
1      0 0 0 0 0 0 0 0 0 0 0 0 0 0
0      0 0 0 0 0 0 0 0 0 0 0 0 0 0
15.  zeros to end simulation
0.      0.      0.00000      0.000      0.000      0      0

```

\*The numbered, italicized lines, corresponding to input card numbers, are for the reader's information only and are not included in the input file.









2-D Unsaturated-Saturated Infiltration of 10W-30 Motor Oil  
8 May 1994

RUN1  
8 20 1 4 0 150 1 0 0 1 0  
0.02000 0. 1000.00 869.00 1.000E-3 1.300E-1  
-9.80 0.00000 1.00 0.100E-04

1  
13  
103425.0 -0.10 0.00000 1.00000  
103425.0 0.00 0.00000 1.00000  
103425.0 0.10 0.00000 0.82000  
103425.0 0.20 0.00000 0.68000  
27580.0 0.30 0.04000 0.55000  
10343.0 0.40 0.10000 0.43000  
7585.0 0.50 0.18000 0.31000  
7447.0 0.60 0.30000 0.20000  
7309.0 0.70 0.44000 0.12000  
7171.0 0.80 0.60000 0.05000  
7033.0 0.90 0.80000 0.00000  
6895.0 1.00 1.00000 0.00000  
6895.0 1.10 1.00000 0.00000

2 0.680  
-98000.0 1.00 -0.3200 1.000  
0.0 0.00 0.6800 0.000

1  
0.100E-11 0.100E-11 0.100E-11

1  
0.300 1.0E-15 0.0  
1.000 1.900 3.610 6.859 13.032 24.761 47.046 89.387  
0.250 0.250 0.250 0.250 0.250 0.250 0.250 0.250  
0.250 0.250 0.250 0.250 0.250 0.250 0.250 0.250  
0.250 0.250 0.250 0.250  
1.000

1  
1 1 1

152  
1 2 3 4 5 6 7 8  
9 10 11 12 13 14 15 16  
17 18 19 20 21 22 23 24  
25 26 27 28 29 30 31 32  
33 34 35 36 37 38 39 40  
41 42 43 44 45 46 47 48  
49 50 51 52 53 54 55 56  
57 58 59 60 61 62 63 64  
65 66 67 68 69 70 71 72  
73 74 75 76 77 78 79 80  
81 82 83 84 85 86 87 88  
89 90 91 92 93 94 95 96  
97 98 99 100 101 102 103 104  
105 106 107 108 109 110 111 112  
113 114 115 116 117 118 119 120  
121 122 123 124 125 126 127 128  
129 130 131 132 133 134 135 136  
137 138 139 140 141 142 143 144  
145 146 147 148 149 150 151 152  
-1 -1 -1 -1 -1 -1 -1 -1

1  
-14700.00 -14700.00 -14700.00 -14700.00 -14700.00 -14700.00 -14700.00 -14700.00 -14700.00  
-12250.00 -12250.00 -12250.00 -12250.00 -12250.00 -12250.00 -12250.00 -12250.00 -12250.00  
-9800.00 -9800.00 -9800.00 -9800.00 -9800.00 -9800.00 -9800.00 -9800.00 -9800.00  
-7350.00 -7350.00 -7350.00 -7350.00 -7350.00 -7350.00 -7350.00 -7350.00 -7350.00  
-4900.00 -4900.00 -4900.00 -4900.00 -4900.00 -4900.00 -4900.00 -4900.00 -4900.00  
-2450.00 -2450.00 -2450.00 -2450.00 -2450.00 -2450.00 -2450.00 -2450.00 -2450.00  
0.00 0.00 0.00 0.00 0.00 0.00 0.00 0.00 0.00  
2450.00 2450.00 2450.00 2450.00 2450.00 2450.00 2450.00 2450.00 2450.00  
4900.00 4900.00 4900.00 4900.00 4900.00 4900.00 4900.00 4900.00 4900.00  
7350.00 7350.00 7350.00 7350.00 7350.00 7350.00 7350.00 7350.00 7350.00  
9800.00 9800.00 9800.00 9800.00 9800.00 9800.00 9800.00 9800.00 9800.00  
12250.00 12250.00 12250.00 12250.00 12250.00 12250.00 12250.00 12250.00 12250.00  
14700.00 14700.00 14700.00 14700.00 14700.00 14700.00 14700.00 14700.00 14700.00  
17150.00 17150.00 17150.00 17150.00 17150.00 17150.00 17150.00 17150.00 17150.00  
19600.00 19600.00 19600.00 19600.00 19600.00 19600.00 19600.00 19600.00 19600.00  
22050.00 22050.00 22050.00 22050.00 22050.00 22050.00 22050.00 22050.00 22050.00  
24500.00 24500.00 24500.00 24500.00 24500.00 24500.00 24500.00 24500.00 24500.00  
26950.00 26950.00 26950.00 26950.00 26950.00 26950.00 26950.00 26950.00 26950.00  
29400.00 29400.00 29400.00 29400.00 29400.00 29400.00 29400.00 29400.00 29400.00  
31850.00 31850.00 31850.00 31850.00 31850.00 31850.00 31850.00 31850.00 31850.00  
0.8500 0.8500 0.8500 0.8500 0.8500 0.8500 0.8500 0.8500 0.8500  
0.8750 0.8750 0.8750 0.8750 0.8750 0.8750 0.8750 0.8750 0.8750  
0.9000 0.9000 0.9000 0.9000 0.9000 0.9000 0.9000 0.9000 0.9000  
0.9250 0.9250 0.9250 0.9250 0.9250 0.9250 0.9250 0.9250 0.9250  
0.9500 0.9500 0.9500 0.9500 0.9500 0.9500 0.9500 0.9500 0.9500  
0.9750 0.9750 0.9750 0.9750 0.9750 0.9750 0.9750 0.9750 0.9750  
1.0000 1.0000 1.0000 1.0000 1.0000 1.0000 1.0000 1.0000 1.0000  
1.0000 1.0000 1.0000 1.0000 1.0000 1.0000 1.0000 1.0000 1.0000  
1.0000 1.0000 1.0000 1.0000 1.0000 1.0000 1.0000 1.0000 1.0000  
1.0000 1.0000 1.0000 1.0000 1.0000 1.0000 1.0000 1.0000 1.0000  
1.0000 1.0000 1.0000 1.0000 1.0000 1.0000 1.0000 1.0000 1.0000  
1.0000 1.0000 1.0000 1.0000 1.0000 1.0000 1.0000 1.0000 1.0000  
1.0000 1.0000 1.0000 1.0000 1.0000 1.0000 1.0000 1.0000 1.0000  
1.0000 1.0000 1.0000 1.0000 1.0000 1.0000 1.0000 1.0000 1.0000  
1.0000 1.0000 1.0000 1.0000 1.0000 1.0000 1.0000 1.0000 1.0000  
1.0000 1.0000 1.0000 1.0000 1.0000 1.0000 1.0000 1.0000 1.0000  
1.0000 1.0000 1.0000 1.0000 1.0000 1.0000 1.0000 1.0000 1.0000  
1.0000 1.0000 1.0000 1.0000 1.0000 1.0000 1.0000 1.0000 1.0000  
1.0000 1.0000 1.0000 1.0000 1.0000 1.0000 1.0000 1.0000 1.0000  
1.0000 1.0000 1.0000 1.0000 1.0000 1.0000 1.0000 1.0000 1.0000  
1.0000 1.0000 1.0000 1.0000 1.0000 1.0000 1.0000 1.0000 1.0000  
1000000 10000 0.10000 1.500 3.1536E07 8 1

1 1 3.4464E-5 0.1013  
1 0 0 0 0 0 0 0 0 0 0 0  
2 1 6.0249E-6 1.0000  
1 0 0 0 0 0 0 0 0 0 0 0  
3 1 1.1447E-5 1.0000  
1 0 0 0 0 0 0 0 0 0 0 0





2-D Unsaturated-Saturated Infiltration of Water  
8 May 1994

```

RUN1
 8 20 1 4 0 100 1 0 C 1 0
0.02000 0. 1000.00 1000.00 1.000E-3 1.000E-3
-9.80 0.00000 1.00 0.100E-04
 1
 13
103425.0 -0.10 0.00000 1.00000
103425.0 0.00 0.00000 1.00000
103425.0 0.10 0.00000 0.82000
103425.0 0.20 0.00000 0.68000
27580.0 0.30 0.04000 0.55000
10343.0 0.40 0.10000 0.43000
7585.0 0.50 0.18000 0.31000
7447.0 0.60 0.30000 0.20000
7309.0 0.70 0.44000 0.12000
7171.0 0.80 0.60000 0.05000
7033.0 0.90 0.80000 0.00000
6895.0 1.00 1.00000 0.00000
6895.0 1.10 1.00000 0.00000
 2
-98000.0 0.680 1.00 -0.3200 1.000
 0.0 0.00 0.6800 0.000
 1
0.100E-11 0.100E-11 0.100E-11
 1
 0.300 1.0E-15 0.0
1.000 1.900 3.610 6.859 13.032 24.761 47.046 89.387
0.250 0.250 0.250 0.250 0.250 0.250 0.250 0.250
0.250 0.250 0.250 0.250 0.250 0.250 0.250 0.250
0.250 0.250 0.250 0.250
1.000
 1
 1 1 1
152
 1 2 3 4 5 6 7 8
 9 10 11 12 13 14 15 16
17 18 19 20 21 22 23 24
25 26 27 28 29 30 31 32
33 34 35 36 37 38 39 40
41 42 43 44 45 46 47 48
49 50 51 52 53 54 55 56
57 58 59 60 61 62 63 64
65 66 67 68 69 70 71 72
73 74 75 76 77 78 79 80
81 82 83 84 85 86 87 88
89 90 91 92 93 94 95 96
97 98 99 100 101 102 103 104
105 106 107 108 109 110 111 112
113 114 115 116 117 118 119 120
121 122 123 124 125 126 127 128
129 130 131 132 133 134 135 136
137 138 139 140 141 142 143 144
145 146 147 148 149 150 151 152
-1 -1 -1 -1 -1 -1 -1 -1
 1
-14700.00 -14700.00 -14700.00 -14700.00 -14700.00 -14700.00 -14700.00 -14700.00
-12250.00 -12250.00 -12250.00 -12250.00 -12250.00 -12250.00 -12250.00 -12250.00
-9800.00 -9800.00 -9800.00 -9800.00 -9800.00 -9800.00 -9800.00 -9800.00
-7350.00 -7350.00 -7350.00 -7350.00 -7350.00 -7350.00 -7350.00 -7350.00
-4900.00 -4900.00 -4900.00 -4900.00 -4900.00 -4900.00 -4900.00 -4900.00
-2450.00 -2450.00 -2450.00 -2450.00 -2450.00 -2450.00 -2450.00 -2450.00
 0.00 0.00 0.00 0.00 0.00 0.00 0.00 0.00
2450.00 2450.00 2450.00 2450.00 2450.00 2450.00 2450.00 2450.00
4900.00 4900.00 4900.00 4900.00 4900.00 4900.00 4900.00 4900.00
7350.00 7350.00 7350.00 7350.00 7350.00 7350.00 7350.00 7350.00
9800.00 9800.00 9800.00 9800.00 9800.00 9800.00 9800.00 9800.00
12250.00 12250.00 12250.00 12250.00 12250.00 12250.00 12250.00 12250.00
14700.00 14700.00 14700.00 14700.00 14700.00 14700.00 14700.00 14700.00
17150.00 17150.00 17150.00 17150.00 17150.00 17150.00 17150.00 17150.00
19600.00 19600.00 19600.00 19600.00 19600.00 19600.00 19600.00 19600.00
22050.00 22050.00 22050.00 22050.00 22050.00 22050.00 22050.00 22050.00
24500.00 24500.00 24500.00 24500.00 24500.00 24500.00 24500.00 24500.00
26950.00 26950.00 26950.00 26950.00 26950.00 26950.00 26950.00 26950.00
29400.00 29400.00 29400.00 29400.00 29400.00 29400.00 29400.00 29400.00
31850.00 31850.00 31850.00 31850.00 31850.00 31850.00 31850.00 31850.00
 0.8500 0.8500 0.8500 0.8500 0.8500 0.8500 0.8500 0.8500
 0.8750 0.8750 0.8750 0.8750 0.8750 0.8750 0.8750 0.8750
 0.9000 0.9000 0.9000 0.9000 0.9000 0.9000 0.9000 0.9000
 0.9250 0.9250 0.9250 0.9250 0.9250 0.9250 0.9250 0.9250
 0.9500 0.9500 0.9500 0.9500 0.9500 0.9500 0.9500 0.9500
 0.9750 0.9750 0.9750 0.9750 0.9750 0.9750 0.9750 0.9750
 1.0000 1.0000 1.0000 1.0000 1.0000 1.0000 1.0000 1.0000
 1.0000 1.0000 1.0000 1.0000 1.0000 1.0000 1.0000 1.0000
 1.0000 1.0000 1.0000 1.0000 1.0000 1.0000 1.0000 1.0000
 1.0000 1.0000 1.0000 1.0000 1.0000 1.0000 1.0000 1.0000
 1.0000 1.0000 1.0000 1.0000 1.0000 1.0000 1.0000 1.0000
 1.0000 1.0000 1.0000 1.0000 1.0000 1.0000 1.0000 1.0000
 1.0000 1.0000 1.0000 1.0000 1.0000 1.0000 1.0000 1.0000
 1.0000 1.0000 1.0000 1.0000 1.0000 1.0000 1.0000 1.0000
 1.0000 1.0000 1.0000 1.0000 1.0000 1.0000 1.0000 1.0000
 1.0000 1.0000 1.0000 1.0000 1.0000 1.0000 1.0000 1.0000
 1.0000 1.0000 1.0000 1.0000 1.0000 1.0000 1.0000 1.0000
 1.0000 1.0000 1.0000 1.0000 1.0000 1.0000 1.0000 1.0000
 1.0000 1.0000 1.0000 1.0000 1.0000 1.0000 1.0000 1.0000
 1.0000 1.0000 1.0000 1.0000 1.0000 1.0000 1.0000 1.0000
 1.0000 1.0000 1.0000 1.0000 1.0000 1.0000 1.0000 1.0000
 1.0000 1.0000 1.0000 1.0000 1.0000 1.0000 1.0000 1.0000
 1.0000 1.0000 1.0000 1.0000 1.0000 1.0000 1.0000 1.0000
 1.0000 1.0000 1.0000 1.0000 1.0000 1.0000 1.0000 1.0000
 1.0000 1.0000 1.0000 1.0000 1.0000 1.0000 1.0000 1.0000
 1.0000 1.0000 1.0000 1.0000 1.0000 1.0000 1.0000 1.0000
 10000 10000 0.10000 1.500 3.1536E07 8 1
 1 1 3.9181E-5 0.0881 0 0 0 0 0 0 0 0 0 0
 1 0 0 0 0 0 0 0 0 0 0 0 0 0
 1 0 0 0 0 0 0 0 0 0 0 0 0 0
 2 1 6.0249E-6 1.0000 0 0 0 0 0 0 0 0 0 0
 1 0 0 0 0 0 0 0 0 0 0 0 0 0
 0 0 0 0 0 0 0 0 0 0 0 0 0 0
 3 1 1.1447E-5 1.0000 0 0 0 0 0 0 0 0 0 0
 1 0 0 0 0 0 0 0 0 0 0 0 0 0

```



2-D Unsaturated-Saturated Infiltration of Phenol  
8 May 1994

```

RUN1
      8 20 1 4 0 100 1 0 0 1 0
      0.02000 0. 1000.00 1053.30 1.000E-3 4.076E-3
      -9.80 0.00000 1.00 0.100E-04

1
13
103425.0 -0.10 0.00000 1.00000
103425.0 0.00 0.00000 1.00000
103425.0 0.10 0.00000 0.82000
103425.0 0.20 0.00000 0.68000
27580.0 0.30 0.04000 0.55000
10343.0 0.40 0.10000 0.43000
7585.0 0.50 0.18000 0.31000
7447.0 0.60 0.30000 0.20000
7309.0 0.70 0.44000 0.12000
7171.0 0.80 0.60000 0.05000
7033.0 0.90 0.80000 0.00000
6895.0 1.00 1.00000 0.00000
6895.0 1.10 1.00000 0.00000
2 0.680
-98000.0 1.00 -0.3200 1.000
0.0 0.00 0.6800 0.000
1
0.100E-11 0.100E-11 0.100E-11
1
0.300 1.0E-15 0.0
1.000 1.900 3.610 6.859 13.032 24.761 47.046 89.387
0.250 0.250 0.250 0.250 0.250 0.250 0.250 0.250
0.250 0.250 0.250 0.250 0.250 0.250 0.250 0.250
0.250 0.250 0.250 0.250
1.000

1
1 1 1
152
1 2 3 4 5 6 7 8
9 10 11 12 13 14 15 16
17 18 19 20 21 22 23 24
25 26 27 28 29 30 31 32
33 34 35 36 37 38 39 40
41 42 43 44 45 46 47 48
49 50 51 52 53 54 55 56
57 58 59 60 61 62 63 64
65 66 67 68 69 70 71 72
73 74 75 76 77 78 79 80
81 82 83 84 85 86 87 88
89 90 91 92 93 94 95 96
97 98 99 100 101 102 103 104
105 106 107 108 109 110 111 112
113 114 115 116 117 118 119 120
121 122 123 124 125 126 127 128
129 130 131 132 133 134 135 136
137 138 139 140 141 142 143 144
145 146 147 148 149 150 151 152
-1 -1 -1 -1 -1 -1 -1 -1
1
-14700.00 -14700.00 -14700.00 -14700.00 -14700.00 -14700.00 -14700.00 -14700.00
-12250.00 -12250.00 -12250.00 -12250.00 -12250.00 -12250.00 -12250.00 -12250.00
-9800.00 -9800.00 -9800.00 -9800.00 -9800.00 -9800.00 -9800.00 -9800.00
-7350.00 -7350.00 -7350.00 -7350.00 -7350.00 -7350.00 -7350.00 -7350.00
-4900.00 -4900.00 -4900.00 -4900.00 -4900.00 -4900.00 -4900.00 -4900.00
-2450.00 -2450.00 -2450.00 -2450.00 -2450.00 -2450.00 -2450.00 -2450.00
0.00 0.00 0.00 0.00 0.00 0.00 0.00 0.00
2450.00 2450.00 2450.00 2450.00 2450.00 2450.00 2450.00 2450.00
4900.00 4900.00 4900.00 4900.00 4900.00 4900.00 4900.00 4900.00
7350.00 7350.00 7350.00 7350.00 7350.00 7350.00 7350.00 7350.00
9800.00 9800.00 9800.00 9800.00 9800.00 9800.00 9800.00 9800.00
12250.00 12250.00 12250.00 12250.00 12250.00 12250.00 12250.00 12250.00
14700.00 14700.00 14700.00 14700.00 14700.00 14700.00 14700.00 14700.00
17150.00 17150.00 17150.00 17150.00 17150.00 17150.00 17150.00 17150.00
19600.00 19600.00 19600.00 19600.00 19600.00 19600.00 19600.00 19600.00
22050.00 22050.00 22050.00 22050.00 22050.00 22050.00 22050.00 22050.00
24500.00 24500.00 24500.00 24500.00 24500.00 24500.00 24500.00 24500.00
26950.00 26950.00 26950.00 26950.00 26950.00 26950.00 26950.00 26950.00
29400.00 29400.00 29400.00 29400.00 29400.00 29400.00 29400.00 29400.00
31850.00 31850.00 31850.00 31850.00 31850.00 31850.00 31850.00 31850.00
0.8500 0.8500 0.8500 0.8500 0.8500 0.8500 0.8500 0.8500
0.8750 0.8750 0.8750 0.8750 0.8750 0.8750 0.8750 0.8750
0.9000 0.9000 0.9000 0.9000 0.9000 0.9000 0.9000 0.9000
0.9250 0.9250 0.9250 0.9250 0.9250 0.9250 0.9250 0.9250
0.9500 0.9500 0.9500 0.9500 0.9500 0.9500 0.9500 0.9500
0.9750 0.9750 0.9750 0.9750 0.9750 0.9750 0.9750 0.9750
1.0000 1.0000 1.0000 1.0000 1.0000 1.0000 1.0000 1.0000
1.0000 1.0000 1.0000 1.0000 1.0000 1.0000 1.0000 1.0000
1.0000 1.0000 1.0000 1.0000 1.0000 1.0000 1.0000 1.0000
1.0000 1.0000 1.0000 1.0000 1.0000 1.0000 1.0000 1.0000
1.0000 1.0000 1.0000 1.0000 1.0000 1.0000 1.0000 1.0000
1.0000 1.0000 1.0000 1.0000 1.0000 1.0000 1.0000 1.0000
1.0000 1.0000 1.0000 1.0000 1.0000 1.0000 1.0000 1.0000
1.0000 1.0000 1.0000 1.0000 1.0000 1.0000 1.0000 1.0000
1.0000 1.0000 1.0000 1.0000 1.0000 1.0000 1.0000 1.0000
1.0000 1.0000 1.0000 1.0000 1.0000 1.0000 1.0000 1.0000
1.0000 1.0000 1.0000 1.0000 1.0000 1.0000 1.0000 1.0000
1.0000 1.0000 1.0000 1.0000 1.0000 1.0000 1.0000 1.0000
1.0000 1.0000 1.0000 1.0000 1.0000 1.0000 1.0000 1.0000
1.0000 1.0000 1.0000 1.0000 1.0000 1.0000 1.0000 1.0000
1.0000 1.0000 1.0000 1.0000 1.0000 1.0000 1.0000 1.0000
10000000 10000 0.10000 1.500 3.1536E07 8 1
1 1 4.1101E-5 0.0836
1 0 0 0 0 0 0 0
0 0 0 0 1.0000
1 0 0 0 0 0 0 0
0 0 0 0
3 1 1.1447E-5 1.0000
1 0 0 0 0 0 0 0

```



2-D Unsaturated-Saturated Infiltration of o-Nitrotoluene  
8 May 1994

RUN1

```

8 20 1 4 0 100 1 0 0 1 0
0.02000 0. 1000.00 1152.90 1.000E-3 2.370E-3
-9.80 0.00000 1.00 0.100E-04
1
13
103425.0 -0.10 0.00000 1.00000
103425.0 0.00 0.00000 1.00000
103425.0 0.10 0.00000 0.82000
103425.0 0.20 0.00000 0.68000
27580.0 0.30 0.04000 0.55000
10343.0 0.40 0.10000 0.43000
7585.0 0.50 0.18000 0.31000
7447.0 0.60 0.30000 0.20000
7309.0 0.70 0.44000 0.12000
7171.0 0.80 0.60000 0.05000
7033.0 0.90 0.80000 0.00000
6895.0 1.00 1.00000 0.00000
6895.0 1.10 1.00000 0.00000
2 0.680
-98000.0 1.00 -0.3200 1.000
0.0 0.00 0.6800 0.000
1
0.100E-11 0.100E-11 0.100E-11
1
0.300 1.0E-15 0.0
1.000 1.900 3.610 6.859 13.032 24.761 47.046 89.387
0.250 0.250 0.250 0.250 0.250 0.250 0.250 0.250
0.250 0.250 0.250 0.250 0.250 0.250 0.250 0.250
1.000
1
1 1 1
152
1 2 3 4 5 6 7 8
9 10 11 12 13 14 15 16
17 18 19 20 21 22 23 24
25 26 27 28 29 30 31 32
33 34 35 36 37 38 39 40
41 42 43 44 45 46 47 48
49 50 51 52 53 54 55 56
57 58 59 60 61 62 63 64
65 66 67 68 69 70 71 72
73 74 75 76 77 78 79 80
81 82 83 84 85 86 87 88
89 90 91 92 93 94 95 96
97 98 99 100 101 102 103 104
105 106 107 108 109 110 111 112
113 114 115 116 117 118 119 120
121 122 123 124 125 126 127 128
129 130 131 132 133 134 135 136
137 138 139 140 141 142 143 144
145 146 147 148 149 150 151 152
-1 -1 -1 -1 -1 -1 -1 -1
1
-14700.00 -14700.00 -14700.00 -14700.00 -14700.00 -14700.00 -14700.00 -14700.00
-12250.00 -12250.00 -12250.00 -12250.00 -12250.00 -12250.00 -12250.00 -12250.00
-9800.00 -9800.00 -9800.00 -9800.00 -9800.00 -9800.00 -9800.00 -9800.00
-7350.00 -7350.00 -7350.00 -7350.00 -7350.00 -7350.00 -7350.00 -7350.00
-4900.00 -4900.00 -4900.00 -4900.00 -4900.00 -4900.00 -4900.00 -4900.00
-2450.00 -2450.00 -2450.00 -2450.00 -2450.00 -2450.00 -2450.00 -2450.00
0.00 0.00 0.00 0.00 0.00 0.00 0.00 0.00
2450.00 2450.00 2450.00 2450.00 2450.00 2450.00 2450.00 2450.00
4900.00 4900.00 4900.00 4900.00 4900.00 4900.00 4900.00 4900.00
7350.00 7350.00 7350.00 7350.00 7350.00 7350.00 7350.00 7350.00
9800.00 9800.00 9800.00 9800.00 9800.00 9800.00 9800.00 9800.00
12250.00 12250.00 12250.00 12250.00 12250.00 12250.00 12250.00 12250.00
14700.00 14700.00 14700.00 14700.00 14700.00 14700.00 14700.00 14700.00
17150.00 17150.00 17150.00 17150.00 17150.00 17150.00 17150.00 17150.00
19600.00 19600.00 19600.00 19600.00 19600.00 19600.00 19600.00 19600.00
22050.00 22050.00 22050.00 22050.00 22050.00 22050.00 22050.00 22050.00
24500.00 24500.00 24500.00 24500.00 24500.00 24500.00 24500.00 24500.00
26950.00 26950.00 26950.00 26950.00 26950.00 26950.00 26950.00 26950.00
29400.00 29400.00 29400.00 29400.00 29400.00 29400.00 29400.00 29400.00
31850.00 31850.00 31850.00 31850.00 31850.00 31850.00 31850.00 31850.00
0.8500 0.8500 0.8500 0.8500 0.8500 0.8500 0.8500 0.8500
0.8750 0.8750 0.8750 0.8750 0.8750 0.8750 0.8750 0.8750
0.9000 0.9000 0.9000 0.9000 0.9000 0.9000 0.9000 0.9000
0.9250 0.9250 0.9250 0.9250 0.9250 0.9250 0.9250 0.9250
0.9500 0.9500 0.9500 0.9500 0.9500 0.9500 0.9500 0.9500
0.9750 0.9750 0.9750 0.9750 0.9750 0.9750 0.9750 0.9750
1.0000 1.0000 1.0000 1.0000 1.0000 1.0000 1.0000 1.0000
1.0000 1.0000 1.0000 1.0000 1.0000 1.0000 1.0000 1.0000
1.0000 1.0000 1.0000 1.0000 1.0000 1.0000 1.0000 1.0000
1.0000 1.0000 1.0000 1.0000 1.0000 1.0000 1.0000 1.0000
1.0000 1.0000 1.0000 1.0000 1.0000 1.0000 1.0000 1.0000
1.0000 1.0000 1.0000 1.0000 1.0000 1.0000 1.0000 1.0000
1.0000 1.0000 1.0000 1.0000 1.0000 1.0000 1.0000 1.0000
1.0000 1.0000 1.0000 1.0000 1.0000 1.0000 1.0000 1.0000
1.0000 1.0000 1.0000 1.0000 1.0000 1.0000 1.0000 1.0000
1.0000 1.0000 1.0000 1.0000 1.0000 1.0000 1.0000 1.0000
1.0000 1.0000 1.0000 1.0000 1.0000 1.0000 1.0000 1.0000
1.0000 1.0000 1.0000 1.0000 1.0000 1.0000 1.0000 1.0000
1.0000 1.0000 1.0000 1.0000 1.0000 1.0000 1.0000 1.0000
1.0000 1.0000 1.0000 1.0000 1.0000 1.0000 1.0000 1.0000
1.0000 1.0000 1.0000 1.0000 1.0000 1.0000 1.0000 1.0000
1000000 1000000 0.20000 1.500 3.1536E07 8 1
1 1 4.4687E-5 0.0764
1 0 0 0 0 0 0 0 0 0 0 0 0 0
0 0 0 0 0 0 0 0 0 0 0 0 0 0
2 1 6.0249E-6 1.0000
1 0 0 0 0 0 0 0 0 0 0 0 0 0
0 0 0 0 0 0 0 0 0 0 0 0 0 0
3 1 1.1447E-5 1.0000
1 0 0 0 0 0 0 0 0 0 0 0 0 0

```













APPENDIX B  
SWANFLOW Output Files

RUN NAME .... 2-D Unsaturated-Saturated Infiltration of Gasoline  
 DATE .... 7 May 1994  
 RUN NO .... RUN1

NUMBER OF BLOCKS IN THE X-DIRECTION (COLUMNS): 8  
 NUMBER OF BLOCKS IN THE Z-DIRECTION (LAYERS): 20  
 NUMBER OF BLOCKS IN THE Y-DIRECTION (SLICES): 1  
 MAXIMUM NUMBER OF NEWTON-RAPHSON ITERATIONS: 4  
 ESTIMATED BANDWIDTH: 0  
 MAXIMUM NUMBER OF TIME STEPS: 100  
 NUMBER OF TIME STEPS BETWEEN PRINTING OUTPUT: 1  
 MAXIMUM NUMBER OF SSOR ITERATIONS: 1

BALANCE ERROR (%) FOR CONTROL OF NEWTON-RAPHSON ITERATION: 0.200000E-01  
 INITIAL TIME (SECONDS): 0.000000  
 DENSITY OF WATER: 1000.00  
 DENSITY OF NONAQUEOUS FLUID: 730.000  
 DYNAMIC VISCOSITY OF WATER: 0.100000E-02  
 DYNAMIC VISCOSITY OF NONAQUEOUS FLUID: 0.450000E-03  
 GRAVITATIONAL ACCELERATION (Z-DIRECTION): -9.80000  
 GRAVITATIONAL ACCELERATION (X-DIRECTION): 0.000000  
 SSOR CONVERGENCE TOLERANCE: 0.100000E-04  
 SSOR RELAXATION FACTOR: 1.00000

NUMBER OF PC VS KR TABLES: 1

DATA SET: 1

PC	SW	KRW	KRN
103425.000	-0.100	0.00000	1.00000
103425.000	0.000	0.00000	1.00000
103425.000	0.100	0.00000	0.82000
103425.000	0.200	0.00000	0.68000
27580.000	0.300	0.04000	0.55000
10343.000	0.400	0.10000	0.43000
7585.000	0.500	0.18000	0.31000
7447.000	0.600	0.30000	0.20000
7309.000	0.700	0.44000	0.12000
7171.000	0.800	0.60000	0.05000
7033.000	0.900	0.80000	0.00000
6895.000	1.000	1.00000	0.00000
6895.000	1.100	1.00000	0.00000

DATA SET: 1 PNWSWR: 0.680

PCAN	SAIR	PRNA	PRA
-98000.000	1.000	-0.32000	1.00000
0.000	0.000	0.68000	0.00000

1 PERMEABILITY SETS

SET 1 0.10000E-11 0.10000E-11 0.10000E-11

1 POROSITY SETS

SET 1 0.30000 0.10000E-14 0.00000

DX

1 1.00 2 1.90 3 3.61 4 6.86 5 13.0 6 24.8 7 47.0 8 89.4

DZ

1 0.250 2 0.250 3 0.250 4 0.250 5 0.250 6 0.250 7 0.250 8 0.250  
 9 0.250 10 0.250 11 0.250 12 0.250 13 0.250 14 0.250 15 0.250 16 0.250  
 17 0.250 18 0.250 19 0.250 20 0.250

DY

1 1.00

1 PROPERTY COMBINATION SETS

SET 1 1 1 1

NUMBER OF ACTIVE BLOCKS

SLICE 1 152

GRID BLOCK NUMBERS

ROW 1	1	2	3	4	5	6	7	8
ROW 2	9	10	11	12	13	14	15	16
ROW 3	17	18	19	20	21	22	23	24
ROW 4	25	26	27	28	29	30	31	32
ROW 5	33	34	35	36	37	38	39	40
ROW 6	41	42	43	44	45	46	47	48
ROW 7	49	50	51	52	53	54	55	56
ROW 8	57	58	59	60	61	62	63	64
ROW 9	65	66	67	68	69	70	71	72
ROW 10	73	74	75	76	77	78	79	80
ROW 11	81	82	83	84	85	86	87	88



```

WATER BALANCE          NAPL BALANCE
CONSTANT PRES          -5089.2          0.00000
SOURCE/SINKS           4811.2          209.40
STORAGE                277.92          -209.40
PER CENT ERROR         -0.84855E-09        -0.13980E-11
    
```

```

STEP NUMBER 31          SIMULATION TIME IN SECONDS 0.946E+08
*****
                        IN MINUTES 0.158E+07
                        IN HOURS 0.263E+05
                        IN DAYS 0.109E+04
                        IN YEARS 3.00
    
```

NAPL SATURATIONS

```

SLICE 1
0.46354 0.46300 0.45017 0.43807 0.41376 0.20619 -0.16653E-15 0.22204E-15
0.45748 0.45767 0.44463 0.43256 0.40821 0.91617E-01 0.13878E-15 0.13878E-16
0.45138 0.45245 0.43902 0.42703 0.29337 0.47964E-02 0.13878E-15 0.11102E-15
0.44521 0.45007 0.44997 0.24397 0.90182E-02 0.12490E-15 0.15266E-15 0.83267E-16
0.16062 0.86762E-01 0.15266E-15 0.11102E-15 0.19429E-15 0.69389E-17 0.90206E-16 0.62450E-16
-0.72858E-16 0.15266E-15 0.23592E-15 0.24286E-16 0.10408E-16 0.48572E-16 0.14572E-15 0.11796E-15
0.00000 0.00000 0.00000 0.00000 0.00000 0.00000 0.00000 0.00000
0.00000 0.00000 0.00000 0.00000 0.00000 0.00000 0.00000 0.00000
0.00000 0.00000 0.00000 0.00000 0.00000 0.00000 0.00000 0.00000
0.00000 0.00000 0.00000 0.00000 0.00000 0.00000 0.00000 0.00000
0.00000 0.00000 0.00000 0.00000 0.00000 0.00000 0.00000 0.00000
0.00000 0.00000 0.00000 0.00000 0.00000 0.00000 0.00000 0.00000
0.00000 0.00000 0.00000 0.00000 0.00000 0.00000 0.00000 0.00000
0.00000 0.00000 0.00000 0.00000 0.00000 0.00000 0.00000 0.00000
0.00000 0.00000 0.00000 0.00000 0.00000 0.00000 0.00000 0.00000
0.00000 0.00000 0.00000 0.00000 0.00000 0.00000 0.00000 0.00000
0.00000 0.00000 0.00000 0.00000 0.00000 0.00000 0.00000 0.00000
0.00000 0.00000 0.00000 0.00000 0.00000 0.00000 0.00000 0.00000
0.00000 0.00000 0.00000 0.00000 0.00000 0.00000 0.00000 0.00000
0.00000 0.00000 0.00000 0.00000 0.00000 0.00000 0.00000 0.00000
0.00000 0.00000 0.00000 0.00000 0.00000 0.00000 0.00000 0.00000
0.00000 0.00000 0.00000 0.00000 0.00000 0.00000 0.00000 0.00000
    
```

```

WATER BALANCE          NAPL BALANCE
CONSTANT PRES          -2476.2          0.00000
SOURCE/SINKS           2338.1          101.76
STORAGE                138.07          -101.76
PER CENT ERROR         0.65985E-09        0.41057E-11
    
```

```

STEP NUMBER 41          SIMULATION TIME IN SECONDS 0.158E+09
*****
                        IN MINUTES 0.263E+07
                        IN HOURS 0.438E+05
                        IN DAYS 0.182E+04
                        IN YEARS 5.00
    
```

NAPL SATURATIONS

```

SLICE 1
0.48089 0.47757 0.47211 0.46142 0.43962 0.38823 0.55788E-01 0.16653E-15
0.47504 0.47209 0.46664 0.45594 0.43411 0.36475 0.41866E-02 0.69389E-16
0.46924 0.46658 0.46114 0.45042 0.42857 0.15915 0.00000 0.15266E-15
0.46352 0.46104 0.45560 0.44488 0.28533 0.83660E-02 0.26368E-15 0.11102E-15
0.46739 0.42984 0.34419 0.17223 0.88123E-03 0.15266E-15 0.14572E-15 0.90206E-16
0.58981E-16 0.12143E-15 0.10408E-15 0.24286E-16 0.76328E-16 0.31225E-16 0.34694E-16 0.18735E-15
0.00000 0.00000 0.00000 0.00000 0.00000 0.00000 0.00000 0.00000
0.00000 0.00000 0.00000 0.00000 0.00000 0.00000 0.00000 0.00000
0.00000 0.00000 0.00000 0.00000 0.00000 0.00000 0.00000 0.00000
0.00000 0.00000 0.00000 0.00000 0.00000 0.00000 0.00000 0.00000
0.00000 0.00000 0.00000 0.00000 0.00000 0.00000 0.00000 0.00000
0.00000 0.00000 0.00000 0.00000 0.00000 0.00000 0.00000 0.00000
0.00000 0.00000 0.00000 0.00000 0.00000 0.00000 0.00000 0.00000
0.00000 0.00000 0.00000 0.00000 0.00000 0.00000 0.00000 0.00000
0.00000 0.00000 0.00000 0.00000 0.00000 0.00000 0.00000 0.00000
0.00000 0.00000 0.00000 0.00000 0.00000 0.00000 0.00000 0.00000
0.00000 0.00000 0.00000 0.00000 0.00000 0.00000 0.00000 0.00000
0.00000 0.00000 0.00000 0.00000 0.00000 0.00000 0.00000 0.00000
0.00000 0.00000 0.00000 0.00000 0.00000 0.00000 0.00000 0.00000
0.00000 0.00000 0.00000 0.00000 0.00000 0.00000 0.00000 0.00000
0.00000 0.00000 0.00000 0.00000 0.00000 0.00000 0.00000 0.00000
0.00000 0.00000 0.00000 0.00000 0.00000 0.00000 0.00000 0.00000
0.00000 0.00000 0.00000 0.00000 0.00000 0.00000 0.00000 0.00000
    
```

```

WATER BALANCE          NAPL BALANCE
CONSTANT PRES          -16762.          0.00000
SOURCE/SINKS           15842.          689.48
STORAGE                920.17          -689.48
PER CENT ERROR         0.10297E-08        -0.11625E-10
    
```

```

STEP NUMBER 53          SIMULATION TIME IN SECONDS 0.315E+09
*****
                        IN MINUTES 0.526E+07
                        IN HOURS 0.876E+05
                        IN DAYS 0.365E+04
                        IN YEARS 9.99
    
```

NAPL SATURATIONS

```

SLICE 1
0.49461 0.49363 0.49217 0.48942 0.47956 0.44647 0.42533 0.65243E-02
0.50570 0.50332 0.49916 0.49158 0.47410 0.44097 0.16990 0.43726E-04
0.49995 0.49784 0.49369 0.48610 0.46860 0.43543 0.12092 0.27756E-16
0.49424 0.49232 0.48818 0.48059 0.46307 0.39515 0.17963E-01 0.27756E-16
    
```





RUN NAME .... 2-D Unsaturated-Saturated Infiltration of Kerosene  
 DATE .... 7 May 1994  
 RUN NO .... RUN1

NUMBER OF BLOCKS IN THE X-DIRECTION (COLUMNS): 8  
 NUMBER OF BLOCKS IN THE Z-DIRECTION (LAYERS): 20  
 NUMBER OF BLOCKS IN THE Y-DIRECTION (SLICES): 1  
 MAXIMUM NUMBER OF NEWTON-RAPHSON ITERATIONS: 4  
 ESTIMATED BANDWIDTH: 0  
 MAXIMUM NUMBER OF TIME STEPS: 100  
 NUMBER OF TIME STEPS BETWEEN PRINTING OUTPUT: 1  
 MAXIMUM NUMBER OF SSOR ITERATIONS: 1

BALANCE ERROR (%) FOR CONTROL OF NEWTON-RAPHSON ITERATION: 0.200000E-01  
 INITIAL TIME (SECONDS): 0.000000  
 DENSITY OF WATER: 1000.00  
 DENSITY OF NONAQUEOUS FLUID: 810.000  
 DYNAMIC VISCOSITY OF WATER: 0.100000E-02  
 DYNAMIC VISCOSITY OF NONAQUEOUS FLUID: 0.205000E-02  
 GRAVITATIONAL ACCELERATION (Z-DIRECTION): -9.80000  
 GRAVITATIONAL ACCELERATION (X-DIRECTION): 0.000000  
 SSOR CONVERGENCE TOLERANCE: 0.100000E-04  
 SSOR RELAXATION FACTOR: 1.00000

NUMBER OF PC VS KR TABLES: 1

DATA SET: 1

PC	SW	KRW	KRN
103425.000	-0.100	0.00000	1.00000
103425.000	0.000	0.00000	1.00000
103425.000	0.100	0.00000	0.82000
103425.000	0.200	0.00000	0.68000
27580.000	0.300	0.04000	0.55000
10343.000	0.400	0.10000	0.43000
7585.000	0.500	0.18000	0.31000
7447.000	0.600	0.30000	0.20000
7309.000	0.700	0.44000	0.12000
7171.000	0.800	0.60000	0.05000
7033.000	0.900	0.80000	0.00000
6895.000	1.000	1.00000	0.00000
6895.000	1.100	1.00000	0.00000

DATA SET: 1 PNWSWR: 0.680

PCAN	SAIR	PRNA	PRA
-98000.000	1.000	-0.32000	1.00000
0.000	0.000	0.68000	0.00000

1 PERMEABILITY SETS

SET 1 0.10000E-11 0.10000E-11 0.10000E-11

1 POROSITY SETS

SET 1 0.30000 0.10000E-14 0.00000

DX

1 1.00 2 1.90 3 3.61 4 6.86 5 13.0 6 24.8 7 47.0 8 89.4

DZ

1 0.250 2 0.250 3 0.250 4 0.250 5 0.250 6 0.250 7 0.250 8 0.250  
 9 0.250 10 0.250 11 0.250 12 0.250 13 0.250 14 0.250 15 0.250 16 0.250  
 17 0.250 18 0.250 19 0.250 20 0.250

DY

1 1.00

1 PROPERTY COMBINATION SETS

SET 1 1 1 1

NUMBER OF ACTIVE BLOCKS

SLICE 1 152

GRID BLOCK NUMBERS

ROW 1	1	2	3	4	5	6	7	8
ROW 2	9	10	11	12	13	14	15	16
ROW 3	17	18	19	20	21	22	23	24
ROW 4	25	26	27	28	29	30	31	32
ROW 5	33	34	35	36	37	38	39	40
ROW 6	41	42	43	44	45	46	47	48
ROW 7	49	50	51	52	53	54	55	56
ROW 8	57	58	59	60	61	62	63	64
ROW 9	65	66	67	68	69	70	71	72
ROW 10	73	74	75	76	77	78	79	80
ROW 11	81	82	83	84	85	86	87	88

ROW 12 89 90 91 92 93 94 95 96  
ROW 13 97 98 99100101102103104  
ROW 14 105106107108109110111112  
ROW 15 113114115116117118119120  
ROW 16 121122123124125126127128  
ROW 17 129130131132133134135136  
ROW 18 137138139140141142143144  
ROW 19 145146147148149150151152  
ROW 20 -1 -1 -1 -1 -1 -1 -1 -1

ALL GRID BLOCKS IN SAME PROPERTY CLASS

INITIAL NAPL PRESSURES

Table with 8 columns of initial NAPL pressures ranging from -14700 to 31850.

INITIAL WATER SATURATIONS

Table with 8 columns of initial water saturations ranging from 0.85000 to 1.00000.

Summary table with columns WATER BALANCE and NAPL BALANCE, listing values for CONSTANT PRES, SOURCE/SINKS, STORAGE, and PER CENT ERROR.

STEP NUMBER 23 SIMULATION TIME IN SECONDS 0.315E+08  
IN MINUTES 0.526E+06  
IN HOURS 0.876E+04  
IN DAYS 365  
IN YEARS 0.999

NAPL SATURATIONS

Table showing NAPL SATURATIONS for SLICE 1 with multiple columns of values ranging from 0.45157 to 0.50633E-03.

```

WATER BALANCE          NAPL BALANCE
CONSTANT PRES          -2490.7          0.00000
SOURCE/SINKS           2352.0          113.90
STORAGE                138.70          -113.90
PER CENT ERROR        -0.10708E-08          -0.18079E-10
  
```

```

STEP NUMBER 29
*****
SIMULATION TIME IN SECONDS 0.491E+08
                  IN MINUTES 0.819E+06
                  IN HOURS   0.136E+05
                  IN DAYS    569.
                  IN YEARS   1.56
  
```

```

NAPL SATURATIONS
SLICE 1
0.46699 0.45402 0.44067 0.39221 0.39985E-01 0.11102E-15 0.00000 -0.55511E-16
0.46843 0.45748 0.44438 0.39357 0.45570E-02 0.12490E-15 0.41633E-16 0.19429E-15
0.47030 0.46091 0.44821 0.17431 0.17432E-03 0.11102E-15 0.55511E-16 0.00000
0.47255 0.46405 0.45719 0.10829 0.00000 -0.40246E-15 0.69389E-16 0.55511E-16
0.47514 0.46719 0.26602 0.70383E-02 0.76328E-16 0.90206E-16 0.41633E-16 0.25674E-15
0.41709 0.29026 0.32711E-01 0.14225E-15 0.76328E-16 0.69389E-16 0.10755E-15 0.79797E-16
0.10554 0.00000 0.00000 0.00000 0.00000 0.00000 0.00000 0.00000
0.00000 0.00000 0.00000 0.00000 0.00000 0.00000 0.00000 0.00000
0.00000 0.00000 0.00000 0.00000 0.00000 0.00000 0.00000 0.00000
0.00000 0.00000 0.00000 0.00000 0.00000 0.00000 0.00000 0.00000
0.00000 0.00000 0.00000 0.00000 0.00000 0.00000 0.00000 0.00000
0.00000 0.00000 0.00000 0.00000 0.00000 0.00000 0.00000 0.00000
0.00000 0.00000 0.00000 0.00000 0.00000 0.00000 0.00000 0.00000
0.00000 0.00000 0.00000 0.00000 0.00000 0.00000 0.00000 0.00000
0.00000 0.00000 0.00000 0.00000 0.00000 0.00000 0.00000 0.00000
0.00000 0.00000 0.00000 0.00000 0.00000 0.00000 0.00000 0.00000
0.00000 0.00000 0.00000 0.00000 0.00000 0.00000 0.00000 0.00000
0.00000 0.00000 0.00000 0.00000 0.00000 0.00000 0.00000 0.00000
0.00000 0.00000 0.00000 0.00000 0.00000 0.00000 0.00000 0.00000
0.00000 0.00000 0.00000 0.00000 0.00000 0.00000 0.00000 0.00000
0.00000 0.00000 0.00000 0.00000 0.00000 0.00000 0.00000 0.00000
0.00000 0.00000 0.00000 0.00000 0.00000 0.00000 0.00000 0.00000
  
```

```

WATER BALANCE          NAPL BALANCE
CONSTANT PRES          -627.97          0.00000
SOURCE/SINKS           594.06          28.769
STORAGE                33.901          -28.769
PER CENT ERROR         0.16151E-08          -0.42728E-11
  
```

```

STEP NUMBER 39
*****
SIMULATION TIME IN SECONDS 0.946E+08
                  IN MINUTES 0.158E+07
                  IN HOURS   0.263E+05
                  IN DAYS    0.109E+04
                  IN YEARS   3.00
  
```

```

NAPL SATURATIONS
SLICE 1
0.48867 0.48211 0.46678 0.43546 0.28568 0.11167E-02 0.11102E-15 0.27756E-16
0.49590 0.48567 0.47042 0.43906 0.16594 0.30511E-05 0.11102E-15 0.27756E-15
0.49798 0.48916 0.47406 0.44265 0.12134 -0.18041E-15 0.13878E-16 0.83267E-16
0.50041 0.49260 0.47770 0.44620 0.57374E-01 0.24980E-15 0.19429E-15 0.19429E-15
0.50315 0.49603 0.48133 0.33539 0.68213E-02 0.13878E-16 0.69389E-16 0.24980E-15
0.50619 0.49945 0.48506 0.12325 0.44364E-05 0.15266E-15 0.22898E-15 0.22898E-15
0.50189 0.43253 0.19645 0.34374E-02 0.00000 0.00000 0.00000 0.00000
0.18956 0.91832E-01 0.00000 0.00000 0.00000 0.00000 0.00000 0.00000
0.00000 0.00000 0.00000 0.00000 0.00000 0.00000 0.00000 0.00000
0.00000 0.00000 0.00000 0.00000 0.00000 0.00000 0.00000 0.00000
0.00000 0.00000 0.00000 0.00000 0.00000 0.00000 0.00000 0.00000
0.00000 0.00000 0.00000 0.00000 0.00000 0.00000 0.00000 0.00000
0.00000 0.00000 0.00000 0.00000 0.00000 0.00000 0.00000 0.00000
0.00000 0.00000 0.00000 0.00000 0.00000 0.00000 0.00000 0.00000
0.00000 0.00000 0.00000 0.00000 0.00000 0.00000 0.00000 0.00000
0.00000 0.00000 0.00000 0.00000 0.00000 0.00000 0.00000 0.00000
0.00000 0.00000 0.00000 0.00000 0.00000 0.00000 0.00000 0.00000
0.00000 0.00000 0.00000 0.00000 0.00000 0.00000 0.00000 0.00000
0.00000 0.00000 0.00000 0.00000 0.00000 0.00000 0.00000 0.00000
0.00000 0.00000 0.00000 0.00000 0.00000 0.00000 0.00000 0.00000
0.00000 0.00000 0.00000 0.00000 0.00000 0.00000 0.00000 0.00000
0.00000 0.00000 0.00000 0.00000 0.00000 0.00000 0.00000 0.00000
  
```

```

WATER BALANCE          NAPL BALANCE
CONSTANT PRES          -4541.2          0.00000
SOURCE/SINKS           4290.9          207.80
STORAGE                250.11          -207.80
PER CENT ERROR         0.47561E-09          -0.13445E-10
  
```

```

STEP NUMBER 50
*****
SIMULATION TIME IN SECONDS 0.158E+09
                  IN MINUTES 0.263E+07
                  IN HOURS   0.438E+05
                  IN DAYS    0.182E+04
                  IN YEARS   5.00
  
```

```

NAPL SATURATIONS
SLICE 1
0.49722 0.49332 0.48877 0.47212 0.41865 0.64023E-01 0.30531E-15 0.83267E-16
0.51412 0.51148 0.49838 0.47577 0.42221 0.37631E-01 0.30531E-15 0.41633E-15
0.52347 0.51497 0.50200 0.47941 0.42572 0.16478E-01 0.41633E-16 0.15266E-15
0.52603 0.51839 0.50559 0.48304 0.33999 0.16796E-02 0.12490E-15 0.19429E-15
  
```



RUN NAME .... 2-D Unsaturated-Saturated Infiltration of p-Cymene [1-Methyl-4-(1-Methylethyl)-Benzene]  
 DATE .... 8 May 1994  
 RUN NO .... RUN1

NUMBER OF BLOCKS IN THE X-DIRECTION (COLUMNS): 8  
 NUMBER OF BLOCKS IN THE Z-DIRECTION (LAYERS): 20  
 NUMBER OF BLOCKS IN THE Y-DIRECTION (SLICES): 1  
 MAXIMUM NUMBER OF NEWTON-RAPHSON ITERATIONS: 4  
 ESTIMATED BANDWIDTH: 0  
 MAXIMUM NUMBER OF TIME STEPS: 150  
 NUMBER OF TIME STEPS BETWEEN PRINTING OUTPUT: 1  
 MAXIMUM NUMBER OF SSOR ITERATIONS: 1

BALANCE ERROR (%) FOR CONTROL OF NEWTON-RAPHSON ITERATION: 0.200000E-01  
 INITIAL TIME (SECONDS): 0.000000  
 DENSITY OF WATER: 1000.00  
 DENSITY OF NONAQUEOUS FLUID: 857.300  
 DYNAMIC VISCOSITY OF WATER: 0.100000E-02  
 DYNAMIC VISCOSITY OF NONAQUEOUS FLUID: 0.340200E-02  
 GRAVITATIONAL ACCELERATION (Z-DIRECTION): -9.80000  
 GRAVITATIONAL ACCELERATION (X-DIRECTION): 0.000000  
 SSOR CONVERGENCE TOLERANCE: 0.100000E-04  
 SSOR RELAXATION FACTOR: 1.00000

NUMBER OF PC VS KR TABLES: 1

DATA SET: 1

PC	SW	KRW	KRN
103425.000	-0.100	0.00000	1.00000
103425.000	0.000	0.00000	1.00000
103425.000	0.100	0.00000	0.82000
103425.000	0.200	0.00000	0.68000
27580.000	0.300	0.04000	0.55000
10343.000	0.400	0.10000	0.43000
7585.000	0.500	0.18000	0.31000
7447.000	0.600	0.30000	0.20000
7309.000	0.700	0.44000	0.12000
7171.000	0.800	0.60000	0.05000
7033.000	0.900	0.80000	0.00000
6895.000	1.000	1.00000	0.00000
6895.000	1.100	1.00000	0.00000

DATA SET: 1 PNWSR: 0.680

PCAN	SAIR	PRNA	PRA
-98000.000	1.000	-0.32000	1.00000
0.000	0.000	0.68000	0.00000

1 PERMEABILITY SETS

SET 1 0.10000E-11 0.10000E-11 0.10000E-11

1 POROSITY SETS

SET 1 0.30000 0.10000E-14 0.00000

DX

1 1.00 2 1.90 3 3.61 4 6.86 5 13.0 6 24.8 7 47.0 8 89.4

DZ

1 0.250 2 0.250 3 0.250 4 0.250 5 0.250 6 0.250 7 0.250 8 0.250  
 9 0.250 10 0.250 11 0.250 12 0.250 13 0.250 14 0.250 15 0.250 16 0.250  
 17 0.250 18 0.250 19 0.250 20 0.250

DY

1 1.00

1 PROPERTY COMBINATION SETS

SET 1 1 1 1

NUMBER OF ACTIVE BLOCKS

SLICE 1 152

GRID BLOCK NUMBERS

ROW 1	1	2	3	4	5	6	7	8
ROW 2	9	10	11	12	13	14	15	16
ROW 3	17	18	19	20	21	22	23	24
ROW 4	25	26	27	28	29	30	31	32
ROW 5	33	34	35	36	37	38	39	40
ROW 6	41	42	43	44	45	46	47	48
ROW 7	49	50	51	52	53	54	55	56
ROW 8	57	58	59	60	61	62	63	64
ROW 9	65	66	67	68	69	70	71	72
ROW 10	73	74	75	76	77	78	79	80
ROW 11	81	82	83	84	85	86	87	88









RUN NAME .... 2-D Unsaturated-Saturated Infiltration of 10W-30 Motor Oil  
 DATE .... 8 May 1994  
 RUN NO .... RUN1

NUMBER OF BLOCKS IN THE X-DIRECTION (COLUMNS): 8  
 NUMBER OF BLOCKS IN THE Z-DIRECTION (LAYERS): 20  
 NUMBER OF BLOCKS IN THE Y-DIRECTION (SLICES): 1  
 MAXIMUM NUMBER OF NEWTON-RAPHSON ITERATIONS: 4  
 ESTIMATED BANDWIDTH: 0  
 MAXIMUM NUMBER OF TIME STEPS: 150  
 NUMBER OF TIME STEPS BETWEEN PRINTING OUTPUT: 1  
 MAXIMUM NUMBER OF SSOR ITERATIONS: 1

BALANCE ERROR (%) FOR CONTROL OF NEWTON-RAPHSON ITERATION: 0.200000E-01  
 INITIAL TIME (SECONDS): 0.000000  
 DENSITY OF WATER: 1000.00  
 DENSITY OF NONAQUEOUS FLUID: 869.000  
 DYNAMIC VISCOSITY OF WATER: 0.100000E-02  
 DYNAMIC VISCOSITY OF NONAQUEOUS FLUID: 0.130000  
 GRAVITATIONAL ACCELERATION (Z-DIRECTION): -9.80000  
 GRAVITATIONAL ACCELERATION (X-DIRECTION): 0.000000  
 SSOR CONVERGENCE TOLERANCE: 0.100000E-04  
 SSOR RELAXATION FACTOR: 1.00000

NUMBER OF PC VS KR TABLES: 1

DATA SET: 1

PC	SW	KRW	KRN
103425.000	-0.100	0.00000	1.00000
103425.000	0.000	0.00000	1.00000
103425.000	0.100	0.00000	0.82000
103425.000	0.200	0.00000	0.68000
27580.000	0.300	0.04000	0.55000
10343.000	0.400	0.10000	0.43000
7585.000	0.500	0.18000	0.31000
7447.000	0.600	0.30000	0.20000
7309.000	0.700	0.44000	0.12000
7171.000	0.800	0.60000	0.05000
7033.000	0.900	0.80000	0.00000
6895.000	1.000	1.00000	0.00000
6895.000	1.100	1.00000	0.00000

DATA SET: 1 PNWSWR: 0.680

PCAN	SAIR	PRNA	PRA
-98000.000	1.000	-0.32000	1.00000
0.000	0.000	0.68000	0.00000

1 PERMEABILITY SETS

SET 1 0.10000E-11 0.10000E-11 0.10000E-11

1 POROSITY SETS

SET 1 0.30000 0.10000E-14 0.00000

DX

1 1.00 2 1.90 3 3.61 4 6.86 5 13.0 6 24.8 7 47.0 8 89.4

DZ

1 0.250 2 0.250 3 0.250 4 0.250 5 0.250 6 0.250 7 0.250 8 0.250  
 9 0.250 10 0.250 11 0.250 12 0.250 13 0.250 14 0.250 15 0.250 16 0.250  
 17 0.250 18 0.250 19 0.250 20 0.250

DY

1 1.00

1 PROPERTY COMBINATION SETS

SET 1 1 1 1

NUMBER OF ACTIVE BLOCKS

SLICE 1 152

GRID BLOCK NUMBERS

ROW	1	2	3	4	5	6	7	8
ROW 1	1	2	3	4	5	6	7	8
ROW 2	9	10	11	12	13	14	15	16
ROW 3	17	18	19	20	21	22	23	24
ROW 4	25	26	27	28	29	30	31	32
ROW 5	33	34	35	36	37	38	39	40
ROW 6	41	42	43	44	45	46	47	48
ROW 7	49	50	51	52	53	54	55	56
ROW 8	57	58	59	60	61	62	63	64
ROW 9	65	66	67	68	69	70	71	72
ROW 10	73	74	75	76	77	78	79	80
ROW 11	81	82	83	84	85	86	87	88

Table with 13 columns (ROW 12-20) and 13 rows of numerical data.

ALL GRID BLOCKS IN SAME PROPERTY CLASS

INITIAL NAPL PRESSURES

Table with 8 columns and 20 rows of initial NAPL pressure values ranging from -14700 to 31850.

INITIAL WATER SATURATIONS

Table with 8 columns and 20 rows of initial water saturation values, mostly 0.85000 and 1.00000.

WATER BALANCE      NAPL BALANCE

Table with 2 columns (WATER BALANCE, NAPL BALANCE) and 4 rows of balance values.

Table with 2 columns (STEP NUMBER 28, SIMULATION TIME IN SECONDS) and 4 rows of simulation parameters.

NAPL SATURATIONS

Table with 13 columns (SLICE 1) and 20 rows of NAPL saturation data for various grid blocks.



0.63689	0.62126	0.52594	0.34706E-02	0.00000	0.00000	0.00000	0.00000
0.63061	0.61738	0.50881	0.14590E-02	0.00000	0.00000	0.00000	0.00000
0.62483	0.61357	0.30800	0.36165E-03	0.00000	0.00000	0.00000	0.00000
0.61948	0.60984	0.20538	0.13806E-03	0.00000	0.00000	0.00000	0.00000
0.61451	0.60622	0.16405	0.55662E-04	0.00000	0.00000	0.00000	0.00000
0.60985	0.60269	0.13220	0.15289E-04	0.00000	0.00000	0.00000	0.00000
0.60548	0.59531	0.10367	0.53324E-06	0.00000	0.00000	0.00000	0.00000
0.60135	0.57440	0.68734E-01	0.00000	0.00000	0.00000	0.00000	0.00000
0.58402	0.55363	0.41771E-01	0.00000	0.00000	0.00000	0.00000	0.00000
0.56055	0.53292	0.21170E-01	0.00000	0.00000	0.00000	0.00000	0.00000
0.53772	0.51223	0.76295E-02	0.00000	0.00000	0.00000	0.00000	0.00000
0.51547	0.33073	0.72234E-03	0.00000	0.00000	0.00000	0.00000	0.00000
0.37465	0.21473E-01	0.00000	0.00000	0.00000	0.00000	0.00000	0.00000
0.00000	0.00000	0.00000	0.00000	0.00000	0.00000	0.00000	0.00000

WATER BALANCE		NAPL BALANCE	
CONSTANT PRES	-448.86		-7.6943
SOURCE/SINKS	432.25		22.494
STORAGE	16.610		-14.800
PER CENT ERROR	0.42271E-03		-0.44562E-03

STEP NUMBER 109  
 SIMULATION TIME IN SECONDS 0.158E+09  
 IN MINUTES 0.263E+07  
 IN HOURS 0.438E+05  
 IN DAYS 0.182E+04  
 IN YEARS 5.00

NAPL SATURATIONS

SLICE 1	
0.70013	0.63188 0.53715 0.89076E-01 0.13878E-15 0.13878E-15 0.38858E-15 0.49960E-15
0.68868	0.64948 0.55671 0.85635E-01 0.74940E-15 0.22204E-15 0.62450E-15 0.13878E-16
0.67819	0.64681 0.57595 0.81085E-01 0.97145E-16 0.27756E-16 0.24980E-15 0.52736E-15
0.66883	0.64326 0.59491 0.75366E-01 0.69389E-16 0.31919E-15 0.45797E-15 0.23592E-15
0.66041	0.63944 0.61001 0.68901E-01 0.34694E-16 0.50654E-15 0.34694E-16 0.55511E-15
0.65276	0.63547 0.60768 0.59899E-01 0.53083E-15 0.32960E-15 0.38164E-16 0.93675E-16
0.64574	0.63139 0.60526 0.50388E-01 0.00000 0.00000 0.00000 0.00000
0.63925	0.62727 0.60275 0.40458E-01 0.00000 0.00000 0.00000 0.00000
0.63320	0.62313 0.60095 0.31198E-01 0.00000 0.00000 0.00000 0.00000
0.62752	0.61902 0.58446 0.22836E-01 0.00000 0.00000 0.00000 0.00000
0.62215	0.61494 0.56748 0.15721E-01 0.00000 0.00000 0.00000 0.00000
0.61704	0.61092 0.54997 0.99688E-02 0.00000 0.00000 0.00000 0.00000
0.61216	0.60695 0.53187 0.53759E-02 0.00000 0.00000 0.00000 0.00000
0.60746	0.60306 0.51308 0.22307E-02 0.00000 0.00000 0.00000 0.00000
0.60291	0.59535 0.36828 0.33635E-03 0.00000 0.00000 0.00000 0.00000
0.59055	0.57206 0.12765 0.13102E-04 0.00000 0.00000 0.00000 0.00000
0.56318	0.54863 0.85549E-01 0.00000 0.00000 0.00000 0.00000 0.00000
0.53510	0.52484 0.47862E-01 0.00000 0.00000 0.00000 0.00000 0.00000
0.50590	0.50040 0.17298E-01 0.00000 0.00000 0.00000 0.00000 0.00000
0.00000	0.00000 0.00000 0.00000 0.00000 0.00000 0.00000 0.00000

WATER BALANCE		NAPL BALANCE	
CONSTANT PRES	-3913.9		-131.10
SOURCE/SINKS	3840.9		199.88
STORAGE	72.956		-68.781
PER CENT ERROR	-0.15041E-01		-0.14490E-03

STEP NUMBER 131  
 SIMULATION TIME IN SECONDS 0.315E+09  
 IN MINUTES 0.526E+07  
 IN HOURS 0.876E+05  
 IN DAYS 0.365E+04  
 IN YEARS 9.99

NAPL SATURATIONS

SLICE 1	
0.70130	0.64865 0.56187 0.43464 0.60890E-02 0.13878E-15 0.66613E-15 0.47184E-15
0.69385	0.65605 0.58144 0.44487 0.49523E-02 0.13878E-15 0.61062E-15 0.83267E-16
0.68341	0.65287 0.60070 0.45499 0.37110E-02 0.69389E-16 0.37470E-15 0.51348E-15
0.67407	0.64928 0.61973 0.46503 0.24667E-02 0.16653E-15 0.68001E-15 0.30531E-15
0.66563	0.64542 0.61902 0.47490 0.15274E-02 0.53429E-15 0.55511E-16 0.50654E-15
0.65792	0.64137 0.61675 0.42433 0.61207E-03 0.33307E-15 0.55511E-16 0.83267E-16
0.65081	0.63720 0.61442 0.26298 0.29018E-03 0.00000 0.00000 0.00000
0.64418	0.63295 0.61204 0.20196 0.16188E-03 0.00000 0.00000 0.00000
0.63797	0.62866 0.60962 0.17600 0.10517E-03 0.00000 0.00000 0.00000
0.63208	0.62436 0.60716 0.15824 0.66835E-04 0.00000 0.00000 0.00000
0.62645	0.62005 0.60467 0.14354 0.39146E-04 0.00000 0.00000 0.00000
0.62105	0.61575 0.60215 0.13112 0.20053E-04 0.00000 0.00000 0.00000
0.61583	0.61146 0.59757 0.12001 0.82515E-05 0.00000 0.00000 0.00000
0.61074	0.60718 0.58153 0.10783 0.17476E-05 0.00000 0.00000 0.00000
0.60576	0.60291 0.56517 0.89062E-01 0.00000 0.00000 0.00000 0.00000
0.60086	0.59151 0.54845 0.65655E-01 0.00000 0.00000 0.00000 0.00000
0.57509	0.56453 0.53136 0.44925E-01 0.00000 0.00000 0.00000 0.00000
0.54374	0.53637 0.51388 0.27006E-01 0.00000 0.00000 0.00000 0.00000
0.51062	0.50669 0.41949 0.87521E-02 0.00000 0.00000 0.00000 0.00000
0.00000	0.00000 0.00000 0.00000 0.00000 0.00000 0.00000 0.00000

RUN NAME .... 2-D Unsaturated-Saturated Infiltration of Water  
 DATE .... 8 May 1994  
 RUN NO .... RUN1

NUMBER OF BLOCKS IN THE X-DIRECTION (COLUMNS): 8  
 NUMBER OF BLOCKS IN THE Z-DIRECTION (LAYERS): 20  
 NUMBER OF BLOCKS IN THE Y-DIRECTION (SLICES): 1  
 MAXIMUM NUMBER OF NEWTON-RAPHSON ITERATIONS: 4  
 ESTIMATED BANDWIDTH: 0  
 MAXIMUM NUMBER OF TIME STEPS: 100  
 NUMBER OF TIME STEPS BETWEEN PRINTING OUTPUT: 1  
 MAXIMUM NUMBER OF SSOR ITERATIONS: 1

BALANCE ERROR (%) FOR CONTROL OF NEWTON-RAPHSON ITERATION: 0.200000E-01  
 INITIAL TIME (SECONDS): 0.000000  
 DENSITY OF WATER: 1000.00  
 DENSITY OF NONAQUEOUS FLUID: 1000.00  
 DYNAMIC VISCOSITY OF WATER: 0.100000E-02  
 DYNAMIC VISCOSITY OF NONAQUEOUS FLUID: 0.100000E-02  
 GRAVITATIONAL ACCELERATION (Z-DIRECTION): -9.80000  
 GRAVITATIONAL ACCELERATION (X-DIRECTION): 0.000000  
 SSOR CONVERGENCE TOLERANCE: 0.100000E-04  
 SSOR RELAXATION FACTOR: 1.00000

NUMBER OF PC VS KR TABLES: 1

DATA SET: 1

PC	SW	KRW	KRN
103425.000	-0.100	0.00000	1.00000
103425.000	0.000	0.00000	1.00000
103425.000	0.100	0.00000	0.82000
103425.000	0.200	0.00000	0.68000
27580.000	0.300	0.04000	0.55000
10343.000	0.400	0.10000	0.43000
7585.000	0.500	0.18000	0.31000
7447.000	0.600	0.30000	0.20000
7309.000	0.700	0.44000	0.12000
7171.000	0.800	0.60000	0.05000
7033.000	0.900	0.80000	0.00000
6895.000	1.000	1.00000	0.00000
6895.000	1.100	1.00000	0.00000

DATA SET: 1 PNWSWR: 0.680

PCAN	SAIR	PRNA	PRA
-98000.000	1.000	-0.32000	1.00000
0.000	0.000	0.68000	0.00000

1 PERMEABILITY SETS

SET 1 0.10000E-11 0.10000E-11 0.10000E-11

1 POROSITY SETS

SET 1 0.30000 0.10000E-14 0.00000

DX

1 1.00 2 1.90 3 3.61 4 6.86 5 13.0 6 24.8 7 47.0 8 89.4

DZ

1 0.250 2 0.250 3 0.250 4 0.250 5 0.250 6 0.250 7 0.250 8 0.250  
 9 0.250 10 0.250 11 0.250 12 0.250 13 0.250 14 0.250 15 0.250 16 0.250  
 17 0.250 18 0.250 19 0.250 20 0.250

DY

1 1.00

1 PROPERTY COMBINATION SETS

SET 1 1 1 1

NUMBER OF ACTIVE BLOCKS

SLICE 1 152

GRID BLOCK NUMBERS

ROW 1	1	2	3	4	5	6	7	8
ROW 2	9	10	11	12	13	14	15	16
ROW 3	17	18	19	20	21	22	23	24
ROW 4	25	26	27	28	29	30	31	32
ROW 5	33	34	35	36	37	38	39	40
ROW 6	41	42	43	44	45	46	47	48
ROW 7	49	50	51	52	53	54	55	56
ROW 8	57	58	59	60	61	62	63	64
ROW 9	65	66	67	68	69	70	71	72
ROW 10	73	74	75	76	77	78	79	80
ROW 11	81	82	83	84	85	86	87	88









RUN NAME .... 2-D Unsaturated-Saturated Infiltration of Phenol  
 DATE .... 8 May 1994 RUN NO .... RUN1

NUMBER OF BLOCKS IN THE X-DIRECTION (COLUMNS): 8  
 NUMBER OF BLOCKS IN THE Z-DIRECTION (LAYERS): 20  
 NUMBER OF BLOCKS IN THE Y-DIRECTION (SLICES): 1  
 MAXIMUM NUMBER OF NEWTON-RAPHSON ITERATIONS: 4  
 ESTIMATED BANDWIDTH: 0  
 MAXIMUM NUMBER OF TIME STEPS: 100  
 NUMBER OF TIME STEPS BETWEEN PRINTING OUTPUT: 1  
 MAXIMUM NUMBER OF SSOR ITERATIONS: 1

BALANCE ERROR (%) FOR CONTROL OF NEWTON-RAPHSON ITERATION: 0.200000E-01  
 INITIAL TIME (SECONDS): 0.000000  
 DENSITY OF WATER: 1000.00  
 DENSITY OF NONAQUEOUS FLUID: 1053.30  
 DYNAMIC VISCOSITY OF WATER: 0.100000E-02  
 DYNAMIC VISCOSITY OF NONAQUEOUS FLUID: 0.407600E-02  
 GRAVITATIONAL ACCELERATION (Z-DIRECTION): -9.80000  
 GRAVITATIONAL ACCELERATION (X-DIRECTION): 0.000000  
 SSOR CONVERGENCE TOLERANCE: 0.100000E-04  
 SSOR RELAXATION FACTOR: 1.00000

NUMBER OF PC VS KR TABLES: 1

DATA SET: 1

PC	SW	KRW	KRN
103425.000	-0.100	0.00000	1.00000
103425.000	0.000	0.00000	1.00000
103425.000	0.100	0.00000	0.82000
103425.000	0.200	0.00000	0.68000
27580.000	0.300	0.04000	0.55000
10343.000	0.400	0.10000	0.43000
7585.000	0.500	0.18000	0.31000
7447.000	0.600	0.30000	0.20000
7309.000	0.700	0.44000	0.12000
7171.000	0.800	0.60000	0.05000
7033.000	0.900	0.80000	0.00000
6895.000	1.000	1.00000	0.00000
6895.000	1.100	1.00000	0.00000

DATA SET: 1 PNWSWR: 0.680

PCAN	SAIR	PRNA	PRA
-98000.000	1.000	-0.32000	1.00000
0.000	0.000	0.68000	0.00000

1 PERMEABILITY SETS

SET 1 0.10000E-11 0.10000E-11 0.10000E-11

1 POROSITY SETS

SET 1 0.30000 0.10000E-14 0.00000

DX

1 1.00 2 1.90 3 3.61 4 6.86 5 13.0 6 24.8 7 47.0 8 89.4

DZ

1 0.250 2 0.250 3 0.250 4 0.250 5 0.250 6 0.250 7 0.250 8 0.250  
 9 0.250 10 0.250 11 0.250 12 0.250 13 0.250 14 0.250 15 0.250 16 0.250  
 17 0.250 18 0.250 19 0.250 20 0.250

DY

1 1.00

1 PROPERTY COMBINATION SETS

SET 1 1 1 1

NUMBER OF ACTIVE BLOCKS

SLICE 1 152

GRID BLOCK NUMBERS

ROW 1	1	2	3	4	5	6	7	8
ROW 2	9	10	11	12	13	14	15	16
ROW 3	17	18	19	20	21	22	23	24
ROW 4	25	26	27	28	29	30	31	32
ROW 5	33	34	35	36	37	38	39	40
ROW 6	41	42	43	44	45	46	47	48
ROW 7	49	50	51	52	53	54	55	56
ROW 8	57	58	59	60	61	62	63	64
ROW 9	65	66	67	68	69	70	71	72
ROW 10	73	74	75	76	77	78	79	80
ROW 11	81	82	83	84	85	86	87	88



```
.....  
                                WATER BALANCE          NAPL BALANCE  
CONSTANT PRES                  -703.68            -1.2165  
SOURCE/SINKS                    664.88            42.080  
STORAGE                         38.798           -40.863  
PER CENT ERROR                 -0.29463E-04      -0.10094E-03  
  
STEP NUMBER 32                  SIMULATION TIME IN SECONDS 0.208E+08  
*****  
                                IN MINUTES 0.347E+06  
                                IN HOURS 0.578E+04  
                                IN DAYS 241.  
                                IN YEARS 0.659  
  
NAPL SATURATIONS  
SLICE 1  
0.35855 0.17297 0.16192E-02 0.27756E-16 0.27756E-16-0.24980E-15-0.16653E-15-0.22204E-15  
0.36262 0.17840 0.26699E-02 0.13878E-16 0.22204E-15-0.30531E-15 0.83267E-16 0.13878E-15  
0.35838 0.18047 0.32657E-02 0.36082E-15-0.69389E-16-0.23592E-15 0.24980E-15 0.69389E-16  
0.35447 0.18125 0.35119E-02 0.83267E-16 0.00000 0.41633E-16-0.18041E-15 0.26368E-15  
0.35065 0.18106 0.35574E-02 0.22204E-15 0.13878E-15-0.27756E-16 0.12490E-15 0.41633E-16  
0.34776 0.18116 0.35038E-02 0.15266E-15 0.21511E-15 0.44409E-15-0.69389E-16-0.10061E-15  
0.34670 0.18296 0.39761E-02 0.00000 0.00000 0.00000 0.00000 0.00000  
0.33420 0.18176 0.33701E-02 0.00000 0.00000 0.00000 0.00000 0.00000  
0.32185 0.17707 0.25743E-02 0.00000 0.00000 0.00000 0.00000 0.00000  
0.30925 0.16832 0.16607E-02 0.00000 0.00000 0.00000 0.00000 0.00000  
0.29592 0.15448 0.86245E-03 0.00000 0.00000 0.00000 0.00000 0.00000  
0.28170 0.13619 0.32776E-03 0.00000 0.00000 0.00000 0.00000 0.00000  
0.26680 0.10032 0.21411E-05 0.00000 0.00000 0.00000 0.00000 0.00000  
0.25127 0.40669E-01 0.00000 0.00000 0.00000 0.00000 0.00000 0.00000  
0.23555 0.27692E-01 0.00000 0.00000 0.00000 0.00000 0.00000 0.00000  
0.21866 0.17309E-01 0.00000 0.00000 0.00000 0.00000 0.00000 0.00000  
0.19875 0.86696E-02 0.00000 0.00000 0.00000 0.00000 0.00000 0.00000  
0.17467 0.29511E-02 0.00000 0.00000 0.00000 0.00000 0.00000 0.00000  
0.10744 0.18466E-03 0.00000 0.00000 0.00000 0.00000 0.00000 0.00000  
0.00000 0.00000 0.00000 0.00000 0.00000 0.00000 0.00000 0.00000  
.....
```

```
.....  
                                WATER BALANCE          NAPL BALANCE  
CONSTANT PRES                  -749.47            -27.030  
SOURCE/SINKS                    731.19            46.277  
STORAGE                         18.278           -19.247  
PER CENT ERROR                 0.13465E-06      -0.90745E-06  
  
STEP NUMBER 38                  SIMULATION TIME IN SECONDS 0.315E+08  
*****  
                                IN MINUTES 0.526E+06  
                                IN HOURS 0.876E+04  
                                IN DAYS 365.  
                                IN YEARS 0.999  
  
NAPL SATURATIONS  
SLICE 1  
0.35850 0.17298 0.31843E-02 0.00000 -0.55511E-16-0.55511E-16-0.11102E-15-0.16653E-15  
0.36312 0.17849 0.56028E-02-0.13878E-16-0.20817E-15-0.33307E-15 0.27756E-16 0.55511E-16  
0.35929 0.18077 0.74103E-02-0.43021E-15-0.13878E-15-0.33307E-15 0.15266E-15 0.20817E-15  
0.35611 0.18211 0.87448E-02 0.97145E-16-0.41633E-16-0.13878E-16-0.15266E-15 0.26368E-15  
0.35362 0.18337 0.98777E-02 0.22204E-15 0.15266E-15 0.48572E-16 0.15266E-15-0.55511E-16  
0.35243 0.18718 0.11347E-01 0.20123E-15 0.25327E-15 0.40246E-15-0.20817E-16-0.10755E-15  
0.35367 0.19722 0.14740E-01 0.00000 0.00000 0.00000 0.00000 0.00000  
0.34380 0.20217 0.14791E-01 0.00000 0.00000 0.00000 0.00000 0.00000  
0.33476 0.20533 0.14322E-01 0.00000 0.00000 0.00000 0.00000 0.00000  
0.32632 0.20732 0.13386E-01 0.00000 0.00000 0.00000 0.00000 0.00000  
0.31827 0.20819 0.12201E-01 0.00000 0.00000 0.00000 0.00000 0.00000  
0.31037 0.20796 0.10919E-01 0.00000 0.00000 0.00000 0.00000 0.00000  
0.30225 0.20657 0.95194E-02 0.00000 0.00000 0.00000 0.00000 0.00000  
0.29339 0.20382 0.82637E-02 0.00000 0.00000 0.00000 0.00000 0.00000  
0.28344 0.19909 0.66951E-02 0.00000 0.00000 0.00000 0.00000 0.00000  
0.27140 0.19112 0.47684E-02 0.00000 0.00000 0.00000 0.00000 0.00000  
0.25499 0.17871 0.26142E-02 0.00000 0.00000 0.00000 0.00000 0.00000  
0.22881 0.15778 0.12354E-02 0.00000 0.00000 0.00000 0.00000 0.00000  
0.17566 0.12458 0.23079E-03 0.00000 0.00000 0.00000 0.00000 0.00000  
0.00000 0.00000 0.00000 0.00000 0.00000 0.00000 0.00000 0.00000  
.....
```

```
.....  
                                WATER BALANCE          NAPL BALANCE  
CONSTANT PRES                  -8872.1            -498.97  
SOURCE/SINKS                    8816.2            557.98  
STORAGE                         55.895           -59.010  
PER CENT ERROR                 -0.70125E-06      -0.27999E-06  
  
STEP NUMBER 46                  SIMULATION TIME IN SECONDS 0.946E+08  
*****  
                                IN MINUTES 0.158E+07  
                                IN HOURS 0.263E+05  
                                IN DAYS 0.109E+04  
                                IN YEARS 3.00  
  
NAPL SATURATIONS  
SLICE 1  
0.35849 0.17298 0.11939E-01-0.19429E-15-0.83267E-16 0.24980E-15-0.22204E-15-0.19429E-15  
0.36322 0.17852 0.21585E-01-0.12490E-15-0.13878E-15-0.24980E-15-0.55511E-16 0.41633E-16  
0.35947 0.18089 0.29510E-01-0.38858E-15-0.97145E-16-0.23592E-15 0.27756E-16 0.26368E-15  
0.35644 0.18240 0.36207E-01 0.22204E-15-0.13878E-15-0.11102E-15-0.69389E-16 0.15266E-15  
0.35421 0.18401 0.42766E-01 0.29837E-15 0.12490E-15 0.97145E-16 0.00000 -0.62450E-16  
.....
```



RUN NAME .... 2-D Unsaturated-Saturated Infiltration of o-Nitrotoluene  
DATE .... 8 May 1994 RUN NO .... RUN1

NUMBER OF BLOCKS IN THE X-DIRECTION (COLUMNS): 8  
NUMBER OF BLOCKS IN THE Z-DIRECTION (LAYERS): 20  
NUMBER OF BLOCKS IN THE Y-DIRECTION (SLICES): 1  
MAXIMUM NUMBER OF NEWTON-RAPHSON ITERATIONS: 4  
ESTIMATED BANDWIDTH: 0  
MAXIMUM NUMBER OF TIME STEPS: 100  
NUMBER OF TIME STEPS BETWEEN PRINTING OUTPUT: 1  
MAXIMUM NUMBER OF SSOR ITERATIONS: 1

BALANCE ERROR (%) FOR CONTROL OF NEWTON-RAPHSON ITERATION: 0.200000E-01  
INITIAL TIME (SECONDS): 0.000000  
DENSITY OF WATER: 1000.00  
DENSITY OF NONAQUEOUS FLUID: 1152.90  
DYNAMIC VISCOSITY OF WATER: 0.100000E-02  
DYNAMIC VISCOSITY OF NONAQUEOUS FLUID: 0.237000E-02  
GRAVITATIONAL ACCELERATION (Z-DIRECTION): -9.80000  
GRAVITATIONAL ACCELERATION (X-DIRECTION): 0.000000  
SSOR CONVERGENCE TOLERANCE: 0.100000E-04  
SSOR RELAXATION FACTOR: 1.00000

NUMBER OF PC VS KR TABLES: 1

DATA SET: 1

PC	SW	KRW	KRN
103425.000	-0.100	0.00000	1.00000
103425.000	0.000	0.00000	1.00000
103425.000	0.100	0.00000	0.82000
103425.000	0.200	0.00000	0.68000
27580.000	0.300	0.04000	0.55000
10343.000	0.400	0.10000	0.43000
7585.000	0.500	0.18000	0.31000
7447.000	0.600	0.30000	0.20000
7309.000	0.700	0.44000	0.12000
7171.000	0.800	0.60000	0.05000
7033.000	0.900	0.80000	0.00000
6895.000	1.000	1.00000	0.00000
6895.000	1.100	1.00000	0.00000

DATA SET: 1 PNWSWR: 0.680

PCAN	SAIR	PRNA	PRA
-98000.000	1.000	-0.32000	1.00000
0.000	0.000	0.68000	0.00000

1 PERMEABILITY SETS

SET 1 0.10000E-11 0.10000E-11 0.10000E-11

1 POROSITY SETS

SET 1 0.30000 0.10000E-14 0.00000

DX

1 1.00 2 1.90 3 3.61 4 6.86 5 13.0 6 24.8 7 47.0 8 89.4

DZ

1 0.250 2 0.250 3 0.250 4 0.250 5 0.250 6 0.250 7 0.250 8 0.250  
9 0.250 10 0.250 11 0.250 12 0.250 13 0.250 14 0.250 15 0.250 16 0.250  
17 0.250 18 0.250 19 0.250 20 0.250

DY

1 1.00

1 PROPERTY COMBINATION SETS

SET 1 1 1 1

NUMBER OF ACTIVE BLOCKS

SLICE 1 152

GRID BLOCK NUMBERS

ROW 1	1	2	3	4	5	6	7	8
ROW 2	9	10	11	12	13	14	15	16
ROW 3	17	18	19	20	21	22	23	24
ROW 4	25	26	27	28	29	30	31	32
ROW 5	33	34	35	36	37	38	39	40
ROW 6	41	42	43	44	45	46	47	48
ROW 7	49	50	51	52	53	54	55	56
ROW 8	57	58	59	60	61	62	63	64
ROW 9	65	66	67	68	69	70	71	72
ROW 10	73	74	75	76	77	78	79	80
ROW 11	81	82	83	84	85	86	87	88





0.21006	0.14014	0.17481E-02-0.27062E-15	0.15266E-15-0.13184E-15	0.10408E-15	0.34694E-15
0.20456	0.12197	0.19406E-02-0.22551E-15	0.69389E-16-0.62450E-16	0.10408E-16	0.93675E-16
0.20314	0.10419	0.24601E-02 0.00000	0.00000	0.00000	0.00000
0.20202	0.10500	0.30640E-02 0.00000	0.00000	0.00000	0.00000
0.20091	0.10579	0.36180E-02 0.00000	0.00000	0.00000	0.00000
0.19973	0.10653	0.41226E-02 0.00000	0.00000	0.00000	0.00000
0.19834	0.10725	0.45792E-02 0.00000	0.00000	0.00000	0.00000
0.19700	0.10794	0.50317E-02 0.00000	0.00000	0.00000	0.00000
0.19569	0.10859	0.55214E-02 0.00000	0.00000	0.00000	0.00000
0.19442	0.10922	0.62766E-02 0.00000	0.00000	0.00000	0.00000
0.19313	0.10983	0.52934E-02 0.00000	0.00000	0.00000	0.00000
0.19164	0.11040	0.51019E-02 0.00000	0.00000	0.00000	0.00000
0.18921	0.11092	0.68625E-02 0.00000	0.00000	0.00000	0.00000
0.18266	0.11123	0.69256E-02 0.00000	0.00000	0.00000	0.00000
0.15707	0.10826	0.48866E-02 0.00000	0.00000	0.00000	0.00000
0.00000	0.00000	0.00000	0.00000	0.00000	0.00000

WATER BALANCE		NAPL BALANCE	
CONSTANT PRES	-8820.5	-606.12	
SOURCE/SINKS	8815.9	611.42	
STORAGE	4.5924	-5.3038	
PER CENT ERROR	-0.10106E-01	-0.11963E-04	

STEP NUMBER 42	SIMULATION TIME	IN SECONDS	0.158E+09
*****		IN MINUTES	0.263E+07
		IN HOURS	0.438E+05
		IN DAYS	0.182E+04
		IN YEARS	5.00

NAPL SATURATIONS

SLICE 1					
0.22644	0.16422	0.92528E-03-0.83267E-16	0.55511E-16-0.11102E-15	0.47184E-15	0.24980E-15
0.22391	0.16044	0.17806E-02-0.30531E-15	0.11102E-15	0.29143E-15	0.36082E-15
0.22099	0.15520	0.25665E-02-0.22204E-15	0.34694E-15-0.69389E-16	0.97145E-16	0.69389E-16
0.21644	0.14956	0.32321E-02 0.00000	0.38858E-15	0.27756E-16	0.97145E-16
0.21006	0.14014	0.36924E-02-0.25674E-15	0.13184E-15-0.11796E-15	0.48572E-16	0.42327E-15
0.20456	0.12197	0.40489E-02-0.17000E-15	0.15613E-15	0.34694E-16	0.15266E-15
0.20314	0.10419	0.50680E-02 0.00000	0.00000	0.00000	0.00000
0.20202	0.10501	0.61731E-02 0.00000	0.00000	0.00000	0.00000
0.20091	0.10579	0.72072E-02 0.00000	0.00000	0.00000	0.00000
0.19973	0.10654	0.81718E-02 0.00000	0.00000	0.00000	0.00000
0.19834	0.10726	0.90688E-02 0.00000	0.00000	0.00000	0.00000
0.19700	0.10794	0.99418E-02 0.00000	0.00000	0.00000	0.00000
0.19570	0.10860	0.10831E-01 0.00000	0.00000	0.00000	0.00000
0.19442	0.10924	0.11952E-01 0.00000	0.00000	0.00000	0.00000
0.19313	0.10984	0.11416E-01 0.00000	0.00000	0.00000	0.00000
0.19165	0.11041	0.11612E-01 0.00000	0.00000	0.00000	0.00000
0.18921	0.11094	0.13605E-01 0.00000	0.00000	0.00000	0.00000
0.18266	0.11125	0.13862E-01 0.00000	0.00000	0.00000	0.00000
0.15707	0.10828	0.99958E-02 0.00000	0.00000	0.00000	0.00000
0.00000	0.00000	0.00000	0.00000	0.00000	0.00000

WATER BALANCE		NAPL BALANCE	
CONSTANT PRES	-27000.	-1857.3	
SOURCE/SINKS	26988.	1871.7	
STORAGE	12.509	-14.448	
PER CENT ERROR	0.18758E-07	-0.78340E-10	

STEP NUMBER 52	SIMULATION TIME	IN SECONDS	0.315E+09
*****		IN MINUTES	0.526E+07
		IN HOURS	0.876E+05
		IN DAYS	0.365E+04
		IN YEARS	9.99

NAPL SATURATIONS

SLICE 1					
0.22644	0.16422	0.21283E-02-0.27756E-16	0.11102E-15-0.13878E-15	0.52736E-15	0.27756E-15
0.22391	0.16044	0.40893E-02-0.41633E-15	0.55511E-16	0.26368E-15	0.15266E-15
0.22099	0.15520	0.58848E-02-0.11102E-15	0.23592E-15-0.55511E-16	0.11102E-15	0.16653E-15
0.21644	0.14956	0.73994E-02 0.49960E-15	0.30531E-15	0.55511E-16	0.24980E-15
0.21006	0.14014	0.84258E-02-0.31919E-15	0.12490E-15-0.13878E-15	0.17347E-15	0.51348E-15
0.20456	0.12197	0.91477E-02-0.32960E-15	0.12837E-15-0.27756E-16	0.16653E-15	0.19776E-15
0.20314	0.10419	0.11280E-01 0.00000	0.00000	0.00000	0.00000
0.20202	0.10501	0.13511E-01 0.00000	0.00000	0.00000	0.00000
0.20091	0.10579	0.15605E-01 0.00000	0.00000	0.00000	0.00000
0.19974	0.10655	0.17567E-01 0.00000	0.00000	0.00000	0.00000
0.19834	0.10727	0.19405E-01 0.00000	0.00000	0.00000	0.00000
0.19700	0.10796	0.21162E-01 0.00000	0.00000	0.00000	0.00000
0.19570	0.10862	0.22877E-01 0.00000	0.00000	0.00000	0.00000
0.19442	0.10926	0.24743E-01 0.00000	0.00000	0.00000	0.00000
0.19314	0.10987	0.25126E-01 0.00000	0.00000	0.00000	0.00000
0.19165	0.11045	0.26100E-01 0.00000	0.00000	0.00000	0.00000
0.18922	0.11099	0.28529E-01 0.00000	0.00000	0.00000	0.00000
0.18266	0.11130	0.29170E-01 0.00000	0.00000	0.00000	0.00000
0.15707	0.10831	0.21655E-01 0.00000	0.00000	0.00000	0.00000
0.00000	0.00000	0.00000	0.00000	0.00000	0.00000



RUN NAME .... 2-D Unsaturated-Saturated Infiltration of Trichloroethene (TCE)  
 DATE .... 8 May 1994 RUN NO .... RUN1

NUMBER OF BLOCKS IN THE X-DIRECTION (COLUMNS): 8  
 NUMBER OF BLOCKS IN THE Z-DIRECTION (LAYERS): 20  
 NUMBER OF BLOCKS IN THE Y-DIRECTION (SLICES): 1  
 MAXIMUM NUMBER OF NEWTON-RAPHSON ITERATIONS: 4  
 ESTIMATED BANDWIDTH: 0  
 MAXIMUM NUMBER OF TIME STEPS: 150  
 NUMBER OF TIME STEPS BETWEEN PRINTING OUTPUT: 1  
 MAXIMUM NUMBER OF SSOR ITERATIONS: 1

BALANCE ERROR (%) FOR CONTROL OF NEWTON-RAPHSON ITERATION: 0.200000E-01  
 INITIAL TIME (SECONDS): 0.000000  
 DENSITY OF WATER: 1000.00  
 DENSITY OF NONAQUEOUS FLUID: 1467.90  
 DYNAMIC VISCOSITY OF WATER: 0.100000E-02  
 DYNAMIC VISCOSITY OF NONAQUEOUS FLUID: 0.566000E-03  
 GRAVITATIONAL ACCELERATION (Z-DIRECTION): -9.80000  
 GRAVITATIONAL ACCELERATION (X-DIRECTION): 0.000000  
 SSOR CONVERGENCE TOLERANCE: 0.100000E-04  
 SSOR RELAXATION FACTOR: 1.00000

NUMBER OF PC VS KR TABLES: 1

DATA SET: 1

PC	SW	KRW	KRN
103425.000	-0.100	0.00000	1.00000
103425.000	0.000	0.00000	1.00000
103425.000	0.100	0.00000	0.82000
103425.000	0.200	0.00000	0.68000
27580.000	0.300	0.04000	0.55000
10343.000	0.400	0.10000	0.43000
7585.000	0.500	0.18000	0.31000
7447.000	0.600	0.30000	0.20000
7309.000	0.700	0.44000	0.12000
7171.000	0.800	0.60000	0.05000
7033.000	0.900	0.80000	0.00000
6895.000	1.000	1.00000	0.00000
6895.000	1.100	1.00000	0.00000

DATA SET: 1 PNWSWR: 0.680

PCAN	SAIR	PRNA	PRA
-98000.000	1.000	-0.32000	1.00000
0.000	0.000	0.68000	0.00000

1 PERMEABILITY SETS

SET 1 0.10000E-11 0.10000E-11 0.10000E-11

1 POROSITY SETS

SET 1 0.30000 0.10000E-14 0.00000

DX

1	1.00	2	1.90	3	3.61	4	6.86	5	13.0	6	24.8	7	47.0	8	89.4
---	------	---	------	---	------	---	------	---	------	---	------	---	------	---	------

DZ

1	0.250	2	0.250	3	0.250	4	0.250	5	0.250	6	0.250	7	0.250	8	0.250
9	0.250	10	0.250	11	0.250	12	0.250	13	0.250	14	0.250	15	0.250	16	0.250
17	0.250	18	0.250	19	0.250	20	0.250								

DY

1 1.00

1 PROPERTY COMBINATION SETS

SET 1 1 1 1

NUMBER OF ACTIVE BLOCKS

SLICE 1 152

GRID BLOCK NUMBERS

ROW 1	1	2	3	4	5	6	7	8
ROW 2	9	10	11	12	13	14	15	16
ROW 3	17	18	19	20	21	22	23	24
ROW 4	25	26	27	28	29	30	31	32
ROW 5	33	34	35	36	37	38	39	40
ROW 6	41	42	43	44	45	46	47	48
ROW 7	49	50	51	52	53	54	55	56
ROW 8	57	58	59	60	61	62	63	64
ROW 9	65	66	67	68	69	70	71	72
ROW 10	73	74	75	76	77	78	79	80
ROW 11	81	82	83	84	85	86	87	88



```

.....
                WATER BALANCE                NAPL BALANCE
CONSTANT PRES      -89.670                    -5.0492
SOURCE/SINKS        87.798                      7.7713
STORAGE             1.8718                     -2.7221
PER CENT ERROR     -0.14896E-04                 -0.79712E-06

```

```

STEP NUMBER 37          SIMULATION TIME IN SECONDS 0.525E+07
*****
                                IN MINUTES 0.874E+05
                                IN HOURS 0.146E+04
                                IN DAYS 60.7
                                IN YEARS 0.166

```

## NAPL SATURATIONS

```

SLICE 1
0.16915 0.10425E-01-0.27756E-16 0.16653E-15 0.30531E-15 0.11102E-15-0.11102E-15 0.24980E-15
0.16559 0.88932E-02-0.27756E-16-0.55511E-16 0.18041E-15 0.41633E-16 0.19429E-15-0.24980E-15
0.15999 0.82134E-02 0.12490E-15 0.22204E-15 0.23592E-15 0.12490E-15-0.83267E-16-0.97145E-16
0.15400 0.69884E-02 0.55511E-16 0.41633E-16-0.55511E-16 0.20817E-15-0.19429E-15-0.13878E-15
0.14566 0.61124E-02 0.11102E-15-0.83267E-16 0.12490E-15 0.21511E-15 0.83267E-16 0.12490E-15
0.12699 0.49645E-02-0.21511E-15-0.90206E-16-0.69389E-16-0.10061E-15 0.12143E-15-0.13184E-15
0.10843 0.40943E-02 0.00000 0.00000 0.00000 0.00000 0.00000 0.00000
0.10838 0.38243E-02 0.00000 0.00000 0.00000 0.00000 0.00000 0.00000
0.10834 0.35112E-02 0.00000 0.00000 0.00000 0.00000 0.00000 0.00000
0.10829 0.30323E-02 0.00000 0.00000 0.00000 0.00000 0.00000 0.00000
0.10825 0.28133E-02 0.00000 0.00000 0.00000 0.00000 0.00000 0.00000
0.10820 0.24883E-02 0.00000 0.00000 0.00000 0.00000 0.00000 0.00000
0.10816 0.20101E-02 0.00000 0.00000 0.00000 0.00000 0.00000 0.00000
0.10811 0.17984E-02 0.00000 0.00000 0.00000 0.00000 0.00000 0.00000
0.10807 0.14740E-02 0.00000 0.00000 0.00000 0.00000 0.00000 0.00000
0.10802 0.98404E-03 0.00000 0.00000 0.00000 0.00000 0.00000 0.00000
0.10799 0.78589E-03 0.00000 0.00000 0.00000 0.00000 0.00000 0.00000
0.10805 0.44976E-03 0.00000 0.00000 0.00000 0.00000 0.00000 0.00000
0.10510 0.11815E-03 0.00000 0.00000 0.00000 0.00000 0.00000 0.00000
0.00000 0.00000 0.00000 0.00000 0.00000 0.00000 0.00000 0.00000

```

```

.....
                WATER BALANCE                NAPL BALANCE
CONSTANT PRES      -489.55                    -39.671
SOURCE/SINKS        487.21                      43.125
STORAGE             2.3398                     -3.4530
PER CENT ERROR     0.45609E-03                     -0.56092E-05

```

```

STEP NUMBER 54          SIMULATION TIME IN SECONDS 0.315E+08
*****
                                IN MINUTES 0.526E+06
                                IN HOURS 0.876E+04
                                IN DAYS 365.
                                IN YEARS 0.999

```

## NAPL SATURATIONS

```

SLICE 1
0.16917 0.54173E-01-0.27756E-16 0.13878E-15 0.22204E-15 0.00000 -0.27756E-16 0.27756E-15
0.16561 0.51654E-01-0.69389E-16 0.41633E-16 0.69389E-16 0.13878E-15 0.55511E-16-0.37470E-15
0.16003 0.49325E-01 0.13878E-15 0.16653E-15 0.23592E-15 0.55511E-16-0.13878E-15-0.83267E-16
0.15405 0.46467E-01 0.41633E-16 0.16653E-15 0.19429E-15 0.45797E-15-0.13878E-15-0.69389E-16
0.14574 0.43009E-01 0.20123E-15-0.31919E-15 0.26368E-15 0.18041E-15-0.13184E-15 0.22204E-15
0.12709 0.37127E-01-0.51001E-15 0.48572E-16 0.16306E-15-0.36776E-15 0.11796E-15-0.20470E-15
0.10854 0.32952E-01 0.00000 0.00000 0.00000 0.00000 0.00000 0.00000
0.10851 0.32634E-01 0.00000 0.00000 0.00000 0.00000 0.00000 0.00000
0.10847 0.32284E-01 0.00000 0.00000 0.00000 0.00000 0.00000 0.00000
0.10844 0.31813E-01 0.00000 0.00000 0.00000 0.00000 0.00000 0.00000
0.10841 0.31530E-01 0.00000 0.00000 0.00000 0.00000 0.00000 0.00000
0.10837 0.31171E-01 0.00000 0.00000 0.00000 0.00000 0.00000 0.00000
0.10834 0.30698E-01 0.00000 0.00000 0.00000 0.00000 0.00000 0.00000
0.10831 0.30421E-01 0.00000 0.00000 0.00000 0.00000 0.00000 0.00000
0.10827 0.30061E-01 0.00000 0.00000 0.00000 0.00000 0.00000 0.00000
0.10824 0.29580E-01 0.00000 0.00000 0.00000 0.00000 0.00000 0.00000
0.10821 0.29313E-01 0.00000 0.00000 0.00000 0.00000 0.00000 0.00000
0.10816 0.28918E-01 0.00000 0.00000 0.00000 0.00000 0.00000 0.00000
0.10721 0.25592E-01 0.00000 0.00000 0.00000 0.00000 0.00000 0.00000
0.00000 0.00000 0.00000 0.00000 0.00000 0.00000 0.00000 0.00000

```

```

.....
                WATER BALANCE                NAPL BALANCE
CONSTANT PRES      -5583.7                    -473.92
SOURCE/SINKS        5570.8                      493.08
STORAGE             12.988                     -19.167
PER CENT ERROR     -0.13838E-06                     -0.10249E-08

```

```

STEP NUMBER 76          SIMULATION TIME IN SECONDS 0.946E+08
*****
                                IN MINUTES 0.158E+07
                                IN HOURS 0.263E+05
                                IN DAYS 0.109E+04
                                IN YEARS 3.00

```

## NAPL SATURATIONS

```

SLICE 1
0.16918 0.11549 -0.83267E-16 0.27756E-16 0.19429E-15 0.83267E-16-0.27756E-16 0.27756E-16
0.16565 0.11204 0.24980E-15 0.27756E-16 0.13878E-16 0.41633E-15-0.11102E-15-0.63838E-15
0.16008 0.10773 0.16653E-15 0.18041E-15 0.36082E-15 0.16653E-15-0.30531E-15-0.43021E-15
0.15412 0.10293 -0.11102E-15 0.30531E-15 0.69389E-16 0.72164E-15-0.41633E-16-0.23592E-15

```



RUN NAME .... Unsaturated-Saturated Infiltration of Tetrachloromethane (Carbon Tetrachloride)  
 DATE .... 8 May 1994 RUN NO .... RUN1

NUMBER OF BLOCKS IN THE X-DIRECTION (COLUMNS): 8  
 NUMBER OF BLOCKS IN THE Z-DIRECTION (LAYERS): 20  
 NUMBER OF BLOCKS IN THE Y-DIRECTION (SLICES): 1  
 MAXIMUM NUMBER OF NEWTON-RAPHSON ITERATIONS: 4  
 ESTIMATED BANDWIDTH: 0  
 MAXIMUM NUMBER OF TIME STEPS: 100  
 NUMBER OF TIME STEPS BETWEEN PRINTING OUTPUT: 1  
 MAXIMUM NUMBER OF SSOR ITERATIONS: 1

BALANCE ERROR (%) FOR CONTROL OF NEWTON-RAPHSON ITERATION: 0.200000E-01  
 INITIAL TIME (SECONDS): 0.000000  
 DENSITY OF WATER: 1000.00  
 DENSITY OF NONAQUEOUS FLUID: 1584.20  
 DYNAMIC VISCOSITY OF WATER: 0.100000E-02  
 DYNAMIC VISCOSITY OF NONAQUEOUS FLUID: 0.969000E-03  
 GRAVITATIONAL ACCELERATION (Z-DIRECTION): -9.80000  
 GRAVITATIONAL ACCELERATION (X-DIRECTION): 0.000000  
 SSOR CONVERGENCE TOLERANCE: 0.100000E-04  
 SSOR RELAXATION FACTOR: 1.00000

NUMBER OF PC VS KR TABLES: 1

DATA SET: 1

PC	SW	KRW	KRN
103425.000	-0.100	0.00000	1.00000
103425.000	0.000	0.00000	1.00000
103425.000	0.100	0.00000	0.82000
103425.000	0.200	0.00000	0.68000
27580.000	0.300	0.04000	0.55000
10343.000	0.400	0.10000	0.43000
7585.000	0.500	0.18000	0.31000
7447.000	0.600	0.30000	0.20000
7309.000	0.700	0.44000	0.12000
7171.000	0.800	0.60000	0.05000
7033.000	0.900	0.80000	0.00000
6895.000	1.000	1.00000	0.00000
6895.000	1.100	1.00000	0.00000

DATA SET: 1 PNWSWR: 0.680

PCAN	SAIR	PRNA	PRA
-98000.000	1.000	-0.32000	1.00000
0.000	0.000	0.68000	0.00000

1 PERMEABILITY SETS

SET 1 0.10000E-11 0.10000E-11 0.10000E-11

1 POROSITY SETS

SET 1 0.30000 0.10000E-14 0.00000

DX

1 1.00 2 1.90 3 3.61 4 6.86 5 13.0 6 24.8 7 47.0 8 89.4

DZ

1 0.250 2 0.250 3 0.250 4 0.250 5 0.250 6 0.250 7 0.250 8 0.250  
 9 0.250 10 0.250 11 0.250 12 0.250 13 0.250 14 0.250 15 0.250 16 0.250  
 17 0.250 18 0.250 19 0.250 20 0.250

DY

1 1.00

1 PROPERTY COMBINATION SETS

SET 1 1 1 1

NUMBER OF ACTIVE BLOCKS

SLICE 1 152

GRID BLOCK NUMBERS

ROW 1	1	2	3	4	5	6	7	8
ROW 2	9	10	11	12	13	14	15	16
ROW 3	17	18	19	20	21	22	23	24
ROW 4	25	26	27	28	29	30	31	32
ROW 5	33	34	35	36	37	38	39	40
ROW 6	41	42	43	44	45	46	47	48
ROW 7	49	50	51	52	53	54	55	56
ROW 8	57	58	59	60	61	62	63	64
ROW 9	65	66	67	68	69	70	71	72
ROW 10	73	74	75	76	77	78	79	80
ROW 11	81	82	83	84	85	86	87	88



```

.....
                WATER BALANCE                NAPL BALANCE
CONSTANT PRES          -146.58                -7.9833
SOURCE/SINKS           142.98                13.665
STORAGE                3.6023                -5.6820
PER CENT ERROR        -0.49463E-04            -0.22668E-05

```

```

STEP NUMBER 28          SIMULATION TIME IN SECONDS 0.525E+07
*****                IN MINUTES 0.874E+05
                        IN HOURS 0.146E+04
                        IN DAYS 60.7
                        IN YEARS 0.166

```

NAPL SATURATIONS

```

SLICE 1
0.17115 -0.19909E-01 0.22204E-15 0.38858E-15 0.55511E-16 0.00000 -0.11102E-15-0.55511E-16
0.16781 0.80393E-02 0.69389E-16-0.83267E-16-0.16653E-15 0.55511E-16-0.11102E-15 0.12490E-15
0.16222 0.70816E-02-0.37470E-15-0.16653E-15-0.97145E-16-0.27756E-16-0.22204E-15 0.20817E-15
0.15625 0.61241E-02-0.83267E-16-0.18041E-15-0.20817E-15-0.41633E-16-0.18041E-15 0.11102E-15
0.14870 0.52812E-02 0.55511E-16-0.90206E-16-0.17347E-15 0.41633E-16-0.41633E-15 0.10408E-15
0.13008 0.42020E-02 0.25327E-15 0.13878E-16-0.39552E-15-0.79797E-16 0.18041E-15 0.15266E-15
0.11165 0.36038E-02 0.00000 0.00000 0.00000 0.00000 0.00000 0.00000
0.11160 0.30642E-02 0.00000 0.00000 0.00000 0.00000 0.00000 0.00000
0.11154 0.29695E-02 0.00000 0.00000 0.00000 0.00000 0.00000 0.00000
0.11149 0.27166E-02 0.00000 0.00000 0.00000 0.00000 0.00000 0.00000
0.11144 0.23200E-02 0.00000 0.00000 0.00000 0.00000 0.00000 0.00000
0.11139 0.21513E-02 0.00000 0.00000 0.00000 0.00000 0.00000 0.00000
0.11134 0.16188E-02 0.00000 0.00000 0.00000 0.00000 0.00000 0.00000
0.11128 0.15380E-02 0.00000 0.00000 0.00000 0.00000 0.00000 0.00000
0.11123 0.12817E-02 0.00000 0.00000 0.00000 0.00000 0.00000 0.00000
0.11120 0.87891E-03 0.00000 0.00000 0.00000 0.00000 0.00000 0.00000
0.11124 0.69512E-03 0.00000 0.00000 0.00000 0.00000 0.00000 0.00000
0.11105 0.42263E-03 0.00000 0.00000 0.00000 0.00000 0.00000 0.00000
0.10642 0.14408E-03 0.00000 0.00000 0.00000 0.00000 0.00000 0.00000
0.00000 0.00000 0.00000 0.00000 0.00000 0.00000 0.00000 0.00000

```

```

.....
                WATER BALANCE                NAPL BALANCE
CONSTANT PRES          -5100.6                -450.60
SOURCE/SINKS           5078.8                485.41
STORAGE                21.850                -34.804
PER CENT ERROR        -0.17576E-06            -0.29528E-08

```

```

STEP NUMBER 37          SIMULATION TIME IN SECONDS 0.315E+08
*****                IN MINUTES 0.526E+06
                        IN HOURS 0.876E+04
                        IN DAYS 365.
                        IN YEARS 0.999

```

NAPL SATURATIONS

```

SLICE 1
0.17117 0.23503E-01 0.22204E-15 0.30531E-15-0.55511E-16 0.13878E-15-0.11102E-15 0.00000
0.16784 0.44052E-01-0.69389E-16-0.55511E-16-0.20817E-15 0.15266E-15-0.13878E-15 0.13878E-15
0.16226 0.41816E-01-0.37470E-15-0.24980E-15-0.11102E-15-0.12490E-15-0.69389E-16 0.20817E-15
0.15630 0.39501E-01-0.16653E-15-0.83267E-16-0.26368E-15-0.27756E-16-0.18041E-15 0.15266E-15
0.14878 0.36731E-01 0.48572E-16 0.90206E-16-0.23592E-15 0.18735E-15-0.34694E-15 0.23592E-15
0.13018 0.31728E-01 0.27062E-15-0.76328E-16-0.53776E-15-0.10755E-15 0.19429E-15 0.72858E-16
0.11176 0.28237E-01 0.00000 0.00000 0.00000 0.00000 0.00000 0.00000
0.11172 0.27725E-01 0.00000 0.00000 0.00000 0.00000 0.00000 0.00000
0.11168 0.27558E-01 0.00000 0.00000 0.00000 0.00000 0.00000 0.00000
0.11164 0.27268E-01 0.00000 0.00000 0.00000 0.00000 0.00000 0.00000
0.11160 0.26866E-01 0.00000 0.00000 0.00000 0.00000 0.00000 0.00000
0.11156 0.26641E-01 0.00000 0.00000 0.00000 0.00000 0.00000 0.00000
0.11151 0.26134E-01 0.00000 0.00000 0.00000 0.00000 0.00000 0.00000
0.11147 0.25977E-01 0.00000 0.00000 0.00000 0.00000 0.00000 0.00000
0.11143 0.25685E-01 0.00000 0.00000 0.00000 0.00000 0.00000 0.00000
0.11139 0.25278E-01 0.00000 0.00000 0.00000 0.00000 0.00000 0.00000
0.11135 0.25043E-01 0.00000 0.00000 0.00000 0.00000 0.00000 0.00000
0.11130 0.24716E-01 0.00000 0.00000 0.00000 0.00000 0.00000 0.00000
0.11019 0.22188E-01 0.00000 0.00000 0.00000 0.00000 0.00000 0.00000
0.00000 0.00000 0.00000 0.00000 0.00000 0.00000 0.00000 0.00000

```

```

.....
                WATER BALANCE                NAPL BALANCE
CONSTANT PRES          -8836.3                -808.46
SOURCE/SINKS           8814.9                842.50
STORAGE                21.371                -34.040
PER CENT ERROR        -0.75431E-06            -0.43515E-08

```

```

STEP NUMBER 45          SIMULATION TIME IN SECONDS 0.946E+08
*****                IN MINUTES 0.158E+07
                        IN HOURS 0.263E+05
                        IN DAYS 0.109E+04
                        IN YEARS 3.00

```

NAPL SATURATIONS

```

SLICE 1
0.17118 0.90372E-01 0.19429E-15 0.27756E-15 0.83267E-16 0.13878E-15-0.27756E-16-0.13878E-15
0.16788 0.99815E-01 0.41633E-16-0.15266E-15-0.12490E-15 0.22204E-15-0.19429E-15 0.13878E-16
0.16232 0.95840E-01-0.49960E-15-0.34694E-15-0.24980E-15-0.26368E-15-0.13878E-16 0.97145E-16
0.15637 0.91652E-01-0.13878E-16 0.55511E-16-0.27756E-15-0.16653E-15-0.27756E-15 0.55511E-16

```





## VITA

David Alan Balthazor

Candidate for the Degree of

Master of Science

**Thesis:** AN EXAMINATION OF DENSITY AND VISCOSITY DEPENDENT INFILTRATION OF IMMISCIBLE NONAQUEOUS PHASE LIQUIDS USING THE NUMERICAL MODEL "SWANFLOW"

**Major Field:** Civil Engineering

### **Biographical:**

**Personal Data:** Born Buchanan, Michigan on February 1, 1964, the son of Donald and Sandra Balthazor.

**Education:** Graduated from Buchanan High School, Buchanan, Michigan in June, 1982. Received the Bachelor of Science Degree in Geology from Michigan State University, East Lansing, Michigan in June, 1987. Earned the Master of Science Degree in Geology from Western Michigan University, Kalamazoo, Michigan in April, 1991. Completed the requirements for the Master of Science Degree in Civil Engineering at Oklahoma State University in July, 1994.

**Professional Experience:** Employed as a graduate research assistant while in residency at Western Michigan University for the Department of Environmental Health and Safety, and for the Department of Geology. Worked for Mobil Exploration and Producing, U.S. in Oklahoma City, Oklahoma as an exploration geologist 1991 to 1992.